NATIONAL AERONAUTICS AND SPACE ADMINISTRATION

Technical Memorandum No. 33-238

Power Systems Related to Operations of a Landed Planetary Capsule

R. G. Ivanoff

JET PROPULSION LABORATORY
CALIFORNIA INSTITUTE OF TECHNOLOGY
PASADENA, CALIFORNIA

June 1, 1965

NATIONAL AERONAUTICS AND SPACE ADMINISTRATION

Technical Memorandum No. 33-238

Power Systems Related to Operations of a Landed Planetary Capsule

R. G. Ivanoff

J. D. Acord, *Manager*
Voyager Guidance and Control

JET PROPULSION LABORATORY
CALIFORNIA INSTITUTE OF TECHNOLOGY
PASADENA, CALIFORNIA

June 1, 1965

Prepared Under Contract No. NAS 7-100
National Aeronautics & Space Administration

CONTENTS

CONTENTS (Cont'd)

TABLES

FIGURES

FIGURES (Cont'd)

ABSTRACT

This Report summarizes the analyses of power sources that have been proposed for use on space capsules to be landed on the planet Mars. The investigation was occasioned by the need to define the advantages and disadvantages of power sources that could provide power for such a landed capsule. The analysis compares the various sources on the basis of weight, operating time, development status, complexity, impact tolerance, and capability to withstand sterilization. Also included is a discussion of the thermal problems that must be considered in the design of radioisotope power systems for this mission. The Appendixes present detailed comparisons between photovoltaic and radioisotopic power systems.

I. INTRODUCTION

The following discussion consists of an analysis of power systems and the criteria which would lead to the selection of one system having the most favorable attributes in meeting the requirements of a Mars landed capsule. Since, at this time, only a very general idea regarding the requirements for such a mission are known, two typical missions are assumed and used as a basis for the power systems selection. The resultant study should provide a means of logically and concisely evaluating the various methods for power generation and eliminate those systems known to be inadequate. It will be the purpose of this study to eliminate immediately those systems which are obviously unsuitable, eliminating the not-so-obvious systems after thorough examination, and finally, expand on systems which appear feasible for the application to a capsule system expected to operate on the Martian surface.

There are, at present, numerous physical phenomena and devices that can be utilized for generating electrical power for space systems. Elimination of any of the major types of power generator systems at this time would be impossible, as each is attractive, to a limited degree, for the power level-mission duration characteristics assumed for a capsule operation. However, physical sources such as springs, capacitors, and friction devices can be eliminated at the outset. Energy density of these sources are extremely low, less than one watt-hour per pound (whr/lb) and are difficult to store for long periods. Capacitors could be utilized for actuating pyrotechnic devices.

Power generation may be reduced to three basic concepts: an energy source or collector, a conversion system, and a waste rejection system. An exception to this separation is, perhaps, the photovoltaic cell. The semiconductor material of the cell performs the entire task of collector, converter, and heat rejection, simultaneously. By reducing the power generation system to this form, tradeoffs become apparent and usually lead to optimizing the system

to form one which more adequately performs to mission requirements. Energy sources can be further categorized as either physical, chemical, or nuclear sources. As shown in Fig. 1, three sources using various methods of conversion can produce an electrical output. The various methods of converting solar, chemical or nuclear energy into electrical power provides the opportunity for complete optimization of the derived power system. As an example, using a parabolic reflector, a physical source of energy, the Sun's thermal energy can be concentrated within a cavity producing the required electrical energy when converted. By careful selection of the converter, either thermionic diodes or thermoelectric elements, a system can be defined which will produce the required power while meeting the maximum number of constraints of the capsule—a system with the greatest utilization factor.

Power systems can also be divided into two different types, dependent on the method of conversion. They are static and dynamic systems. In the preceding paragraph, an example of a static system was presented in which the energy from a physical source was converted directly into electrical power without the use of moving parts. In the dynamic system there is an intermediate step requiring the primary source of power to be converted first to mechanical power and then to the desired electrical power. An example of the dynamic system can be seen in Fig. 1. Using a chemical source of energy, a monopropellant fuel, conversion to a hot gas by combustion or decomposition of the fuel produces mechanical energy by driving a turbine; this energy is transmitted through a shaft to a generator, whose rotor is rotated through a magnetic field producing a current to the capsule load.

Up to the present time, spacecraft electrical power requirements have been relatively small, usually under 200 w, and have been met by primary batteries or by arrays of solar cell systems backed up by secondary batteries for dark and peak demand periods. There have been exceptions such as the radioisotope thermoelectric generators used in the Transit navigational satellites and the nuclear thermoelectric SNAP-10A system. However, power requirement estimates used for future power systems designs have anticipated a growth in the power

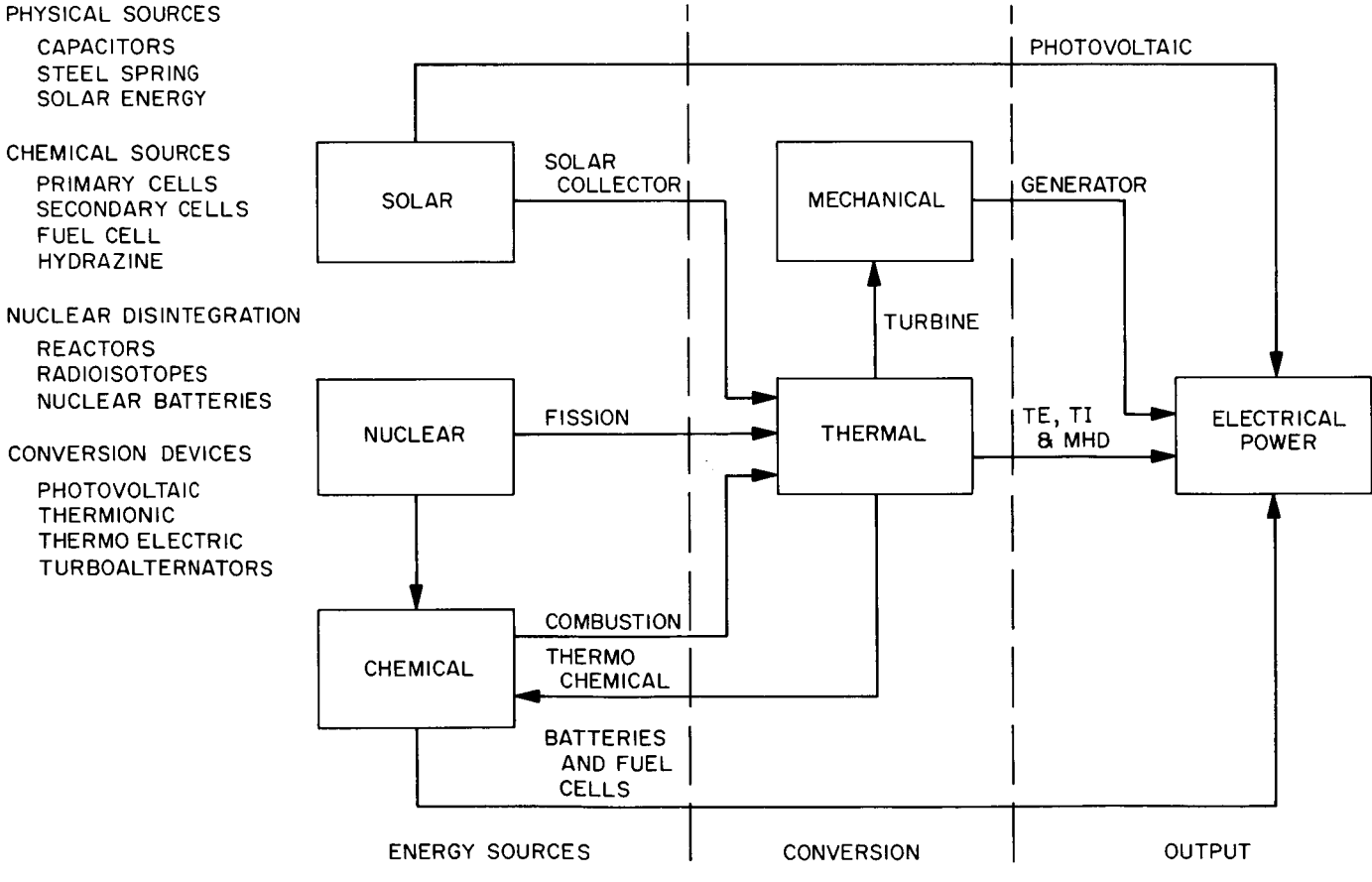

Fig. 1. Relationship between source of energy and desired electrical power output

level required for future missions. This has led to research and development of sources and converters to produce power in excess of 1 kw and as high as 10 Mw. These systems do not, in all cases, lend themselves to small power levels and it is these levels, less than 500 w, that are most likely to be the requirements for the earlier landed capsule operations. It will be shown in later sections that solar cells and batteries are still applicable for the expected and assumed capsule mission, but do not produce the optimum system for all the constraints imposed by the mission and planet characteristics. It then becomes mandatory to investigate all power systems to determine which are applicable and of these, which are optimum for the capsule system.

II. OBJECTIVES AND REQUIREMENTS

There were three objectives of this study:

1. To evaluate all power sources and energy converters to determine which are applicable to a capsule system that could be landed on the Martian surface
2. To present the technical information resulting from this study in a usable form as a guide in the development of selected power systems
3. To develop two specific capsule configurations and mechanize acceptable power systems that will meet the needs of the mission while conforming to the mission and capsule requirements

The analysis is bounded by the following conditions regarding mission and systems of interest:

1. Electrical power is the only desired form of energy output.
2. Power requirements may be supplied by separate systems or a single source for each of four assumed mission portions, i.e., a delivery system; a low power, short life system; a high power, long life system.
3. Analysis shall include promising developments of power systems as well as current components to the extent that performance can be demonstrated by 1970.
4. System power levels are mission discreet and defined by the power profiles of Figs. 2 and 3.
5. Load durations are as defined in Tables 1 and 2 with most power systems designed for a relatively constant load. Consideration is thus given to energy storage systems that can be applied for the short duration peak load applications.

To analyze all systems that are available as power sources and conversion devices, it becomes necessary to define a typical mission so that all systems are evaluated for the same constraints and mission objectives to make any comparison meaningful. To this end, two landed capsule systems are defined and the selection of power systems will be based on their capability to fulfill the requirements of these missions.

A. Capsule I

Capsule I is selected on the basis of providing an absolute minimum of landed operation and could be a capsule designed to provide initial information on the characteristics of the Martian surface which would be used in the design of larger, more sophisticated systems for later Mars opportunities. It would consist of:

1. A delivery system, D_1, for the flight phases from preseparation to impact.
2. A parachute deployment upon entry to the Martian atmosphere.
3. A survival system, S, for operation on the planet surface. Maximum operating time of 40 hr consisting of two periods of five hr each for communication and data retrieval, separated by a 30-hr passive period during which science data are obtained. The first communications period would be used to transmit engineering and entry data immediately after impacting the planet. Science data which are gathered and stored during the passive period would be transmitted during the last communication period.

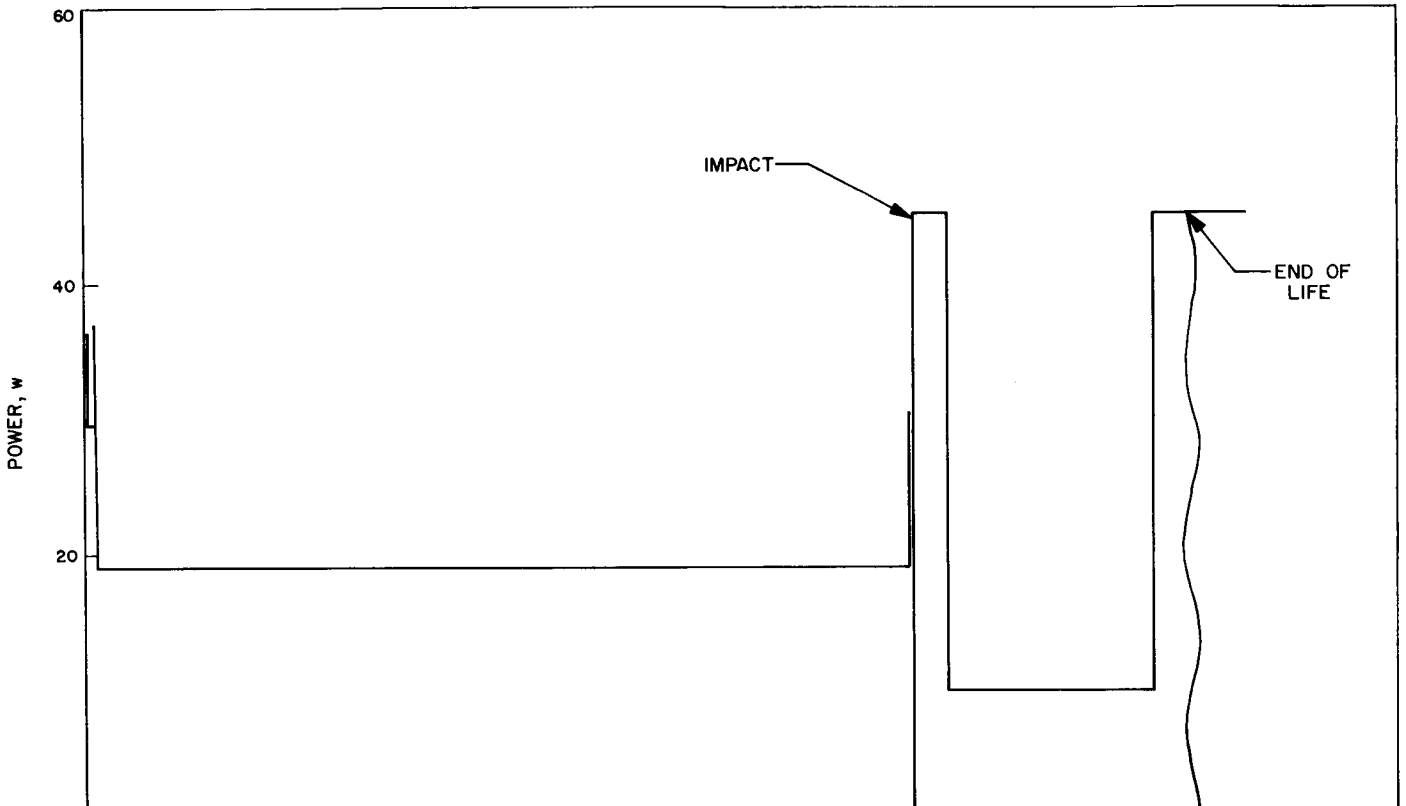

Fig. 2. Power profile for minimum-life capsule

Table 1. Minimum-life capsule system power matrix

Subsystem	Flight phase (power in watts)								
	Preseparation: capsule on internal power 0.5 hr	Separation & spin up 5 min	Coast to deflection motor firing 1 hr	Despin 5 min	Coast to entry 5 days	Chute deployment 10 min	Capsule descent 15 min	Landed operation	
								Active comm. period (2) 5 hr each	Passive period 30 hr
Capsule bus timer	3	3	3	3	3	3	3	—	—
Spin control	5	10	5	10	—	—	—	—	—
VHF transmitter, 3 bits/sec	10	10	10	10	10	10	10	—	—
Data encoder	5	5	5	5	3	5	5	—	—
Capsule bus total	23	28	23	28	16	18	18	—	—
Raw power required	29	36	29	36	19	21	21	—	—
Survival timer	—	—	—	—	—	—	—	1	1
S-band FSK transmitter	—	—	—	—	—	—	—	30	—
Data storage & encoder	—	—	—	—	—	3	3	4	1
Survival science	—	—	—	—	—	—	—	2	1
Temperature control	—	—	—	—	—	4	4	—	4
Survival capsule total	—	—	—	—	—	7	7	37	7
Raw power required	—	—	—	—	—	10	10	40	10

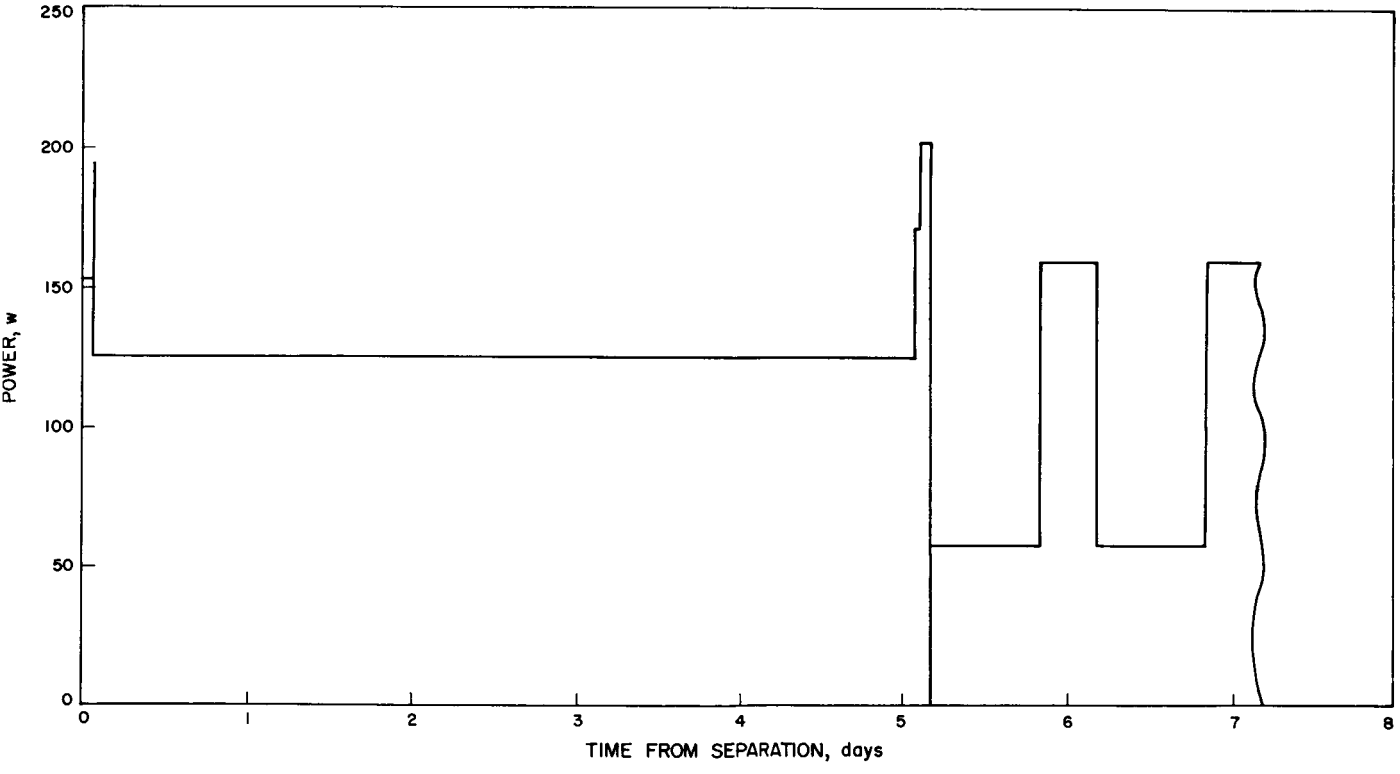

Fig. 3. Power profile for long-life capsule

Selection of power systems for this capsule may provide power either for the delivery system, D_1, or the survival system, S, or both. They must be capable of supplying power as defined by the power profile shown in Fig. 2 and the power matrix of Table 1. The capsule, during the cruise period, is expected to have random orientation, and its only stabilization is provided by spinup prior to the deflection maneuver from the spacecraft bus.

Table 2. Maximum-life capsule system

Subsystem	Flight phase (power in watts)											
											Diurnal cycle, 6 mo	
	Preseparation (Capsule on internal power) ~½ hr		Separation to deflection maneuver ~1 hr	Deflection maneuver ~5 min		Cruise to entry 5 days, max	Entry to chute deployment 3–10 min		Descent to impact 10–20 min		Deployment and erection of lander equipment ½–2 hr		Passive observation period 16–18 hr/day	Active communication period; Earth near Zenith 6–8 hr/day
Capsule attitude control	30 w, 3-axis inertial		30 w, 3-axis inertial	30 w, 3-axis inertial		10 w, Sun plus roll rate limit	—		—		—		—	—
Capsule autopilot	—		—	30 w		—	—		—		—		—	—
Sequencer and timer	3		3	3		3	5		5		5		3	3
VHF transmitter 30 bits/sec, 100 w raw input	100		100	100		100[a]	100		100		100		—	—
Radar altimeter, 30 w raw input	—		—	—		—	30		30		—		—	—
Command receiver, 10 w raw input	—		—	—		—	—		—		10		10	10
S-band PSK transmitter, 100 w raw input	—		—	—		—	—		—		—		5	100
Data storage system	—		—	—		—	10		10		5		5	5 plus peaks for TV recording
Lander deployment & erection system	—		—	—		—	—		—		20		1	1
North seeking and antenna pointing	—		—	—		—	—		—		15		1	5 plus peaks
Science-atm & biological	—		—	—		—	5		5		10		10	5
TV	—		—	—		—	—		—		—		—	5 plus peaks
Data encoding system	5		5	5		5	10		10		10		2	10
Total power[b]	138		138	168		118	160		160		175		37	144 plus peaks
Raw power[c]	154		154	197		126	173		173		203		46	159

Separation | Jettison motor | Jettison aft cone; deploy chute | Impact | S/C set, end relay operation

[a] May be cycled if operating from energy limited source.
[b] Does not include power for temperature control if required.
[c] This power includes the inefficiency of the conversion equipment.

B. Capsule II

This design is made on the basis of long life requirements for the landed operation in measuring atmospheric and biological data of the planet's surface. Although this is not to infer a maximum capsule configuration, it is meant to be a realistic landed capsule model. Capsule II for this study consists of:

1. A parachute deployment upon entry to the Martian atmosphere.
2. The deployment and erection of the landed capsule after impact. This includes alignment of the capsule to the local vertical, determination of tru North, and pointing the communication antenna.
3. A maximum operating life of 6 mo with a diurna cycle which consists of 16 to 18 hr per day gather ing and storing science data and 6 to 8 hr per da of communications when Earth is near Zenith.

This capsule system can be broken down again into capsule bus system and a survival capsule for landed operation. It can further be broken down by stipulatin a landed capsule system called L_1 with a maximum lif of 3 to 6 mo; L_2 will have 2- to 5-days maximum capability

Fig. 3 illustrates the power profile for this capsule, while Table 2 indicates the power matrix. It is assumed that this capsule design will incorporate an attitude control system in the capsule bus and provide orientation to a fixed reference, such as the Sun during the cruise period.

The choice of any particular power system will depend on which can best meet all the requirements of the defined mission. The criteria for which each power source and conversion device will be examined, pertains directly to the mission requirements and capsule design. Listed without regard to importance, these are:

1. Objectives
2. Scientific instruments
3. Surface operational characteristics
4. Payload weight and volume limitations
5. Mission duration
6. Reliability and system complexity
7. Surface environment
8. Cost
9. Adaptability to sterilization
10. Impact tolerance while operating; while off
11. Complexity of integration into the capsule system with maximum compatibility
12. Ease of thermal control
13. Availability
14. Growth potential
15. Development risk
16. Operation hazards

Of the above criteria, it is difficut to determine which are the more important in the selection of power systems. If this were known, a weighting factor could be applied to each and the systems analyzed and selected on the basis of the highest total summation of these factors. However, factors such as cost, system integration, and operational characteristics do not lend themselves as readily to a rigorous mathematical analysis as does either the system weight or reliability. Therefore, it becomes necessary to select a system on experience as well as mathematical proofs, because those requirements which cannot be defined precisely play an important part in the power system selection.

III. POWER SOURCES FOR A LANDING CAPSULE

Although space applications impose many unique restrictive requirements upon power systems, many systems have been or are being developed from long known principles which can be used directly in these applications. In addition to those requirements applied by the space environment, which imposes restrictions on the selection of power systems, is the restriction to the power level required. The trend in the development of future power systems, is to develop systems capable of high power levels of operation. However, the development of reliable, high efficiency, long life, low power systems have not progressed to the extent that a selection is readily available and can be specified for a particular mission. Each unit now available has unique advantages. The selection of any one for a particular requirement becomes more a process of elimination of systems which are unacceptable because they do not perform satisfactorily to the mission requirements.

With the requirements presented in Section II as the criteria for selection, each of the power sources and conversion devices is analyzed, first on a general basis providing a definition of the major characteristics of that method of power generation. Secondly, a specific design for each of the assumed landers will be developed to determine its feasibility for inclusion into the capsule systems. It is to be emphasized that, although computations can be performed in most cases, these computations can only be used as indicators and they do not represent a finalized system.

A. Chemical Sources

Chemical sources of energy which can be converted to electrical energy can be subdivided into three types:

1. Direct conversion generators: Fuel cells, so-called, produce electrical energy directly from the initial products of the chemical reaction.
2. Intermediate thermal generators: These are composed of a chemical source of energy which can be decomposed. The combustion product is then used in an open loop thermodynamic cycle to drive a dynamic conversion unit to produce mechanical energy, which is again converted to electrical energy by a generator. The dynamic conversion takes the form of a turbine or a reciprocating engine, which drives the generator.
3. Electrochemical batteries and regenerative fuel cells: These are methods of producing theoretically reversible energy, which is stored in the chemical form and converted to electrical energy for short periods of time upon demand by the system and later restored to the chemical form by a secondary power system. The secondary system regenerates the combustion products.

The basic attractiveness of using electrochemical units is the fact that the output is a direct conversion to electrical energy. Much higher efficiencies can be expected as a result.

1. Nonregenerative Fuel Cells

Direct conversion generators are those systems in which energy is derived from a continually supplied chemical reaction and converted directly into electrical energy. This scheme bypasses the conversion to heat process and the associated mechanical to electrical processes. The energy produced is in the form of low voltage, dc electrical energy produced with relatively high efficiency. When the chemical fuel is expended the chemical reaction ceases and electrical power is no longer available. A typical example of this type of energy source is the nonregenerative fuel cell.

In this fuel cell the fuel and oxidant are fed directly to the electrodes (Fig. 4), where the chemical action takes place. The cell shown in the Figure is a modified Bacon cell utilizing a liquid electolyte. The fuel is injected at the anode electrode, where it is oxidized, releasing electrons to the external circuit. The oxidizer, injected at the

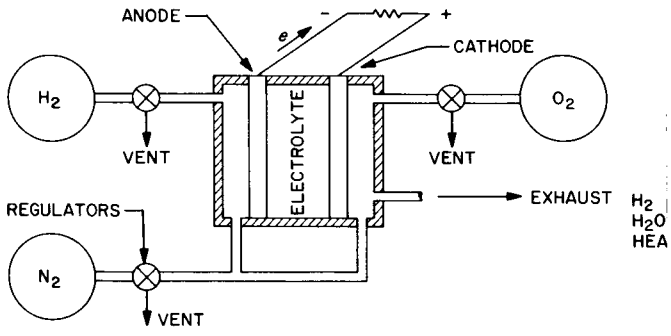

Fig. 4. Nonregenerative fuel cell

cathode, diffuses through the cathode and is reduced by the electrons that have come from the anode by way of the external load. The pressure of the reactants is maintained at a slightly higher pressure than the electrolyte pressure. This pressure differential retains the electrolyte within its defined compartment of the cell and establishes a meniscus at the pore interface of the electrodes. The reaction occurs at this interface.

Since fuel cells using hydrogen as a fuel and oxygen as the oxidizer have the lowest equivalent weight and are in a greater state of development, this criteria will be used to limit or restrict consideration to these cells for primary fuel cell usage. The overall chemical action which occurs is expressed by the chemical equation:

$$H_2 + \tfrac{1}{2}O_2 \rightarrow H_2O + \text{heat} + \text{electrical energy}.$$

The reaction which occurs at the anode is:

$$H_2 + 2OH^- \rightarrow 2H_2O + 2e^-$$

at the cathode:

$$\tfrac{1}{2}O_2 + H_2O + 2e^- \rightarrow 2OH^-$$

Hydrogen is ionized at a tri-phase reaction site at the anode. The electrons traverse the external load and combine with water from the electrolyte and with oxygen to form hydroxyl ions at the cathode as shown in the last equation. The hydroxyl ions migrate through the electrolyte to the anode and combine with the ionized hydrogen to produce water and more electrons. Thus, water is produced at the anode with basic electrolytes (in other fuel cell concepts an acidic electrolyte is used and in this case water is produced at the cathode). Circulation of

the excess hydrogen gas is used to remove product water from the fuel cell system. A buildup of this water in the cell would dilute the electrolyte, which under constant operating temperature would increase the vapor pressure of the aqueous solution as well as reducing the amount of free hydroxyl ions to react with hydrogen. The electron flow would thereby be reduced.

This type of system has a high theoretical reliability, but requires a large quantity of fuel and must get rid of the product of the reaction. Water must be expelled external to the system. Heater power from an external source is required to keep the reactants at a minimum temperature of 0°F indicating a secondary source of power is required in order to start the reaction. Efficiency of the fuel cell is not limited by the Carnot cycle meaning a theoretical efficiency of 100% could be obtained. This is limited, however, to 55 to 65% by polarization of the electrodes and the electrolyte, IR drops, and corrosion.

Except for fuel cell designs for the Gemini, Apollo, and Lunar Excursion Module, LEM, programs, fuel cell work remains in the research and development stage. There are no fuel cells for space applications now in operation which can prove state-of-the-art. The most advanced fuel cells at this time are those using hydrogen–oxygen as the fuel–oxidizer. These systems have not reached the point in development where they can be defined as proven power systems, and further development over the next few years is required to produce a proven system. For this reason, fuel cells are not acceptable for a landed systems design.

A typical fuel cell can be calculated to determine the fuel–oxidizer requirements and to obtain an estimate of an ideal system's weight. From these calculations, a relative comparison would show a fuel cell system to be competitive with other sources of power if the ideal system could be attained. As an example, using the power profile shown in Fig. 3, a fuel cell will be sized to provide the power requirements during the period from separation from the spacecraft until impact on the Martian surface.

The following assumptions are made:

1. Voltage output required is 28 v
2. Power required by the capsule, and auxiliary equipment internal to the fuel cell shall be an average of 200 w
3. The fuel cell shall have the following characteristics:

$$A = 87\ \text{cm}^2$$

$$J_{\max} = 100\ \text{ma/cm}^2$$

$$E_{c_{\min}} = 0.40\ \text{v/cell}$$

$$E_o = 0.9\ \text{v/cell}$$

$$\alpha = 5\ \text{lb/1000 cm}^2$$

$$b = 0.005\ \Omega\text{-cm}$$

$$\beta = 0.0022\ \text{lb/gm}$$

$$\text{Electrolyte concentration} = 30\%\ \text{KOH}$$

$$\text{Operating temperature} = 175°\text{F}$$

$$\text{Operating pressure} = 1.5\ \text{atm}$$

Loss in the current density J becomes more pronounced with operating time because of the cell materials not remaining invariant. Losses are primarily due to chemical polarization, concentration polarization and resistance polarization. These losses become significant with time, reducing the current density of the cell to a limited value. The limited value can be determined from the expression

$$J_L = -\frac{\alpha}{\beta T} + \left[\left(\frac{\alpha}{\beta T}\right)^2 + \frac{\alpha E_0}{\beta b T}\right]^{1/2} \qquad (1)$$

When the maximum operating time is 122 hr:

$$J_L = 41.1\ \text{ma/cm}^2$$

the cell operating voltage is found from the equation

$$E_{max} = E_0 - bJ_L = 0.70\ \text{v} \qquad (2)$$

Since the fuel cell voltage varies between 0.4 and 0.7 v, a value of 0.55 v/cell is used to determine the total number of cells required for an operating voltage of 28 v. A total of 51 cells are required and the output voltage will vary from 20.4 to 35.6 v or 28 ±27%. This voltage variation will require a great deal of regulation before distribution to the load.

$$\text{the current } I = J_L A = 3.58\ \text{amp} \qquad (3)$$

and the power $= E_o I = 100$ w so that two parallel sets of 51 cells are required for a total of 102 cells.

a. Fuel requirements. Fluid flow rates are determined from Faraday's laws of electrolysis and stoichiometry. The hydrogen consumption is calculated from:

Consumption.

$$W_{H_C} = \frac{NI}{\sigma} \tag{4}$$

$$= \frac{102\,(3.58)}{1.21 \times 10^4} = 3.02 \times 10^{-2}\ \text{lb/hr}$$

Moisture removal.

$$W_{H_D} = W_{H_C}\frac{P - P_v}{P_v} \tag{5}$$

For 30% KOH, the vapor pressure is $P_v = 0.276$ at 175°F

$$W_{H_D} = 3.02 \times 10^{-2}\frac{1.5 - 0.276}{0.276} = 13.4 \times 10^{-2}\ \text{lb/hr}$$

Total hydrogen flow rate.

$$W_{H_T} = W_{H_C} + W_{H_D} \tag{6}$$

$$= 0.1642\ \text{lb/hr}$$

b. Oxygen flow rate.

Consumption.

$$W_{O_C} = 7.94\,W_{H_C} = 0.240\ \text{lb/hr} \tag{7}$$

Purge. A small continual purge of the oxygen side of the fuel cell reduces the amount of cell impurities.

$$W_{O_P} = 0.05\,W_{O_C} = 0.012\ \text{lb/hr} \tag{8}$$

Total oxygen flow rate.

$$W_{O_T} = W_{O_C} + W_{O_P} = 0.252\ \text{lb/hr} \tag{9}$$

c. Water removal rate. Water produced by the reactants must be removed at a rate equal to its production in order to maintain the electrolyte concentration.

$$W_{H_2O} = 8.94\,W_{H_C} = 0.270\ \text{lb/hr} \tag{10}$$

d. Total reactant weights. The reactant weights required for completion of a 122-hr mission are:

Hydrogen.

$$H_2 = W_{HT}\,T = 0.1642\,(122) = 20.0\ \text{lb} \tag{11}$$

Oxygen.

$$O_2 = W_{OT}\,T = 0.252\ \text{lb/hr}\,(122) = 30.8\ \text{lb} \tag{12}$$

Fuel storage may well be one of the limiting factors in the design of a practical fuel cell system. Storage in a high pressure gas form is difficult to achieve for extended missions. Use of cryogenic liquid storage is more practical but not necessarily easier to contain. Absorption of heat through the container walls creates an increased pressure and/or evaporation can occur. Although large systems using storage containers with a larger volume to area ratio are not affected as readily as smaller systems, any loss through evaporation must be considered and provided for. Design of super-insulator materials to limit the fuel loss to a reasonable level may be achieved, but even with the insulation, storage of the fuel for over six months during a spacecraft transit will produce enough loss to at least double the weight of the fuel that has to be carried. Also, a 25% allowance should be provided for the effect of variable factors such as temperature, electrolyte concentration, and rate of moisture removal. Therefore, the reactant weights are:

$$H_2 = 2.25 W_{HT}\,T = 45\ \text{lb}$$

$$O_2 = 2.25 W_{OT}\,T = 69.4\ \text{lb}$$

e. Fuel tankage weight. The weight of the fuel tanks and all the appurtenances, such as regulators, is assumed to be twice that of the total fuel weight.

$$W_F = 2\,(H_2 + O_2) = 229\ \text{lb} \tag{13}$$

f. Fuel cell weight. The specific cell weight is given by the expression

$$W_{cs} = 33.3\text{v}\,(1 - \text{v})\ \text{w/lb} \tag{14}$$

$$= 33.3\,(0.779)\,(0.22) = 5.74\ \text{w/lb}$$

$$W_c = \frac{P}{W_{cs}} = \frac{200}{5.74} = 34.8\ \text{lb} \tag{15}$$

The total fuel cell system weight is then:

$$W_{FC} = H_2 + O_2 + W_F + W_C = 378 \text{ lb} \qquad (16)$$

To the total weight derived must be added the weight of a storage battery to provide temperature control prior to fuel cell startup. This is to maintain the stored fuel above 0°F and heat the fuel prior to injection into the fuel cell. Also the electrical conversion equipment must be added.

g. Conclusion. Although calculations can be performed to determine some of the fuel cell characteristics, it must be recognized that the results are idealistic and may be hard to achieve. Since only laboratory models have thus far been demonstrated, additional development of the fuel cell must be done to make it an acceptable space power system. When the problems of water removal, removal of impurities, ion exchange membranes, electrolyte containment, and reductions in the heat transfer and polarization losses are solved, the fuel cell will be a competitive source of energy.

Because the system is not now state-of-the-art, the additional constraints of sterilization and impact survival can hardly be attained. Other mission requirements as listed in Section II which cannot be achieved are:

1. Surface operation. The open loop fuel cell would require a large amount of fuel for surface operation for the longer missions, which would also violate the weight and volume limitations. Used reactants in the form of water would pollute the Martian environment and impede science experiments.
2. Integration into the capsule system, although not complex, would still require a secondary power source for some peak loads. When the electrical load changes, the rate of the electrochemical reaction at the electrode surface must also change. This requires a change in the amount of fuel and oxidizer and a higher or lower rate of water removal. The inability to immediately adjust to the new power level can be caused by insufficient fuel or oxidizer being available, flooding or drying of the electrodes by the product water, or a change in the operating temperature. All of these can cause a transient instability in the voltage at the new power level.

The response behavior of a fuel cell is not good at this time and would be a major development effort. The reliability required would, therefore, call for a second source of power adding more weight and complexity to the overall system. It is concluded that the fuel cell is not an acceptable source of power at this time.

2. Hydrazine Fueled Turboalternator

The second type of system, utilizing chemical energy as its source, can best be described as one which uses the combustion products of the decomposed chemical through a thermodynamic cycle to obtain mechanical or electrical energy. Examples of this type of power source are many and varied. The jet engine is a typical example. These systems need not depend upon an external source to initiate the reaction, but rather contain this internal to the system in the form of some catalyst to perform the decomposition of the fuel. Usually these systems are open loop in that when work has been obtained from the fuel, it is exhausted to the external environment.

Although there are a number of chemicals which can be used as a fuel for a dynamic system, monopropellant hydrazine fuel is considered herein because it has a relatively high energy availability for a low decomposition temperature. Extensive analysis has been made on the use of hydrazine for this application and also for use as guidance correction propulsion on spacecraft. These are documented in the bibliography and references. For this reason, the hydrazine fueled turboalternator is considered to be the best example of this type of system for discussion.

The liquid hydrazine, stored under pressure, is passed over a catalyst, which causes decomposition of the hydrazine to form nitrogen, hydrogen, and ammonia. These gases are injected into a turbine chamber under pressure providing the turbine drive. A generator coupled to the turbine by a shaft converts the mechanical work of the turbine into electrical energy. The dynamic system utilizes the Rankine thermodynamic cycle. The gas is expanded through the turbine after having been heated under constant pressure. Work is removed from the expanded gas, which is then exhausted from the system.

a. Capsule designs. A representative hydrazine turboalternator power system consists of a propellant supply unit, gas generator, accumulator, and turboalternator unit as shown in the system schematic of Fig. 5.

The hydrazine and helium at 900 psia are contained in the spherical titanium tank separated by a bladder or other expulsion device. A sufficient quantity of helium gas is stored to completely expel the fuel. The tank is designed to withstand the expected pressure of 1400 psia resulting from the heat sterilization temperature of 293°F. Pressure

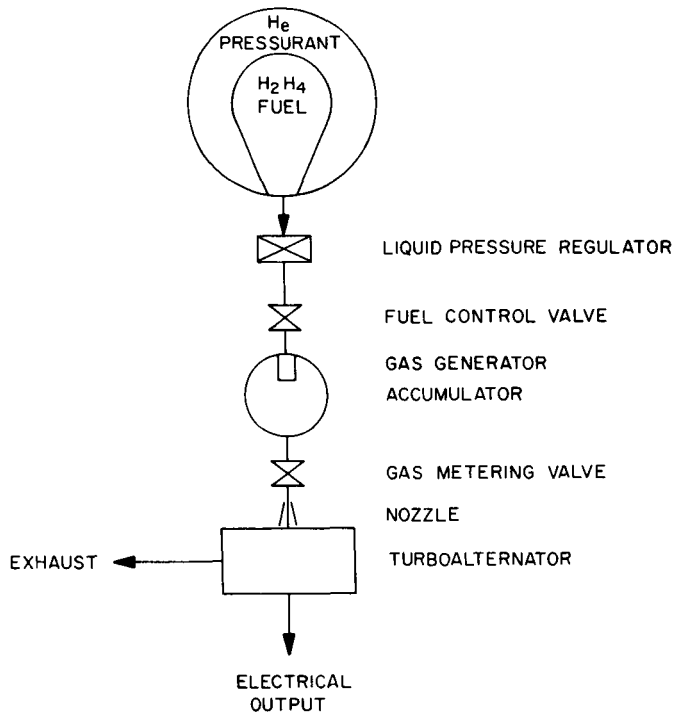

Fig. 5. Hydrazine turboalternator system

regulated fuel is supplied to the gas generator upon actuation of the solenoid control valve.

It is noted that the bladder or other expulsion device would not be necessary in a capsule that is oriented with respect to the gravity or acceleration direction. The gas flow to the turbine can be controlled by the metering valve installed between the turbine and the accumulator. This valve will be controlled by an electronic device which senses the turboalternator speed. An electrical signal will be sent to the electromechanical actuator, which in turn will adjust the gas flow to produce the desired power output.

The effect of fuel hydrostatic head on the storage tank, created by the impact force of 5000 *g*, has been investigated for the hard landing capsule power system. This imposes an additional pressure of 182 psi per in. of fuel depth.

Hydrazine is admitted to a reaction chamber containing a spontaneous catalyst bed which decomposes the fuel into gases. An ammonia dissociation fraction of 75% is recommended for the turbine designed for long operation so that the resulting gas temperature will be 1500°F. Because the minimum feasible liquid flow injection rate into the gas generator is considered to be greater than the turbine gas demand for the two power outputs under consideration, an accumulator is required to store the excess decomposition gas. The gas generator is enclosed within the accumulator, permitting the heat transferred from the chamber wall to heat the stored gas during the gas generator cycle of intermittent operation. A high strength material, under high temperatures, such as Haynes Alloy No. 25 is recommended for fabrication of the accumulator.

Based on the capsule description given in Section II, calculations were made to determine the fuel requirements and weight of hydrazine systems for the landed operation of the two capsules. The delivery system (required from spacecraft separation until entry) has been excluded from consideration for this type of power system. For the low power capsule, the omission is based upon the improbability of producing a dynamic system of such complexity to operate at so low a level as 19 to 30 w. For the Capsule II delivery system, the exclusion is based on the size and weight of the fuel requirements for the five days of continuous operation; the thrust effect on the capsule from gas expulsion and the effects this would have on the rest of the capsule design ($\approx$0.1 lb force total).

In designing this hydrazine system, it is assumed that a secondary source of power is available to provide thermal control power and power during the passive operational periods. If the power for the passive or science periods were supplied by the hydrazine system, the lower power requirements would require throttling valves and regulator systems for the reduced gas flow rates required. Startup of the hydrazine system must be achieved from an external source, which also indicates a requirement for a secondary power source. For a non-restartable system, valve actuation for startup may be achieved at impact by a *g* valve or activated squib valve, after impact by a timer. For restart capability, a solenoid or additional squibs and power to activate them are required. The hydrazine turboalternator is thus designed to operate during the active periods of the landed operation.

The following constraints on the operating time are used for the design:

1. For the low power configuration, the total operating time of the hydrazine system is 10 hr. This is separated into two 5-hr periods with 30 hr of passive operation occurring between each active period.
2. For Capsule II the total operation time is divided into five 8-hr periods separated by 16 hr of passive operation.

The impulse turbine design features assumed for this design are listed in Table 3. Heat sterilization is not expected to be a problem for either design.

Table 4 lists the estimated masses for the two systems. The calculations used to obtain the mass values in the table are based upon the design schematically depicted in Fig. 5. This mechanization is only a sample design but the system mass should be fairly independent of the system design and configuration. The major contributor to the system mass in most cases will be the fuel and tankage. The fuel mass is proportional to the total energy required and the system efficiency. The tank mass is proportional to the propellant mass and the operating pressure, and is a function of the sterilization temperature and impact acceleration requirements.

Table 3. Turbine design features

System	S	L_2
Turbine power, w	45	333
Tip diam, in.	2.50	2.50
Material	Titanium	Titanium
Blade velocity, ft/sec	3270	3270
Turbine velocity, rpm	300,000	300,000
Inlet pressure, psia	200	200
Pressure ratio	30:1	30:1
Inlet temperature, °F	1500	1500
Adiabatic efficiency	0.35	0.40
Gas flow rate, lb/hr	0.504	3.384
Turbine outlet temperature, °F	440	440

Table 4. Hydrazine turboalternator mass and size parameters

System	S	L_2
Power output, w	40	300
Energy output, whr	400	12,044
Fuel (N_2H_4), lb	5.05	137.5
Tankage + He, lb	2.68	61.9
Liquid regulator, lb	1.25	1.25
Valving, lb	0.50	0.55
Gas generator, lb	0.25	0.25
Accumulator, lb	0.15	0.60
Tubing, connectors, misc., lb	0.25	0.30
Turbine, lb	0.50	0.75
Generator, lb	0.75	1.25
Total weight, lb	11.38	204.35
Specific energy, whr/lb	35.2	59.0
Battery capacity, whr	206	1770.0
Battery weight, lb	10.3	88.4
Fuel tank diam, in.	8.38	25.22
Accumulator diam, in.	3.00	5.50
Turbine diam, in.	2.50	2.50

The value of specific propellant consumption used to determine the fuel weight was a conservative value of greater than 10 lb/kw-hr. To show the effect of fuel requirements for extended missions, we could assume the maximum life for the Capsule II design of 6 mo. The fuel required would be 4000 lb and the tankage would increase to 600 lb. It is apparent then, operation of this system would be limited in duration.

To the total weights shown in Table 4 must be added any regulation and electrical conversion equipment. Also, for a system that is not throttled, a secondary source of electrical energy must be added to provide power during the passive periods. For system S, a primary battery with a capacity of 130 whr and a weight of 6.5 lb must be used. For system L_2, a rechargeable battery must be used with power to recharge being supplied from the hydrazine system while it is in operation. In order to supply 46 w for the total passive period, a battery with a capacity of 1770 whr and weighing 88.4 lb would be required. In this case, it might be advantageous to throttle the turbine at constant speed, which would only add approximately 38 lb to the system. The battery weight is based on the use of a zinc-silver oxide battery having a specific energy of 20 whr/lb and discharged to a depth of 50%. The battery is recharged during the active communications period when 141 w are available from the hydrazine power source. The weight and capacity values given do not reflect any battery sizing for reliability considerations, but does provide a 20% degradation margin. Secondary power sources are discussed in the next Section.

Because this is an open loop system, the combusted gases are exhausted externally; so there is no requirement for a radiator to radiate thermal energy. However, to minimize any force exerted by the exhaust gas during descent, equal proportions of the gas should be exhausted from the capsule in opposite directions. Materials which can be used in removing the exhaust product are stainless steel alloys (302, 304 and 347), nickel, inconel, copper, and monel. These materials will not be affected by contact with the gas products. Teflon, Mylar, rubber, KEL-F, and polyethylene could be used for limited periods.

An obvious disadvantage of this system is the pollution of the Martian atmosphere with hydrogen, nitrogen, and ammonia. Although sterilization of the fuel can be

achieved, any science requirements which prevent the dispersion of gases which were originally external to the Martian atmosphere would prohibit the use of this system as well as the fuel cell discussed earlier.

The freezing point of pure hydrazine is 0°C so thermal control would probably have to be provided. However, if the turboalternator system is isolated from the other spacecraft systems, or it is determined that the other systems do not require thermal control, the freezing point can be depressed to −37°C through the use of additives, without a loss in overall performance.

b. High impact shock considerations. The previous capsule designs have considered the high impact requirements for the capsule systems. This resulted in a slight increase in weight for the fuel tankage in order to survive the high impacts. The rotating members of turboalternators for landed power systems can be designed for extreme ruggedness. The rotating members are relatively massive, short, and devoid of fragile or projecting components. The housings can be made equally rugged. The major problem in ruggedizing a turboalternator is to somehow guarantee that the bearings will not be damaged during the impact. Techniques are presently being devised by the Jet Propulsion Laboratory which permit the use of standard ball bearings in ruggedized rotating machinery. The method which has proven most successful is an omni-directional wafer-spring bearing mount which permits the supported rotating mass to bottom against its enclosure before bearing loads become high enough to cause damage.

One such fabricated spring was a 1.375-in. O.D., 0.030-in. thick, 2024 aluminum wafer with three concentric 0.25-in. deep corrugations. A 0.50-in. O.D. ball bearing was mounted in the inside diameter of the wafer spring. The spring constants for this particular spring were 28,600 lb/in. in the radial direction and 21,700 lb/in. in the thrust direction.

To evaluate the spring system, a fixture was fabricated to house the springs and bearings with a mass supported between them. The mass was a steel disc 0.45-in. thick and 1.5 in. in diameter weighing approximately ¼ lb. The mass was suspended on two ½-in. O.D., ¼-in. I.D., 143-lb capacity ball bearings. The radial and thrust direction clearances between the mass and housing were 0.005 in.

Tests were conducted at impact levels of 10,000 *g*'s in both radial thrust directions with velocity changes of approximately 180 ft/sec. At these levels the only failures were bearing separator failures. Phenolic separators fractured when impacted in the thrust direction. Metal separators failed by yielding the crimped tabs. This problem was solved by spot welding the metal separator ribbons together. Snap rings and bearing shields came off during thrust direction impacts, so for later tests they were removed. Despite the use of a light series bearing, these tests showed that this technique prevented bearing damage. Because some turboalternators utilize spring centering of the rotating member, this technique should be easily applied to a high impact turboalternator.

All of the above mentioned tests were conducted with the rotation mass at rest. To get some indication of the problems of impacting a rotating device, the steel disc, which was used as a mass in the earlier tests, was fashioned into a crude air turbine. Since a high-speed tachometer was not available at the time of the test, it was determined only that the rotating speed was greater than 30,000 rpm. The exact speed was not known. The shock test was conducted such that the bearings were loaded radially during impact while the turbine was being operated. The unit received a shock of 13,000 *g*'s after traveling at a maximum velocity of 173 ft/sec. The angular deceleration of the turbine at impact was not determined. However, immediately following the impact, the turbine attained its original speed and was allowed to operate for 2½ hr. There was no indication of bearing damage while the unit was operating. After the 2½ hr of operation, the unit was disassembled; and some bearing Brinelling was found. However, this was probably due to faulty spring selection.

The tests, which have been conducted, indicate the spring-mounted bearing technique has good potential for turboalternator application. In all the tests conducted using this system, the amount of deflection of the springs, to permit the rotating mass to rest against the housing, was determined from the rated load capability of the bearing. It would appear that the load capability given by the manufacturers should be adjusted by a factor for high impact applications. Controlled testing should determine this factor.

c. Conclusions. It appears feasible to design a hydrazine fueled turboalternator system for landed operation on the Martian surface. Design for sterilization and hard impact can be achieved within a relatively small packaging volume. It has the advantages of not being affected either by space or the Martian environment and can be stored for long periods prior to operation.

A disadvantage is that to prevent transfer of heat to sensitive components during operation, the accumulator and other hot surfaces would have to be insulated.

As shown in Table 4, for short duration operations, this power source would provide a relatively high specific energy. When the operating time becomes long or power requirements vary, the fuel supply must be made larger or the system mechanized to provide a variable flow rate. An alternative is the use of a secondary power source during these periods. This would detract from the specific energy of the chemical source, reduce reliability and add complexity to the design.

An additional point should be emphasized: dynamic systems maximize their high performance characteristics by operation at high temperatures and high turbine speeds.

Turboalternators have been built for, and operated by, the AEC at power levels as low as 55 w. The performance characteristics of such a system could be expected to be somewhat lower than that obtained with higher power units. JPL has not built a hydrazine fueled turboalternator for nearly 10 yr, but literally thousands of turboalternator systems using various solid and liquid fuels have been built for guided missile and torpedo applications. Some of these have used hydrazine for the fuel. The estimated development time for the systems specified herein would be about 3 yr. The pacing items in the development are:

1. Turbine: There may be problems in the design and development of an efficient, low power turbine. The operating time of the turbine should not be critical with a turbine inlet temperature of 1500°F. Present gas turbines now run longer at much higher temperatures.
2. Gas generator and accumulator: Expected problems are the development of a gas generator injector for low fuel flow and the development of a long service, spontaneous catalyst bed.
3. Liquid pressure regulators and valves: There may be a design problem associated with these components because the flow rates being below that of present systems. One company has solved this problem by using a pulsed system in which the turbine and alternator rotating mass serves as a flywheel.

This system then, appears to be feasible for limited use and should be considered for short duration applications up to several hr, but not for long durations.

3. Electrochemical Batteries and Regenerative Fuel Cells

Of all the potential power sources available today, electrochemical batteries have the lowest power levels and are relatively heavier in proportion to their power output. Their operating life times are usually short and dependent upon environmental conditions. They are, however, among the most reliable power sources now available for orbital space applications. Consequently, they are used extensively throughout the industry. As a matter of fact, so few power systems exist which can provide power under all conditions of load and mission requirements, that hardly any space system or launch vehicle is launched without batteries for energy storage. Future applications will continue to demand batteries, even in some cases where they are heavier or larger than an alternate but less reliable system, provided the power requirements are small.

Although the demands for electrochemical batteries have helped to produce improved cells, the requirements for operation have become more severe. The result has been a lag in the improvement of cells for longer life, higher outputs and better power to weight ratios. The major goal in battery improvement is in these areas. Secondary batteries with higher reliability, greater temperature range, extended storage and cycle life, and continuous trickle charge acceptance capability need further development.

Thermal batteries have been developed to produce a relatively low specific energy (10 whr/lb) and operating times of less than 20 min. Future development of this type of battery, predicts an increase in specific energy to 50 whr/lb and durations to three days. These batteries can easily be shock hardened and sterilized. Use of this type of battery will not be considered for the capsule design because of the short operating time, the low specific energy, the difficulty in testing such a device and the inability to stay abreast of other hardware development and increase in demands for capsule power and operating times which are expected.

Regenerative (secondary) fuel cells have been in the research and development stage for the last several years but none have been made operational. At this time there are no regenerative systems which are competitive with conventional electrochemical batteries. The low efficiencies, high temperatures and the requirement for a secondary system, such as solar or nuclear energy to regenerate the fuel cell reactants, removes the use of this type system from consideration at this time.

Primary batteries, defined as energy storage systems in which a single discharge is obtained, have much higher energy densities than can be obtained from secondary or rechargeable batteries. These batteries continue to be used for power requirements up to a few kw for short duration power demands. This is because of their high reliability and simplicity as well as their ability to provide all the power requirements of a system with a short duration life. They are also used extensively to provide power when a primary source is unable to supply the peak demand. Primary batteries, as compared to other power systems for long duration space applications, are heavy and bulky. They are, however, easily built to meet the severe mechanical requirements of launch, vacuum effects of space, and zero gravity effects.

Most primary batteries now being considered for space use are silver zinc (AgZn) since they offer the lowest weight or conversely, the highest energy density. The use of this battery has been demonstrated successfully on the *Ranger* lunar spacecraft and the *Mariner Mars* spacecraft. The batteries used on these missions have demonstrated their capabilities to provide power during periods when the photovoltaic solar panels were not aligned to the Sun and to withstand the temperatures and environs of space for long periods. In addition, a limited number of cycles were performed during systems tests, and recharged after the initial space maneuvers on the *Mariner* vehicle. These were well controlled recharges. These spacecrafts have demonstrated the capabilities of the AgZn primary battery.

Secondary batteries have had extensive use on Earth orbiting satellites in conjunction with solar panels. The solar panels provide the primary source of power during the sunlit portion of the orbit as well as additional power to recharge the secondary battery, which is discharged providing the power during the orbit shadow periods. The type of secondary battery is dependent upon the length of the shadow period, the number of orbits required, the length of time to recharge, and the energy required from the battery during the shadow period. Nickel cadmium (NiCd), silver cadmium (AgCd) and silver zinc are the three types of batteries considered as secondary power sources at this time. Of the three, NiCd have been used most often; silver cadmium have been used on a limited number of satellites. The only advantage in selecting a NiCd secondary battery is to obtain very long cycle life and charge characteristics which are very good. This type of battery has a poor energy density and is very bulky in comparison to the AgCd and AgZn cells. Silver cadmium cells have been flight demonstrated on satellites, and, although the cycle life is only half that of the NiCd, it is expected to approach, and perhaps surpass, the NiCd in cycle life in the next few years. In addition, it has a specific energy twice that of the NiCd.

The silver zinc secondary battery is superior to both the NiCd and AgCd in energy density and size. Unfortunately, it requires a more stringent operating temperature range and it has the lowest cycle life capability. It cannot sustain as high a charge-discharge rate as the other batteries. Performance of this battery has not been demonstrated in space. Selection of the AgZn secondary battery would be on the basis of:

1. Low depth of discharge (for repeated cycles)
2. Long recharge time
3. Spacecraft weight and volume limitations
4. Low cyclic requirements

Table 5 presents an estimate of the state-of-the-art in sealed silver zinc primary batteries and on the three previously discussed secondary batteries. The values given are maximum in each case and start with the year 1967 (which assumes a definition of requirement during 1965). These values can be reasonably expected if continual development is pursued at the current rate. It should be emphasized that no more than one of the maximum values can be achieved in the design of any one battery. As an example, the higher temperature in the table would reduce the battery life to minutes or hours depending on the type battery. Each of the maximum values can be achieved at the sacrifice of the other requirements listed. Other battery design parameters affected include:

1. Discharge current
2. Depth of discharge
3. Overcapacity requirements
4. Recharge current
5. Overcharge capability
6. Trickle charge current

These design parameters must also be considered in design of the electrochemical battery.

Two severe requirements for landed systems are not reflected by the figures listed in Table 5. These are impact and sterilization requirements. Batteries which must sur

Table 5. Estimated state-of-the-art batteries

Primary batteries	1967	1969	1971	1973
Sealed AgZn				
95% capacity retention at 70°F	1 yr	1½ yr	1½ yr	2 yr
whr/lb	100	110	115	120
Storage life	2 yr	3 yr	4 yr	5 yr
whr/in.^{3}	2.0	2.2	2.3	2.5
Operating temperature range, internal	−60° to 160°F	−60° to 200°F	−60° to 250°F	−60° to 300°F
Secondary batteries				
Sealed AgZn				
95% capacity retention at 70°F	1 yr	1½ yr	1½ yr	2 yr
whr/lb	60	70	75	80
Storage life	2 yr	2½ yr	3 yr	4 yr
whr/in.^{3}	2.0	2.1	2.2	2.3
Cycles before failure at 30% depth of discharge	500	700	1000	1500
Operating temperature range, internal	−60° to 160°F	−60° to 200°F	−60° to 250°F	−60° to 300°F
Sealed AgCd				
95% capacity retention at 70°F	1 yr	1½ yr	2 yr	2½ yr
whr/lb	30	32	34	35
Storage life	2 yr	3 yr	4 yr	5 yr
whr/in.^{3}	1.69	1.75	1.78	1.81
Cycles before failure at 30% depth of discharge	2000	3000	4000	5000
Operating temperature range, internal	−40°F to 165°F	−40°F to 200°F	−40°F to 250°F	−40°F to 300°F
Sealed NiCd				
whr/lb	15	15	16	17
Storage life	5 yr	5 yr	6 yr	6 yr
whr/in.^{3}	0.50	0.50	0.53	0.55
Cycle life at 30% depth of discharge	10,000	12,000	14,000	15,000
Operating temperature range, internal	0–200°F	0–250°F	0–300°F	0–300°F

vive impact of 5000 *g* or greater, are yet to be developed. An impact testing program has been initiated at JPL to investigate this problem. Testing to date has been done on existing cells; none of which have been specifically designed to withstand high impact levels. The results of tests on silver zinc and silver cadmium cells indicate the impact problem can be solved. Mechanical design of the battery for impact would increase its overall weight producing a decrease in the specific energy below the values presented in the table. Additional problems involving test philosophy would need resolving, as pointed out below.

Sterilization of batteries presents a more formidable problem, the consequences of which are not fully known at this time. However, a considerable amount of research and development has been done in the industry to date on heat sterilization of silver zinc batteries. The AgZn system was chosen because of its inherently high specific energy. There is no reason to believe AgCd or NiCd could not also be selected, since the main problems are with the separator and cell case materials rather than with the basic electrode system, although the electrodes are also affected. A brief summary of the research and development work funded by JPL and the planned continuation is given below.

JPL has sponsored several R&D contracts including a present contract to develop an organic separator capable of withstanding the sterilization environment in a sealed cell. Fifty-one different types of material have been fabricated and tested under this contract with the selection of two as being possible candidates. A complete evaluation has not yet been performed. An inhouse effort is in progress to test and evaluate existing materials for use in cell cases. A second contract, for the development of an alternate type of organic separator, is in the final stages of negotiation.

An RFP has been sent out which includes tasks for cell case and electrochemical research and development, cell fabrication and test, and battery fabrication and test. An inhouse research and development effort is to be established. This effort will include all phases of the work to be done. Some delay is expected until suitable lab space is available.

In addition to the JPL effort, General Electric (GE) together with Eagle-Picher, claims to have developed a heat sterilizable silver zinc battery using organic separators. However, some degree of conjecture and uncertainty exists since inconsistent and contradictory reports have come from the two companies. Also, the test procedure being used is not necessarily to the JPL specifications.

Two heat sterilizable silver zinc batteries using different types of inorganic separators are being developed, one by GE, the other by Douglas Aircraft. The two inorganic separators are both inherently high resistance materials, necessitating low-rate discharges. Also, the Douglas inorganic separator appears to be a relatively fragile device. At present, Lewis Research Center (LRC), the cognizant

NASA facility, imposes a very low level shock and vibration specification. LRC has been asked by JPL to consider the implementation of the shock and vibration levels given in footnote 1.

The research, testing and discussions with various battery companies have indicated certain specific areas which either require the additional research and development or which may impose certain constraints on the capsule. These problems are listed below. Although the word battery is used, in the final design several discrete batteries may be employed. Also, it should be understood that any or all the problems or constraints may be solved or changed in some respect by the planned development phase:

1. The battery must be in the discharged state (silver and zinc oxide) during the entire sterilization procedure. The battery must be fabricated in the discharged state and not charged until after the final sterilization cycle. The reason is that in the charged state during sterilization the silver-oxide plate is partially decomposed to silver and gaseous oxygen causing high internal pressures.

   Once a cell has been charged, it cannot be completely discharged to the silver zinc-oxide state. Consequently no charging can be done until after the completion of sterilization. The battery may be charge/discharge cycle limited. This implies that the capsule operations must be conducted primarily on external power with limited drain on the battery. One topping off may be done either prior to launch or prior to capsule spacecraft separation.

   It is assumed that the final sterilization cycle will take place a few days before launch. An allowance must be made at this time, up to 72 hr, for battery charging. The exact time cannot be determined until the battery capacity and maximum charge rates are known. Since more than one battery will probably be used, provisions should be made for simultaneous charging.

2. The impact testing to date has shown that the battery must be in the charged state to survive. The zinc oxide (discharged state) is too fragile and the plate will disintegrate at impact. This is acceptable, since the battery must be in the charged state at planetary impact. However, this constraint and the one stated above are incompatible with the flight acceptance test procedure. No one battery can be FA tested in the historical sense of FA testing all flight units. To survive sterilization it must be discharged, to survive impact it must be charged, no charging can be done until after sterilization, therefore, an alternate FA test procedure must be established. This applies at both the power subsystem level and the capsule system level.

3. The battery may be a low rate device, requiring rate limited discharging as well as charging. This constraint is manifested as poor voltage regulation and internal temperature rise during high rate charge or discharge. This results in a lengthy charge time as stated above and also limits the peak power available for such operations as radio transmission, pyrotechnic events (in the event acceptable capacitors cannot be obtained) or the use of attitude control (A/C) gas valves. In view of this possible discharge rate limitation, imposed by the battery, a similar constraint must be imposed on the user subsystems, setting upper limits on the ratio of peak power to average power and on di/dt.

   If a rate limitation does exist, it may be necessary to use several batteries for load separation. This is especially true for the radio transmitter.

   This rate limitation is caused by high resistivity separator materials. Some organic separators developed have a significantly higher resistivity than the cellophane used on the *Ranger* and *Mariner* batteries. The present inorganic separators are an order of magnitude higher in resistivity than the new material. This is one of the areas of major concentration for research and development.

4. The selection of a case material to use for the individual cells is also one of the major areas of concentration. The main effect the choice will have on the final battery is weight. However, the difference between alternate choices is small. The case material must have the strength to withstand impact. Also there must be no internal voids in the cell construction, this may require relatively large quantities of potting compounds. In addition to the impact requirements, the case material must meet these other requirements: (1) be capable of withstanding high internal pressures during sterilization (2) be capable of a metal to plastic seal for the electrodes (3) be capable of being sealed and staying sealed for the life of the battery, and (4) be capable of withstanding the somewhat corrosive environment of a 40% KOH solution at 145°C.

[1]G. C. Cleven, "Design Specification Heat Sterilizable, Impact Resistant Power Subsystem Battery A," Jet Propulsion Laboratory Specification GMP-50437-DSNA, August 23, 1965.

Such a material does not exist so far as is known, though several possible ones are being tested.

5. The last major area of concentration is in the cell configuration. Here some compromises may be necessary between the possibly conflicting design requirements for impact survival, sterilization survival, plate configuration giving maximum cross sectional area, plate configuration giving maximum capacity, cell configuration in the assembled battery, and the number of discharge/charge cycles required.

The specific energies attainable for various battery designs are subject to many variables. The figures of 25 and 45 whr/lb, given in footnotes 1 and 2, respectively, represent design goals only and should not be assumed in design calculations. It is felt that, at the present time, a specific energy of 20 whr/lb, should be assumed for both the batteries defined in the specifications cited. Any weight savings gained by removing the impact survival requirement in footnote 2 will be offset by the requirement for a large number of cycles. If both impact survival and cycle life are required, 15 whr/lb should be assumed.

These specific energies are approximations only and should be considered as such. They will be revised, up or down, when quantitative data are available to justify it.

A comparison of the three common alkaline systems is given in Table 6 for existing non-sterilizable batteries. It can be seen that AgZn has two distinct advantages, a high specific energy and a high per-cell voltage. It has a more restrictive operating temperature range, however. It was conservatively estimated, above, that the attainable specific energy for sterilizable AgZn batteries of several designs range from 15 to 20 whr/lb. Similar decreases in specific energy can be expected for the AgCd and NiCd batteries designed to the same specifications. Any attempt to put quantitative values to these specific energies would be pure guess work and, therefore, of limited usefulness. If the separator and case material capable of being sterilized are developed, it is felt that these may be used with the AgCd battery. The AgCd may be required for use with a long duration mission imposing cyclic operation on the battery. The AgZn battery is inherently cycle limited, but at the expense of weight could be capable of up to 200 cycles at 50% depth of discharge. The AgCd battery presently is capable of more than 200 cycles at 75% depth of discharge. However, because of the nominal factor of 2 difference in specific energy, the effective specific energy for cyclic operation is still higher for AgZn.

[1]G. C. Cleven, "Design Specification Heat Sterilizable, Impact Resistant Power Subsystem Battery A," Jet Propulsion Laboratory Specification GMP-50437-DSNA, August 23, 1965.

[2]G. C. Cleven, "Design Specification Heat Sterilizable, Impact Resistant Power Subsystem Battery B," Jet Propulsion Laboratory Specification GMP-50436-DSNA, August 23, 1965.

Table 6. Properties of existing non-sterilizable secondary batteries

Parameter	AgZn	AgCd	NiCd
Specific energy[a] (whr/lb)	35–70	15–25	8–12
Maximum cell voltage at end of charge	1.95	1.55	1.45
Minimum cell voltage at discharge	1.35	1.05	1.10
Nominal plateau voltage	1.58	1.10	1.2
Nominal charge rate,[b] amps	0.25C	0.4C	5C
Operating temperature range, °F	59–95	14–104	14–104

[a]The range of values exists because of the various designs in use.
[b]C is defined as the battery capacity in amp-hr. A charge rate of C would be equal to C amp for 1 hr.

Using the above information, an attempt is made to determine the required battery capacity and an approximate weight assuming an impactable, sterilizable battery is the only available power source for the capsule.

a. Capsule I. The total capacity required to supply all the needs of this capsule from spacecraft separation until end of landed operation would be the summation of the requirements for each segment as defined in the power matrix, Table 5. Therefore, the total capacity is 3,042 whr assuming the battery or batteries are fully charged at separation.

If an allowance for battery degradation is assumed to be 20% the required capacity is 3,650 whr, the total battery weight is 183 lb. If two separate batteries are used, one for the delivery system (D_1) and one for the survival capsule (S), the capacities and weights would be as shown in Table 7.

b. Capsule II. In the same manner used above, battery sizing for this capsule produces the capacity and weight values as shown in Table 7. It is obvious that the use of batteries alone is prohibitive for this capsule operation. The minimum weight power system would be a 1000 lb assuming a minimum communications period during capsule cruise and the minimum operational life on the planet's surface.

Table 7. Capacity and weight summary

System	Weight, lb	Capacity, whr
Capsule I	183	3650
D_1	126	2570
S	42	845
Capsule II	—	—
D_2[a]	927	18.54×10^3
$D_2 + L_2$	1.51×10^3	30.2×10^3
$D_2 + L_1$	23.1×10^3	46.3×10^4
L_2	583	11,657
L_1	22.2×10^3	44.3×10^4
D_2 (25% Communications)[b]	387	7745

[a] D_2 is defined as the delivery system for Capsule II from spacecraft separation until impact.

[b] Communications time has been reduced to 25% operation per day or 6 hr/day during cruise.

If a constant power source could be assumed as a primary source of power and the battery utilized for peak loads, the battery would now be selected as a secondary battery capable of recycling. As an example of this type of system, assume a constant power source supplying a constant X watts. Further assume a primary battery is used to supply the power in excess of the constant power source during the cruise (D_2) period and a secondary silver zinc battery is used for the landed operation (L_1). The secondary battery would thus have a specific energy of 15 whr/lb and a 50% depth of discharge to insure long recycle capability.

To determine the power output, X, of the constant power source, the total battery capacity used must also be determined:

$$C_1 = (P_1 - X)\,T_1 \tag{17}$$

where

C_1 = Capacity in whr discharged from the battery during the landed active communications period

P_1 = Power required during the active period in w

T_1 = Time of active period in hr

During the passive period of landed operation, the battery can be recharged. During this period the excess power from the constant power source must recharge the battery to 120% of the original discharge, to account for losses in the battery charger and the battery charge efficiency. The amount available for charge then is:

$$C_1 = \frac{(X - P_2)\,T_2}{1.2} \tag{18}$$

where

P_2 = Power required during the passive period in w

T_2 = Time for passive period in hr

Since the capacity in Eq. (18) must equal that of Eq. (17) the constant power source must have a value of

$$X = \frac{1.2P_1T_1 + P_2T_2}{1.2T_1 + T_2} \text{ w} \tag{19}$$

$$= \frac{1.2\,(159)\,(8) + 46\,(16)}{25.6} = 88.5 \text{ w}$$

Having determined the power of the constant power source, both primary and secondary batteries may be determined:

Secondary battery for landed operation.

$$\begin{aligned} C_S &= 2.4C_1 \\ &= 2.0\,(X - P_2)\,T_2 \text{ from Eq. (18)} \\ &= 2.0\,(88.5 - 46)\,16 \\ &= 1{,}360 \text{ whr @ } 91 \text{ lb} \end{aligned} \tag{20}$$

Primary battery for cruise operation.

$$C_p = 1.2\Sigma\,(P_n - X)\,T_n \tag{21}$$

where

P_n = Power required for time T_n of each mode of the cruise phase.

This equation implies that the primary battery must be sized to provide the power required during cruise, which is in excess of that supplied by the constant power source

$$C_p = 5{,}850 \text{ whr @ } 293 \text{ lb}$$

If a radioisotope thermoelectric generator with an energy density of 1.5 w/lb is assumed for the constant power source, the total weight would be 443 lb for this system as compared to 23,100 lb for the all battery system as shown in Table 7.

The selection of primary power sources using batteries only for peak loads is discussed again in later sections. The objective here is to show the significance of battery utilization and the impact it can have on a capsule system. Also, it points out the need for a sterilizable secondary battery.

For the example shown, the time for a complete discharge/charge cycle was considered to be an Earth day of 24 hr. This consists of an 8-hr discharge and a 16-hr charge time. The discharge/charge rates for this example are $C/16$ to $C/27$ and $C/11$ to $C/18$ for silver zinc and silver cadmium, respectively. These are well within the present capabilities and can be expected for sterilizable batteries of either type. If a mission duration of more than six Earth months is intended, AgCd should be considered. The choice should be based on the effective specific energies of each when considering the number of cycles, depth of discharge allowable, charge rates and capacity loss with cycling. The NiCd battery is capable of thousands of cycles of short duration involving high rate charging. This makes it useful for such applications as Earth satellites in 100-min orbits but its low specific energy makes it less than attractive for capsule operations. A silver zinc battery will be used for the capsule unless precluded by some development problem or where long life involving cyclic operation is required.

It should be noted that the battery weights for all of the cases above are minimum and assume an ideal situation. No consideration is given for redundancy or increasing reliability by other means. If any other designs are considered, the weights should be increased accordingly. Additional examples of battery sizing are given in later sections.

c. Conclusions. Electrochemical batteries for use as energy storage and for providing power during peak load periods on a cyclic basis are well established in spacecraft use. Because of the mission requirements for sterilization of all capsule systems, the design of batteries is no longer assured. If the requirements of present battery programs are met, electrochemical cells can be obtained but at a more reduced specific energy than is now available.

Also to be considered in a capsule design is the increase in system weight, to provide reliability. To provide maximum reliability, redundancy in batteries would be required. The number of batteries is dependent upon the reliability of each individual battery. Assuming the required energy is supplied by two batteries in parallel, a third can be added to provide 50% redundancy. For this example any one of the batteries could fail, and the other two could still supply the required energy. The number of batteries, as stated above, is dependent upon the specific design. What is shown here is the increased weight and system complexity in order to charge multiple batteries.

Unless an extremely limited capsule mission is anticipated, or another source of power is used to provide the largest majority of power, batteries are not recommended. This is based on the expected weight penalty when sterilization is required. If the specific energy is doubled over what is now expected, it would still be impractical to design anything but a minimum system using only a battery as a power source.

B. Solar Energy

The use of solar energy to develop electrical power has many unique qualities for application on long life spacecraft. Once outside the Earth's atmosphere, insolation from the Sun becomes a constant; and if utilized, represents an extensive source of energy in the form of light or thermal energy. With the use of a number of conversion devices, the energy available from the Sun can be transformed into the required electrical energy. As an energy source for space missions, the Sun represents the most reliable, unchanging, source of energy available for conversion to useful power. Although this source of energy is essentially free, several requirements are placed on the vehicle and on the power system when using the Sun's energy. For all deep space transits, there are periods in which the spacecraft must go through the Earth's shadow and perform maneuvers. During these periods solar energy will not be available, and other onboard power sources must be provided to keep the spacecraft operable. Orbital vehicles also pass through successive shadow periods with the same results. Landed capsules using the Sun's energy must contend with the characteristics of the planet, such as its period of axial rotation, which with its period of revolution, determines the length of Sun time per day. The planet's surface environment and atmosphere may reduce the amount of solar irradiance significantly, and therefore, must be considered. Thus, energy storage is required in all cases where power is demanded during shadow and/or night periods. A second spacecraft requirement, due to utilization of solar energy, is precise orientation of the vehicle such that the Sun axis is continuously positioned to the axis of the solar collector.

The amount of solar energy available to the vehicle will be dependent upon the mission characteristics. The energy flux from the Sun has been measured at one astronomical unit (1 AU, the mean distance from Earth to Sun) to be 140 mw/cm^2 above the Earth's atmosphere (air mass zero). Since the energy flux decreases with the square of the distance from the Sun, the flux is reduced to 50 mw/cm^2 at 1.67 AU—the distance to Mars when at

aphelion. In addition, the energy flux is reduced by any atmosphere present when measured from a planet's surface. For Earth the energy flux is reduced to 100 mw/cm^2 on the surface (air mass one).

The Martian atmosphere presents an attenuating medium for solar energy in the wavelength region spanned by the spectral response of a solar cell (4,000 Å to 11,000 Å). The presence of argon, carbon-dioxide and nitrogen gases account for essentially all of the losses in light intensity due to the atmosphere of Mars. Of these three gases, nitrogen is believed to be by far the most abundant. There is definitely water vapor present also. However, the maximum amount of precipitable water is estimated at about 20×10^{-4} cm. This amount of water can cause less than 1% light absorption at the water absorption bands centered at wavelengths of 0.94 and 1.10 μ, and also those centered at higher wavelengths. The loss of light intensity is, therefore, due to Rayleigh scattering and molecular absorption. The attenuation at any wavelength may be expressed as

$$\frac{I(\lambda)}{I_0(\lambda)} = e^{-\alpha(\lambda)1} \tag{22}$$

where $\alpha(\lambda)$ is the absorption coefficient and (1) is the effective absorber length. For a vertical path through the atmosphere, it is convenient to define a vertical (or normal) attenuation coefficient.

$$R_N(\lambda) = \frac{I(\lambda)_N}{I_0(\lambda)_N} \tag{23}$$

The attenuation for sunlight not passing through the atmosphere normal to the surface is then

$$R(\lambda) = [R_N(\lambda)]^{\sec\theta} \tag{24}$$

where θ is the angle between the solar radiation vector and the normal to the surface. We may also use average values of $R_N(\lambda)$ over wavelength intervals where either or both the solar spectrum and absorption coefficient do not change by a large amount. The width of the interval will determine the accuracy of the attenuated solar cell power obtained. For our purpose we may break the response bandwidth into (1000Å = 0.1μ) intervals and consider the percentage of total spectral response ($\Delta S/S$) in each interval. The product of ($\Delta S/S$) and $R_N(\lambda)$ for each interval will give the reduced power ratio (P/P_o) for that interval. The sum of all of these values of P/P_o will give the ratio of the total power available on the surface of Mars to that available outside the atmosphere for the following conditions:

1. Complete Sun orientation both below and above the atmosphere
2. Same temperature below and above the atmosphere
3. Sunlight passing through the atmosphere normal to the surface

Table 8 shows a tabulation of these calculations. The result is that for conditions 1, 2, and 3, the power output operating on the surface of Mars will be 75% of the power available outside the atmosphere.

Table 8. Ratio of total available power, Mars surface vs outside the atmosphere

$\Delta\lambda$ (μ)	$\Delta S/S$	$R_N(\lambda)$	P/P_o
0.40–0.51	0.05	0.3	0.015
0.51–0.61	0.12	0.6	0.072
0.61–0.71	0.16	0.8	0.128
0.71–0.81	0.20	0.8	0.160
0.81–0.91	0.23	0.8	0.184
0.91–1.00	0.20	0.8	0.160
1.00–1.10	0.04	0.8	0.032
TOTAL	100%	—	0.751

Solar energy may be converted directly into electrical energy by a photovoltaic cell. Also, the photon energy may be first converted to thermal energy, and subsequently, converted into electrical power by either static or dynamic energy conversion devices. In general conversion devices which convert the solar flux directly into electrical energy do not require concentrating the solar energy; however, when an intermediate conversion of solar energy is required, a concentrator is normally used to extract the maximum thermal energy. Usually the operating temperature range of the conversion devices is much higher in the latter case and requires the concentrator for the high thermal energy collection.

1. Solar Concentrators

Solar concentrators are being extensively investigated with significant results primarily in the smaller diameter one-piece collectors. Most efforts are aimed at achieving fabrication reproducibility, resistance to launch and space environments, high concentration ratios and structural strength. Figure 6 is a photograph of a 50-in. diam sola

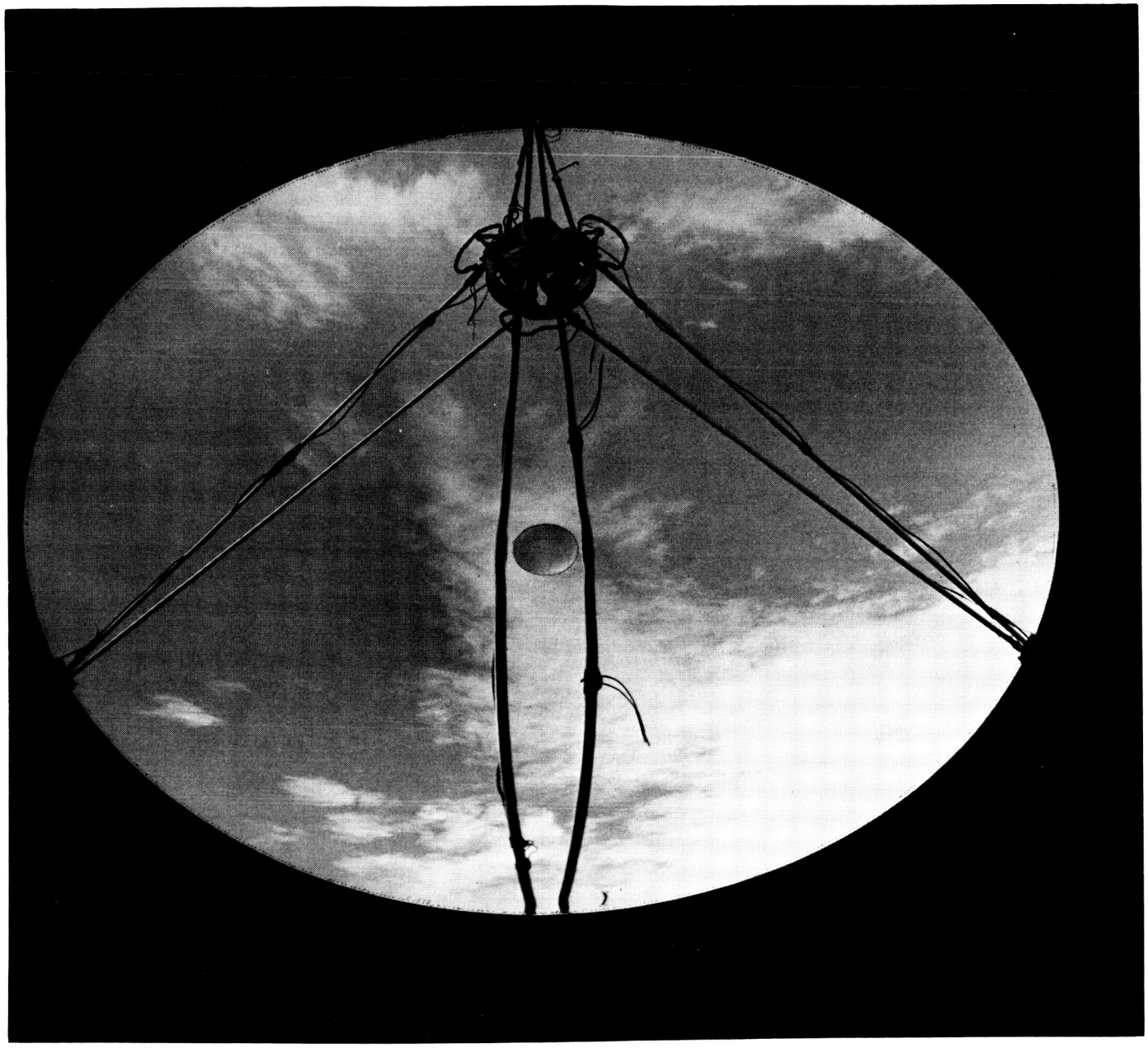

Fig 6. 50-in. solar concentrator with thermionic generator at the focal point

concentrator with a 60-deg rim angle which has successfully undergone seven vibration tests at the *Mariner Mars* type approval level. Although the one-piece concentrator is not the only collector being developed, it has reached a higher degree of development with the highest performance to date. The accurate focusing required for solar thermionic and solar dynamic systems is only available with the precise, one-piece, rigid collectors. Considerable effort is presently being expended to develop formed, inflatable and unfurlable petal concentrators to improve their performance. At the present they are competitive only in lighter weight and smaller storage volume. The one-piece concentrator is the heaviest of all types, due to its solid construction using nickel electroforming. Future development will reduce its weight 60% by using aluminum as the mirror surface. Figure 7 shows a one-piece, 9.5-ft diam concentrator now undergoing evaluation at JPL.

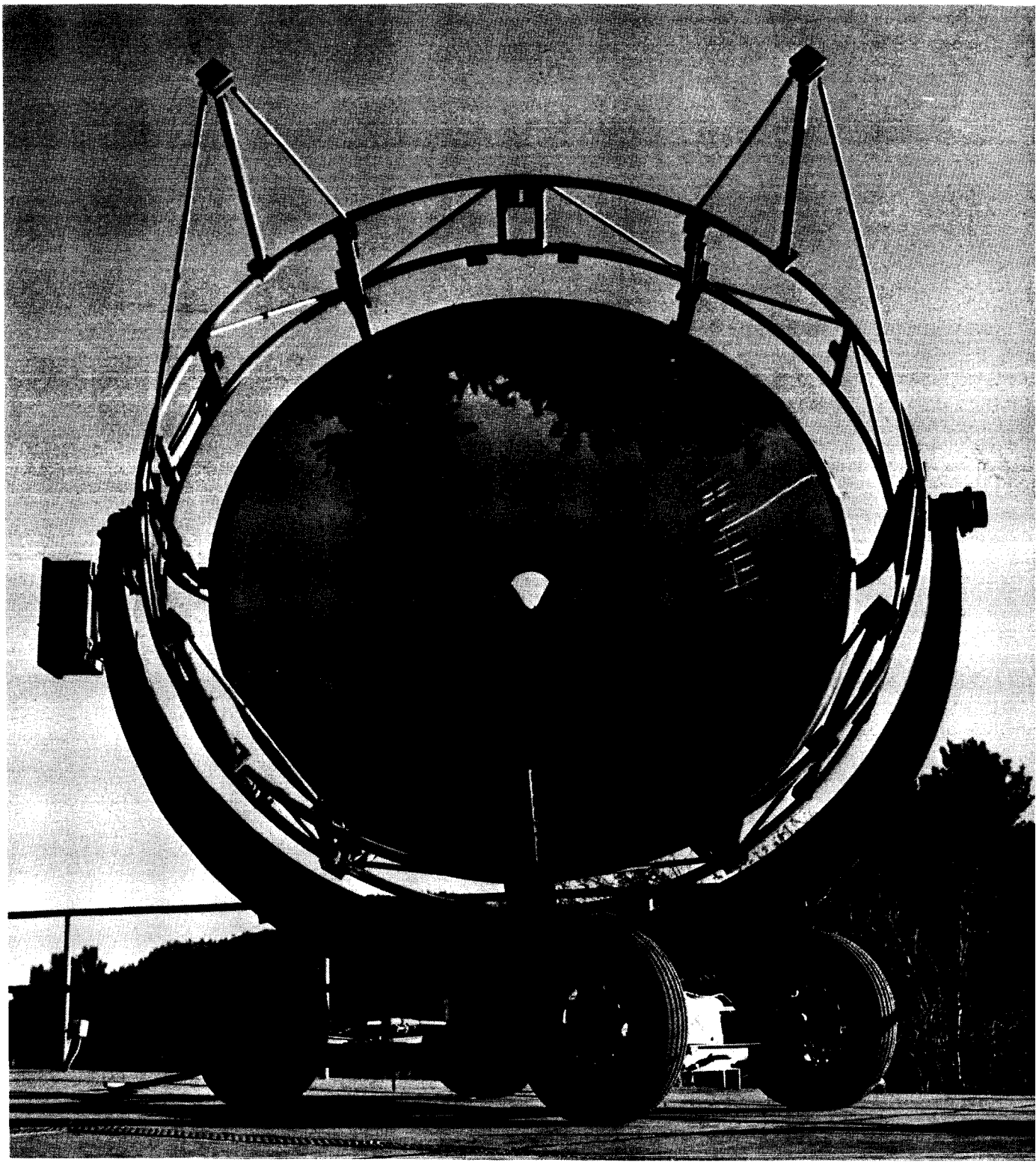

Fig. 7. 9.5-ft diam solar concentrator on portable mount

The conversion of thermal energy collected with the solar concentrator can take many forms: closed cycle turbine, thermionic, thermoelectric and regenerative fuel cell. In solar dynamic systems a collector focuses the solar flux into a cavity containing the working fluid. Rankine, Brayton or Sterling cycles are generally considered for such devices and their characteristics are discussed in the section on conversion devices (Section IV). In dynamic systems, the cycle selection must be based on an optimization of the collector size and the radiator surface area required to radiate the system waste heat. If the temperature of operation is low, a penalty is paid in radiator size, since the area is proportional to the fourth power of temperature. This area will increase rapidly at low temperatures. However, if the operating temperature is high, the collector area and mass increases, since the area is directly proportional to the thermal energy collected.

Solar thermoelectric systems can take two forms. Flat plate thermoelectric panels are manufactured in the form shown in Fig. 8. This is a lightweight, radiation resistant power source, which absorbs thermal energy through an optical coating on the collector surface. The heat is conducted through an aluminum foil to the element hot junction, through the thermoelements where part of the heat is converted to useful power, and the remainder is rejected to the element cold junction. Rejected heat is conducted away from the element cold junction and rejected to space by the radiating back panel surface. Test panels have been fabricated and tested on Air Force satellites with degraded performance being experienced. At this time, this type of solar panel cannot be considered because:

1. Inefficiency of optical coatings for temperatures of 200 to 250°C
2. Fabrication techniques are insufficient at this time
3. Efficient, reliable thermoelectric elements for low temperatures (100 to 200°C) are not available
4. Problems in erection, deployment and orientation require solutions
5. Thermal energy available at Mars aphelion would be so low a solar concentrator would be required introducing non-uniform heat flux problems
6. At Mars distance, this system is not competitive with solar cells

The concentrator-thermoelectric power system takes advantage of the higher temperature characteristics of thermoelectric materials now being fabricated. A parabolic concentrator is used to concentrate the incident solar flux on the heat absorber of a thermoelectric generator, located at the focal point of the solar collector. To date, several models have been made of this concept with limited success. The efficiency was found to be less than 4% and the specific energy was 2.3 w/lb with an insolation of 140 mw/cm^2. Considerable development in thermoelements is necessary to make this type system competitive with solar cells.

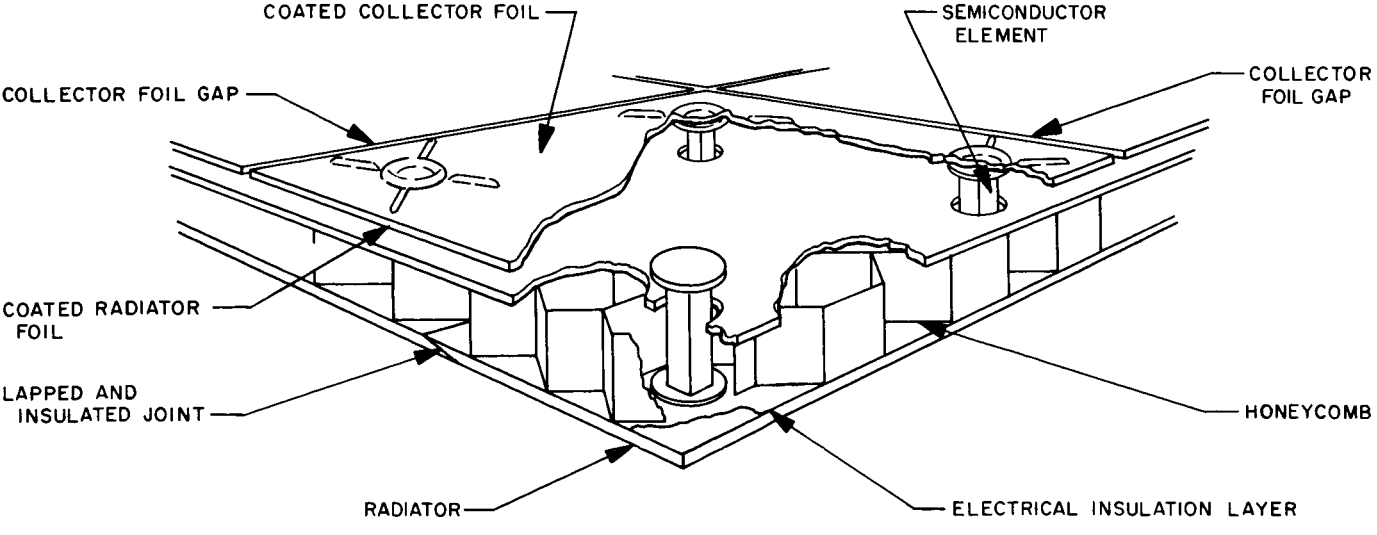

Fig. 8. Schematic of flat plate thermoelectric panel

Solar thermionic space generators have been the subject of intensive development for the past 5 yr, and are now at a point where actual flight data are all that is lacking. A thermionic generator consists of a number of cesium vapor thermionic converters, mounted with their heated surfaces directed toward the center of a cavity in which solar energy is focused by the concentrator (Fig. 6). The converter itself is basically an electron tube, which converts heat directly into electrical power by thermionic emission. Ground tests of these systems have yielded efficiencies of about 8%.

While the feasibility of these various systems has been demonstrated, additional improvements are required before they can be seriously considered for space applications as required for the landed capsule now under study. Two significant problems connected with the solar concentrator alone are serious enough to forestall their use on this type requirement.

The accuracy of orientation of the solar concentrator toward the Sun is a very significant parameter. Figure 9 shows the loss of thermal energy with increasing mis orientation of the concentrator to the normal Sun line As shown, solar cells are not affected by small angula errors and dynamic systems have lost only 10% of tota power with an error of 35 min of arc. Solar thermioni output, however, decreases rapidly for an error greate than 14 min of arc. The significant difference is due t the requirement for a smaller cavity aperture for th thermionic generator. Any error larger than shown i the Figure would cause the flux pattern at the collecto focal point to be too diffuse for efficient thermal absorp tion. An orientation error of one degree on the thermioni system would cause generator burnup, due to the con centrated energy impinging on converter piece parts no designed to withstand the thermal energy. A control sys tem is obviously required to control concentrator mis orientation by providing signals to align the collecto axis precisely to that of the Sun. For solar thermioni systems with a 1.0-in. cavity aperture, the maximun allowable misorientation would be ±14 min of arc, whic is within present state-of-the-art of attitude control sys tems, but add excess weight and complexity.

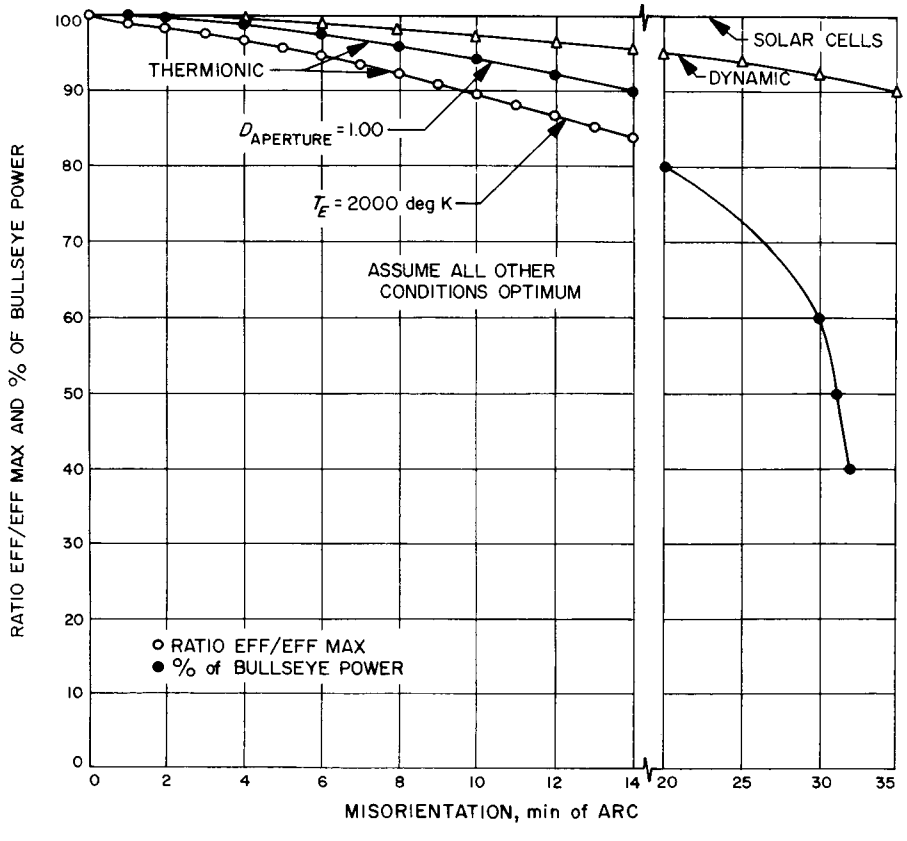

Fig. 9. Solar systems power degradation as a function of misorientation to the normal Sun line

The Martian surface environment reduces the effectiveness of solar concentrators and photovoltaic cells. Wind, sand and dust affect the surfaces of both concentrators and solar cell cover glasses. The reflective surface of a concentrator must be highly polished and geometrically accurate to obtain optimum efficiency. Collection of dust or pitting of the surface by high velocity sand particles would reduce the efficiency. Simulated micrometeorite tests performed at NASA Lewis Research Center on reflective surfaces indicates a loss of 35 to 70% of the reflectance at wavelengths between 0.2 and 1.0 μ. This range is particularly important, since 71% of the solar intensity concentrated by the collector is in this wavelength range. It is difficult to directly correlate this data to the effects which may be present on the Martian surface; however, this much degradation from particles of 2- to 14-μ diam (used by NASA LRC) would indicate that comparable damage could be expected from the larger particles on the surface of Mars. Additional concentrator problems occur from distortion of the reflective surface without extensive structural support to withstand impact.

There are substantial data to indicate solar concentrators used with both static and dynamic conversion techniques will be successful and extremely useful for both Earth and space vehicles in the near future. However, they cannot be fully established as practical at this time. The use of solar systems utilizing the intermediate thermal conversion step cannot be considered on the Capsule I configuration, because no attitude control is available for precise orientation of the solar concentrator. For Capsule II, landed operation cannot be considered, because of the expected surface environment as explained above and due to the added requirements imposed by the accuracy of Sun tracking. A simple sizing analysis can be performed for the cruise mode (D_2) of the Capsule II system. Table 9 is the projected performance data for solar thermionic power systems extrapolated from presently known data. These data can be used to obtain a relative sizing of a solar thermionic system for the Capsule II delivery system. The area of the concentrator must be sized to provide the thermal power required to operate the generator at the optimum temperature. This is determined by the following equation:

$$A_m = \frac{P_t}{\eta_{ca} I_s} \tag{25}$$

The thermal power input to the generator cavity P_t is determined by the output power required or

$$P_t = \frac{P_o}{\eta_g} \tag{26}$$

For a rim angle of 45 deg, the approximate concentrator diam is that of a circular cylinder or

$$d = \left(\frac{4}{\pi} A_m\right)^{1/2} \tag{27}$$

Table 9. Projected solar thermionic performance data

Factor	Solar concentrator									
	1966	1967	1968	1969	1970	1971	1972	1973	1974	1975
	Ni	Ni Al	Ni Al	Ni Al	Ni Al Be	Al Be Mg	Al Be Mg	Al Be Mg	Al Be Mg	Al Be Mg
Maximum diam, ft	9.5	9.5	9.5	15	15	15	15	15	15	15
Collector efficiency, %	70	75	75	75	75	75	75	75	80	80
Collector-absorber N_{c-a}, %	63	67.5	67.5	67.5	67.5	67.5	67.5	67.5	72	72
Collector density (11/ft^2)	1.0	0.8	0.8	0.6	0.6	0.5	0.5	0.5	0.5	0.5
Obscuration, %	5	4	4	3	3	3	3	3	2.5	2.5
Rim angle, deg	45 60	55	55	55	55	55	55	55	55	55
Max slope error (min of arc)	15	10	10	10	10	10	8	8	8	8
Converter and generators	—	—	—	—	—	—	—	—	—	—
Converter power density (w/cm^2) (S_p)	24	30	20[a]	20	20	20	20	20	25	25
Converter weight, lb	0.6	0.6	0.4	0.4	0.4	0.3	0.3	0.25	0.25	0.25
Generator efficiency, %	12	12	12	12	12	12	12	15	15	15

[a] See operating temperature.

Combining Eqs. (25) and (26) the diam is

$$d = \left(\frac{4}{\pi}\frac{P_o}{\eta_{c-a}\eta_g I_s}\right)^{1/2} \tag{28}$$

If the solar thermionic system is sized to provide an average cruise load of 126 w, the concentrator diam will be 6.7 ft and weigh 35.4 lb. The number of converters required to make up the generator as determined from Eq. (29) is 2.1.

$$\text{Number of converters} = \frac{P_o}{S_p A_e} \tag{29}$$

To satisfy this requirement and provide redundancy as well as utilization of the cavity area, 4 converters would be used as 2 parallel sets of two. The output voltage of this configuration would be 1.2 v, which is difficult to use without conversion. A battery required to supply peak power would require a capacity of 400 whr. The total weight of concentrator, generator, generator support structure and battery would be 62 lb. This does not consider the weight addition to attitude control for precise orientation or deployment mechanisms to deploy the concentrator.

2. Solar Cells

Photovoltaic cells, which provide direct conversion of solar radiation into electrical power, have become the most reliable type of power system in use today for space applications. Long life satellites and planet probe spacecraft have been almost exclusively dependent upon the solar cell for power. Solar cell systems have progressed rapidly from small devices providing low power outputs to large arrays of cells such as the solar panels used on *Ranger* and *Mariner Mars*. The *Mariner* spacecraft uses 70.4 ft^2 of solar panel area to produce a power output of 680 w.[3] Future developments anticipate a growth to power levels in kw with cells which can be packaged in rolls and unfurled like window shades.

Solar cells, in various configurations, are ideally suited to provide spacecraft power and, even with no improvements, will probably continue to be the most used power device on satellites and spacecraft for the next 5 or 10 years. While development efforts were applied with specific emphasis on silicon materials for cell fabrication, other materials are now being developed which, having a higher theoretical efficiency, should produce highe levels with no increase in cell area or weight.

Development of silicon cells is also being pursued t provide increases in efficiency and power handling capa bility and decreases in the cell weight. The ultimate powe density of solar cell arrays is now considered to b 20 w/lb. Presently, the *Mariner Mars* has a value c 9.6 w/lb, at one astronomical unit (AU), which is the bes that has been flown to date. Major improvements ar required in the mechanical area primarily in the structur hinging and packing of solar cells. Additional improve ment can be achieved by improving the temperatur characteristics of solar cells and by using thinner cells.

Efficiency of current bare silicon cells is approximatel 12%. In the past the P on N silicon cell has been th cell used on satellites and spacecraft. The newer N on P cells, having comparable performance to the older type have been found to be superior to P on N in resistanc to radiation effects. It is for this reason that futur applications of silicon cells will utilize the N on P cel almost exclusively. Since the silicon cell has been devel oped, much has been learned about its characteristic and most engineers feel that very little can be done t improve upon this type. However, continual develop ment is being directed toward reduction of temperatur gradients within the cells. Because the cell efficienc decreases with increase in cell temperature, a decreas in cell absorptivity of infrared radiation would decreas the cell temperature; and therefore increase its outpu power. Any expected increase will be minimal, an therefore, research is in progress on other cell material such as gallium arsenide, cadmium sulfide and gallium telluride.

Gallium arsenide has been produced in limited quan tities with efficiencies between 8 and 9%. A few cell have attained 11% at air mass one. The temperature an radiation resistances of this cell, compared to silicon, ar much better and the theoretical efficiency is much highe This indicates much better performance can be expected but this has not been proven to date. The present stat of development of this and the other cell material indicates they do not warrant further consideration a this time. Therefore, this Report will be confined to th fully developed silicon solar cell.

Up to the present time, cell thickness has been main tained between 18 to 22 mils. The *Mariner Mars* uses cell of 20-mil thickness. This was generally though necessary for strength considerations in cell processin

[3]Measured at a solar intensity of 130 w/ft^2 and a temperature of 55°C.

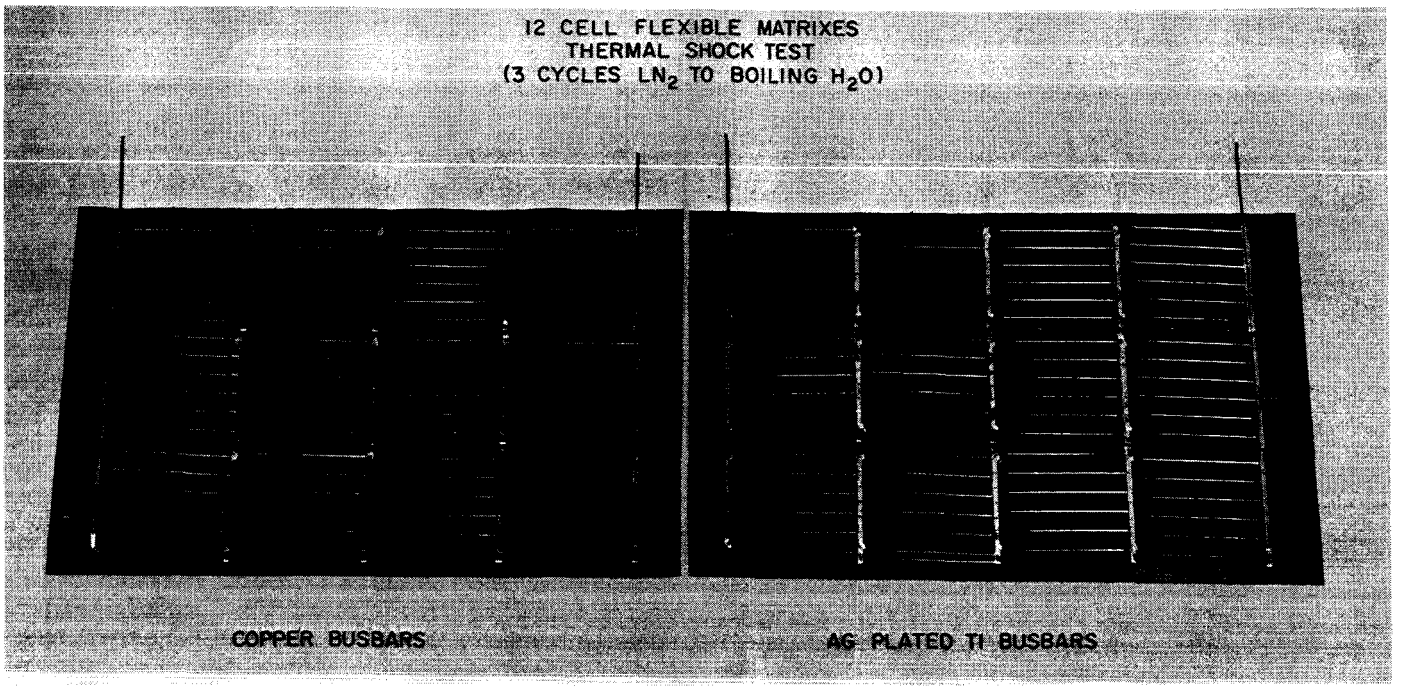

Fig. 10. N on P silicon solar cells, 8-mils thick, mounted on a flexible substrate

and handling. Advances in technology have made the cutting of thinner slices of silicon practical and breakage has been reduced by development of handling procedures. Because of this, the trend is toward the development of thinner solar cells from 8 to 14-mils thick. This represents a weight reduction of 35 to 55% for cells. Figure 10 illustrates two 12 cell, N on P silicon solar cell modules. The cells are 8-mils thick and are mounted on a flexible substrate. These cells are now undergoing tests at JPL to determine their performance characteristics. The photograph shows the results of thermal shock tests and their effect on cells connected using copper and silver plated busbars. The results indicate that silver plated busbars reduce the cell damage produced by thermal shock. Figure 11 indicates the variation in cell performance for the three types of silicon cells as a function of Sun probe distance. Although the 8-mil cells have a reduced specific energy over the other cells, the fact that they are 60% lighter in weight may be significant in their selection for future spacecraft power systems.

Solar cells have distinct limitations, which must be considered before their selection for a particular mission. These are:

1. Sensitivity to damage by radiation
2. Unusability during dark periods, thus requiring energy storage
3. High cost
4. Sensitivity to physical damage from manufacture, handling and operational environment

A transparent cover glass is placed on each solar cell, that is spectrally selective, to reduce the absorption of infrared radiation, which reduces the temperature buildup within the cell. The cover glass also protects the cell from damage by hard particle radiation and from erosion by micrometeorites. In the past, a thickness of 6 mils was thought to be a practical minimum for protection of the cells. Recent studies have indicated the cover thickness will have to be increased to 20 mils to protect solar panels on a Mars transit from the effects of solar flare protons. This will, of course, reduce the specific energy of the panels considerably. The use of the thin N on P cell would appear to offset this decrease slightly. The requirement for the thicker cover glass on solar cells used on a capsule will be dependent upon the design of the panel configuration. If the cells are exposed to solar radiation during the entire transit period to Mars, the thicker cover glass will be required. If the panel configuration is such that exposure does not occur until capsule separation, it is unlikely the protection will be required. Should the thicker cover glass be required, a decrease in the cell efficiency can be expected from increased diffraction within the glass as well as a decrease

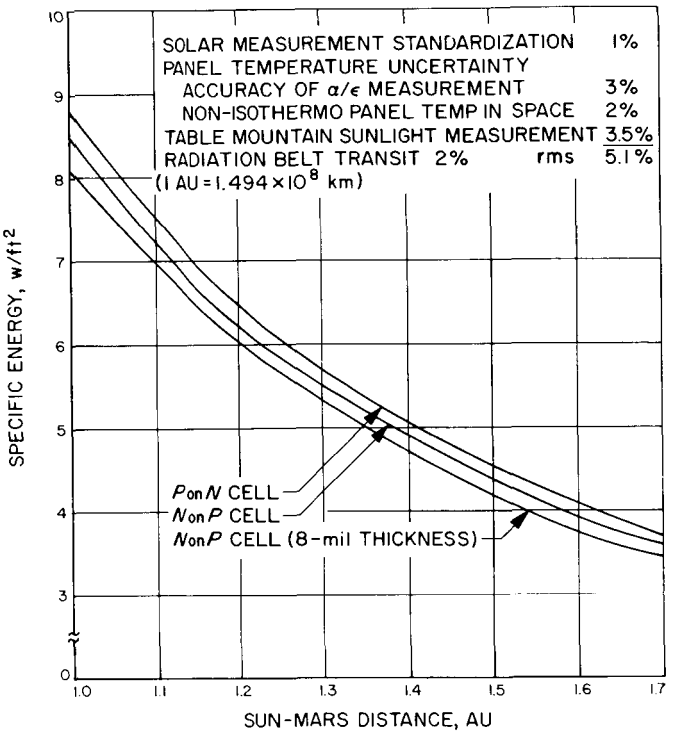

Fig. 11. Solar cell specific energy as a function of distance from the Sun

in transmission of light to the cell because of the adhesive required to hold the cover glass.

To determine the desirability of using solar cells for a capsule transit after separation from the main spacecraft and for use on a landed system, several factors must be considered before and during system design. The power output of solar cells vary directly with the cosine of the angle of incidence of illumination. Hence, orientation of the panels within a few degrees is desirable for maintaining constant power. A capsule in transit can, however, have cells affixed to the surface of the capsule so that essentially constant power is delivered to the load regardless of orientation with respect to the Sun. However, the number of cells used in an unoriented system for a given power load will be much greater than for an oriented system, since only a small portion of the cells would be effectively producing power.

For landed operation several other factors are also significant. Silicon cells are extremely brittle and only small strains are tolerable. For this reason, design of a landed system of solar cells is difficult, because impact levels exceed any previous stresses ever applied to cells. Methods are being investigated to insure survival, but it is doubtful a design can be achieved which stays within the constraints of capsule design as now conceived. Se ondly, the Martian environment is essentially hostile t solar cell use. As pointed out earlier, the atmosphere su rounding Mars presents an attenuating medium, whic will reduce the power output of the solar cell array b 25%. In addition, temperature effects on the surface wi cause further reductions in the cell output even for a Su oriented array. For the *Mariner Mars* spacecraft the sol panel temperature at Mars encounter has been estimate to be −10°C maximum. The same array operating on th surface of Mars would have (assuming the surface ten perature is the same as the array temperature) a temper ture of +10°C. This also assumes no convection coolin which may be present due to winds prevailing near th surface.

The Mars encounter maximum power from th *Mariner IV* solar panels is estimated at 4.5 w/ft² an 4.5 w/lb (at −10°C). The Mars surface operation fo solar illumination normal to the array and the Martia surface is, therefore,

$$(0.75)\,(0.90)\,(4.5\ \text{w/ft}^2) = 3.0\ \text{w/ft}^2$$

and 3.0 w/lb. The factor 0.90 derives from a temperatur power loss of 0.5%/°C. Lightweight arrays now und development by the power sources group may achiev 6.0 w/lb and 3.0 w/ft² on the surface of Mars.

In addition, physical damage to the cells may occur a a result of dust storms on the planet's surface. It is n known at this time what damage can be sustained by th cells. Surface erosion of the cell cover glass, pitting o scratches would reduce the amount of illumination t the cell. A more likely consequence would be the sed mentation of fine dust particles on the cell surface, th movement of wind and dust and the resultant buildu of a static charge across a panel surface increasing th dust collection. Experiments to evaluate these effec should be performed under simulated conditions to d termine the exact nature of the problem. Such experimen could show that particles of sizes and/or velocities great than those believed to exist on Mars are necessary to cau significant performance degradation.

3. Capsule Solar Panel Design

Design of capsules using solar panels as the prima source of power would be done in the same manner with previous systems. However, because the design f the delivery systems for Capsules I and II are similar, th will be discussed together, as will the landed operation It is unlikely that the panels used during the crui

operation could also be used for landed operations, since the planet entry and impact constraints could not be met by unfurled or deployed solar arrays.

a. Capsule delivery system design. The most significant difference in the Capsule I delivery system, D_1, as opposed to that of Capsule II (D_2) is that it has no Sun orientation. Because the body is randomly oriented, a sufficient solar cell area must be provided to give an equivalent area of illuminated surface to supply the required power. Figure 12 shows the 16-ft-*Apollo* configuration of a capsule with several mounting positions for the solar cells. The most troublesome orientation is with the Sun normal to the heat shield. To provide power for this case, either separate panels must be used or the cells must be mounted directly on the heat shield. Although the panels could be dropped before entry or left on to burn up in the atmosphere, and the cells could burn off the heat shield at entry, either solution would complicate the mechanical and aerodynamic problems. The total cell area required for an unoriented capsule would be 3.7 times that required with constant insolation of a Sun normal to the solar cells.

For both delivery systems, the panel will be sized to provide the power required during the long duration coast to entry phase. A battery will be required to provide peak and entry power in the case of D_1 and for D_2 the battery provides peak, entry, and maneuver power. For D_1 the solar panels must supply 19 w. From Fig. 11 at a Sun–Mars distance of 1.5AU a specific energy of 4.4 w/ft² can be assumed and the total required panel area is thus 5.2 ft² providing a 20% allowance for degradation.

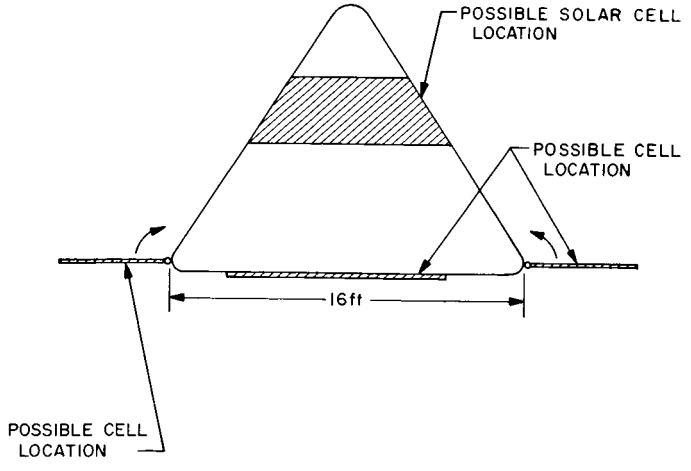

Fig. 12. *Apollo* configuration with possible solar cell locations

Because the cells are unoriented, the total area requirement is 19.5 ft². At approximately 0.45 lb/ft² for the solar cells, excluding any structural material necessitated by adding the cells, a solar cell weight of 8.7 lb would result. A battery with a capacity of 50 whr weighing 2.5 lb would be adequate. In practice, the battery would probably weigh more than shown due to the larger fraction of the total weight needed for the battery case. The total power source weight is therefore 11.2 lb.

For the Capsule II system, since Sun orientation is maintained, the solar cell area would be 34.4 ft² to provide a cruise power of 126 w. If the cells are mounted on the *Apollo* body, at a 33 deg angle to the Sun, the required solar area would increase to 63 ft². For the worst area case, with the cells mounted on the *Apollo* body, the total cell weight would be 28.4 lb. The required battery capacity and weight would be 400 whr and 20 lb, respectively.

b. Capsule landed system design. As in part *a*, the landed systems design is similar in all but one respect. For the Capsule II landed system, the operational time required on the surface has a profound effect on system sizing. Because this is greater than a few days, a secondary battery would be required, which not only effects the battery size, but also the overcapacity required from the solar cells to recharge the battery during the periods of sunlight. A power systems analysis for landed operation of a photovoltaic system has been performed and appears in Appendix A.

The analysis was performed for an asynchronously-loaded solar cell power system. Although the analysis does not consider the effects of battery sterilization as pointed out in Section III-A-3, it remains valid but somewhat optimistic in battery size. The following major conclusions from the analysis were reached:

1. A solar array for a Mars equatorial lander must be sized for peak load (active communication) period during eclipse.

2. A battery for a Mars equatorial lander must be sized for peak load period during eclipse, but increased by charge rate limitations imposed by peak load during sunlight.

3. Effective solar array specific weight is approximately 0.44 lb/w, due to angle of incidence of solar insolation, atmospheric attenuation, and shape of $P_g(\phi)$ function.

4. Effective battery specific weight is approximately 14 to 23 whr/lb (at 100% depth of discharge) due to charge rate limitation and temperature (for the AgCd battery assumed).

For the survival system (S) of Capsule I, solar panel use is doubtful. Since there is no provision for Sun orientation on this capsule, it would be difficult to provide the panel area which would be required to reduce the size battery as shown in Table 7. Addition of an erection and Sun orientation system to this capsule to provide the peak communications power (40 w) from solar panels, would reduce the battery weight by 60%. However, the erection system would be attributed to the power system from a weight standpoint and the overall reduction in weight would be approximately 16% or 3 lb. Therefore, surface environment and minimum system improvement by use of solar cells are sufficient criteria to preclude their use on this system.

The landed systems for Capsule II (L_1 and L_2) are similar and differ only in the length of operating time. This has no effect on the basic sizing of the solar panel system other than perhaps the battery. To do a system sizing, several assumptions need to be made as pointed out in Appendix A. It is assumed that the Martian dark period is no greater than its daylight period for the length of landed operation. It is further assumed, half of the communication period or peak load occurs during the dark period. This is based on the desirable condition of the science gathering occurring during equal portions of day and night. The significance of the assumption is that the solar panel must be sized larger to provide an overcapacity (μ_R) to recharge the secondary battery used to provide power for night operations.

Therefore, from Appendix A:

$\alpha = 0.5$ and $K = 0.5$ (see Appendix A, Fig. A-1)

$T_e = \alpha T_o = 0.5\,(24.62) = 12.31$ hr

$\phi = T_p/T_o = 8/24.62 = 0.325$

$\delta P = P_p/P_1 - 1 = (159/46) - 1 = 2.46$

from Eq. (A-5), $\phi_T = 0.06$ which is less than ϕ, and therefore, Eq. (A-4) is used to determine the panel overcapacity due to battery recharge requirements.

$$\mu_R = \frac{\alpha + \phi\delta P\,[h + k(1-h)]}{h(1-\alpha)} = 4.4$$

and

$$\mu_R = P_g/R - 1 \text{ or } P_g = P_1\,(\mu_R + 1)$$

Therefore, the source power $P_g = 46\,(5.4) = 248$ w. This is the power required from the solar panels during sunlight operation to supply the load and recharge the battery.

In Appendix A, Eq. (A-9) is used to determine the specific weight of the solar panels at a Sun–Mars distance of 1.55 AU. The value of 0.22 lb/w given is typical for a panel such as used on the *Mariner Mars* flyby and includes structural weight of the panel. However, in this case a structural weight which is heavier must be assumed for impact requirements. The value of 0.105 lb/w is directly attributable to the solar cells. A specific weight of 1 lb/ft² is assumed for panel structures which is approximately twice that of the *Mariner* structures. In addition, a landed capsule would experience a decrease in solar insolation after 6 mo of operation and if landed at 1.55 AU, the Sun–Mars distance would increase to 1.67 AU by end of life and the specific weight would, therefore, increase to 0.1465 lb/w excluding structures.

An error of ±5 deg in alignment of the solar panels to the Sun normal is assumed; the attitude control system requirements are thus eased although this error will normally be no greater than ±1 deg. Therefore, from Eq. (A-9)

$$a_g = 0.1465 \sec 10 \text{ deg } (0.75)^{-\sec 10 \text{ deg}} \text{ lb/w}$$

$$= 0.1835 \text{ lb/w}$$

the solar cell weight: $W_s = a_g P_g = 45.5$ lb

The specific energy of N on P cells at 1.67 AU from Fig. 11 and the equation

$$S_e = 3.7\,(0.9) \cos 10 \text{ deg } (0.75)^{\sec 10 \text{ deg}}$$

$$= 2.46 \text{ w/ft}^2$$

the panel area is $A_p = P_g/S_e = 101$ ft². Assuming a structural weight of 1 lb/ft² for the solar panels they would weigh 101 lb.

The secondary battery must be sized to provide the energy for the system during dark periods. To insure a cycle life with a minimum of 200 cycles, the depth of discharge d should not exceed 50% of the total battery

capacity (AgZn battery). Allowing 20% for degradation, the battery capacity would be

$$E_R = 1.2 \frac{P_1}{d} T_o (\alpha + k\phi\, \delta P) = 2450 \text{ whr}$$

and would weigh 163 lb. The total weight of the system would be 310 lb.

4. Conclusion

Solar dynamic, thermionic and thermoelectric systems are not developed sufficiently at this time to demonstrate reliable and efficient operation at the power levels of interest here. They also suffer significant penalties from mechanical constraints such as articulation of the solar concentrator, impact survival, flux control and surface environment. At this time the concentrator alone represents a major development problem for applications proposed here.

Solar thermionic systems can be made available and may also appear acceptable from a weight, volume and cost standpoint. However, flight experience, operating life, correlation of ground test data to space flight, reliability and spacecraft compatibility have not been demonstrated. Reduction in the solar constant in transits away from the Sun are not compatible with this system's requirement for high temperature for efficient operation. Serious consideration must be given for using this system for high power levels and for operation on spacecraft near the Sun. Its usefulness for outer planet probes and surface operation on these planets is reduced by the lower solar insolation, requirements for accurate alignment and the possible planet environment it may encounter. Crossovers between the use of solar thermionic and photovoltaics, on a weight basis alone, depend considerably on the power levels with photovoltaics appearing more favorable at the low power levels.

Solar cells will continue to play a dominant role in spacecraft design for transit and orbital missions. Of all the power systems which use solar energy for conversion to electrical power, solar cells alone can be designed and integrated into a spacecraft with ease. Although they have demonstrated their usefulness in space and in Earth orbits, operation on a foreign surface such as Mars is doubtful due to mechanical design constraints and expected surface conditions. Sterilization of solar systems does not represent a problem and has been demonstrated on solar panels. However, surface operation is limited by the planet's diurnal period. Because solar cells are Sun dependent, energy storage must be incorporated in the system design for any night operation. This imposes additional constraints on the solar panels where long life must be obtained, to adequately recharge the battery.

Thin solar cells may offer a weight saving on future spacecraft but additional tests and analysis must be performed to improve electrical characteristics. Significant improvements have been made in other solar cell materials such as thin film cadmium-sulfide. Their efficiencies, however, are still too low in mass lots to be considered in solar panel designs. Silicon N on P cells are the only type to be considered at this time because of their high efficiency and resistance to hard radiation in the space environment. Therefore, solar panels using silicon N on P photovoltaic cells appear satisfactory for transit vehicles in space, but are not recommended for Mars surface use without proof of surface conditions more favorable than now assumed.

C. *Nuclear Sources*

Nuclear sources provide energy in the form of heat, either by the fission process, as obtained in a nuclear reactor, or by the decay of a radioactive isotope (radioisotope). The thermal energy, thus obtained, can be converted to electric power by either static or dynamic conversion devices. The relatively high energy content and life of the nuclear sources make them extremely attractive for long life space missions. Even for missions of several months duration, only nuclear and solar systems can be considered. Chemical sources including batteries must be eliminated due to the fuel requirements and the associated weight.

In nuclear reactors, energy is obtained by neutron induced fission of uranium in which approximately 85% of the energy appears as kinetic energy of the fission fragments. The heat generated in the reactor core is transported away from the core by a liquid coolant loop to a suitable conversion device, whereby, the heat is partially converted to electrical power and the remainder rejected by radiation.

Radioisotopes release heat by the spontaneous decay of the isotope, in which radiations emanating from the radioactive material are absorbed within the source and container, releasing their kinetic energy in the form of heat. Although the heat produced by the isotope can be carried off by a coolant loop for dynamic conversion, it is more convenient and less complex to locate the conversion device close to the radioisotope container.

The major advantages of nuclear energy sources are:

1. Long life
2. Continuous power which is accurately predictable
3. Insensitivity to external environment
4. High power per unit area
5. Requires no specific orientation
6. The available thermal energy is independent of the operating temperature
7. Mass of fuel required is dependent upon the power required and not the total energy to be supplied
8. No energy storage is required on a system (optimization may dictate energy storage)
9. Ruggedness of design

Nuclear sources are not without disadvantages. Although there are few, they are so significant that mission requirements may very well dictate the selection of another source. They are:

1. Radiation hazard to equipment, science and personnel. The level of radiation flux emitted from a nuclear source places stringent constraints on the design of the power system itself to provide adequate safety during launch and the life of the mission. In addition, requirements for safe handling on the ground and design of the vehicle to provide installation without damage to the vehicle or its components during the mission life are required.
2. Materials problems due to radiation, thermal stress and high operating temperatures.
3. Thermal control and heat rejection on a vehicle with nuclear systems becomes more complex.

1. Nuclear Reactor

The power available from the fission products in a nuclear reactor cannot be duplicated by any other power source in existence today. For high power, long operational life power systems, reactors are the most promising for future space operations. However, the mass of a reactor and the associated shielding necessary to reduce the large neutron flux from the reactor makes it impossible for it to compete with other power systems at low power levels.

Although the enriched uranium fuel required to obtain the needed thermal energy is extremely small, there is a necessary critical mass of the fissile material required to maintain the fission process within the reactor. This is a consequence of the reactor being neutron physics, rather than heat transfer limited, and results in a reactor core weight which is essentially independent of the power level. Therefore, the specific weight of very small power plants would be quite high. As an example, since approximately 200 Mev total energy is released per fission of U^{235}, there are 3.12×10^{10} fissions/sec-w. The mass of U^{235} needed to produce X thermal w/day is $1.05 \times 10^{-6} X$ g. For 5 kw of thermal energy, this would mean a requirement for 5 mg of U^{235} for each day of operation or a total of 2 g for 1 yr at the above power level. This is well below the mass required for criticality of the reactor fission process. Low power reactors currently being developed are designed for operation below the level where fuel loadings are in excess of the critical mass, and thus, can supply any level of thermal power that a power plant requires without needing additional fuel.

The major nuclear reactor development for space power is being carried out in the AEC SNAP (Systems for Nuclear Auxiliary Power) programs. Several types of reactors capable of a wide range of thermal power and core temperatures have reached varying stages of development, including the launch and partial success of the SNAP-10A system. At the present time, the SNAP-2/10A unit is the only reactor of any interest for a landed system. However, the SNAP-2/10A reactor represents the smallest physical size reactor obtainable. The lower power requirements of the landed system defined in this study could not reduce this size appreciably, but may indeed increase it to provide reliable control and cooling in deep space. The weight, therefore, would be approximately 450 lb for the reactor and its associated systems, but excluding shielding.

In addition, the radiation from the reactor is far more severe than that from a radio isotope of an equivalent thermal power. This is due to the excessive neutron flux and gamma radiation emitted in the fission process. The shield weight would be determined by the allowable dose levels for the scientific experiments and the most sensitive components integrated over the mission life. Other factors are: (1) separation distance of reactor from rest of capsule equipment, (2) geometric design of the shield, and (3) scattering variations. This would lead to a shield weight of 200 to 700 lb. It is apparent weights of this magnitude could not be made available for a capsule power system, and therefore, nuclear reactors are not the logical source of power for low level operation.

2. Radioisotope Power Sources

Compared with nuclear reactors, radioisotope heat sources are relatively low in power output per unit mass,

and are thus, constrained to more modest power level requirements. At low power, radioisotopes can provide the most compact source of thermal energy available today. This is due in part to the fact that the thermal energy produced by the particle emission of the decay process, occurs at a constant, predetermined rate. Existing power systems in the SNAP space program, utilizing nuclides, have power levels of less than 25 w electrical and use static conversion techniques. However, the first SNAP generator, the SNAP-1, used dynamic conversion in the form of a mercury rankine cycle turboalternator. This unit was cancelled before tests were complete and the unit fueled. Dynamic conversion techniques are again being studied for applications at power levels above 1 kw electrical. The expected lifetime of a radioisotope power source is dependent, in part, on the isotope used as the fuel. Units have been built for mission life times of 90 days to 5 yr and could, with long half-life fuels be extended to longer periods. Two navigational satellites, launched in 1963 utilizing Pu-238 fueled thermoelectric generators (RTG), are still operational.

When a radioisotope decays spontaneously to a more stable element, it emits energetic particles or photons in the process. Each decay results in the liberation of energy, which is mainly contained in the emitted particles and photons in the form of kinetic energy. Collisions of these particles within the fuel and container releases this energy and slows the particle. The principle types of particles emitted are α-particles, β-particles and γ-radiation; in general radioisotopes are either α-emitters, β-emitters or γ-emitters.

Alpha-particles are energetic helium nuclei, which are emitted at discrete energy levels having a range of $\sim$1 to 10 cm in air depending on their energies. Thus, an α-emitting radioisotope contained within a thin container, will have the majority of the α-particles absorbed within the isotope itself, and only those produced at the surface will escape to be absorbed by the container. All the energy of decay is available as thermal energy. When the α-particle is absorbed, it captures two electrons and evolves as helium gas. For this reason, void spaces must be left in α-emitting generator containers to contain this gas. In practice, the void space may be made equal to or greater than the volume of the isotopic material. Because the α-particles are absorbed within the fuel and container, it would appear that no radiation hazard exists with this type material. Unfortunately, neutrons are emitted from collisions with the α-particles and from the spontaneous fission process. In addition, γ-radiation can also be emitted when the α-particle does not release its total energy and must decay to the zero energy level. Radioisotopes emitting α-particles generally have higher power densities than those produced by β-emitters and generally less radiation effects than that of β-fuels. They are, however, more expensive to produce since β-emitters are produced as waste products of the fission reactor; α-emitters are produced by irradiation of another isotope.

Beta-particles are electrons with velocities approaching that of light and are emitted in a broad spectrum of energies. Because of this high energy, the β-particle is more penetrating than α-particles and have a range of $\sim$50 to 1500 cm in air, again depending on the energy. The deflection of β-particles from their path by nuclei give rise to a continuous x-ray spectrum known as *Bremsstrahlung*. This radiation has an intensity roughly proportional to the square of the atomic number of the nucleus and to the energy of the β-particle. Because of the higher penetration power of the β-particle, a higher proportion of them will escape from the radioisotope to be absorbed by the container wall and generator proper. This means the container thickness must be greater than in the case of the α-emitters and energy will be lost by the production of *Bremsstrahlung*. When the β-particles are absorbed, they also give rise to parasitic γ-radiation.

Gamma-radiation is electromagnetic radiation, which accompanies nuclear transitions, and the photons emitted have energies which are characteristic of the isotopes and the energy level transcended. The absorption of this radiation occurs by various mechanisms, whereby, the photon energy is dissipated. High density material provides the greatest attenuation. However, the penetration power is much greater for γ-radiation than for α-particles or β-particles requiring heavy shielding for absorption. This produces a decrease in the energy absorbed per unit volume, reducing the number of applications of γ-emitting radioisotopes.

Each specific radioisotope has its own characteristic values of rate of decay, spectrum of identity, and intensity of emitted radiation. The power available depends on the decay scheme and the rate of decay which, unlike nuclear fission, is not capable of control but decays exponentially at a rate characteristic of the particular isotope. This decay process is independent of temperature, density, concentration, radiation, etc. It is governed by an exponential law relating the number of atoms present to the number originally present. Since each atom produces a characteristic specific energy during the decay, the energy at any time can be determined by

$$P_t = P_o e^{-\lambda t} \tag{30}$$

where P_t is the thermal power available at time t, and P_o is the original power available. Gamma is the radioactive decay constant and represents the time for the activity of the isotope to be reduced to one half its original value.

$$\lambda = \frac{\ln 2}{T_{1/2}} = \frac{0.6931}{T_{1/2}} \tag{31}$$

From Eq. (30), it can be seen that the initial specific power is largely determined by the half-life of the selected radioisotope. The significance of this fact can be seen in the initial selection of a high power density nuclide, Table 10. A short half-life is a result, and for short missions this leads to better utilization of a costly and hard to obtain fuel. On the other hand, for a long mission this may lead to the requirement for a fuel overloading to compensate for the short half-life, Table 11. This would lead to the requirement for providing a method to *dump* the initial excess energy available (power flattening).

The essential trade-offs in selection of a nuclide then are in the half-life, power density and problems caused by the decay process. In addition, cost, safety, fuel availability and required shielding must be considered before a fuel is selected.

All but a few of the more than 1000 nuclides can be eliminated from consideration by excluding all that have half-lives of less than 100 days and power densities of less than 0.1 w/g. This arbitrary limit ensures a practical energy source mass and a reasonable half-life, that must be considered in the design because of manufacture, processing, encapsulating, testing, shipping and installation time, in addition to actual operational time. In addition, some fuels may require aging to remove daughter nuclides which contaminate the fuel source and produce excessive radiation. By setting the above limits, the fuels are limited to those in Table 10. Applying the criteria for minimum λ and *Bremsstrahlung* radiation, reduces the selection to the last five in the table, namely Pm-147, Po-210, Pu-238, Cm-242 and Cm-244.

The remaining five radioisotopes provide a wide choice of half-lives and power densities as well as radiation hazards. The selection of any one is more difficult and each must be considered in light of the mission criteria, to determine which is optimum. Of the five, four are α-emitters which are produced in reactors by irradiation of heavy elements. Since α-emitters have energy ranges of 5 to 7 Mev and most of the energy released by the α-particles is usable in the form of heat, they permit higher thermal power densities than do β-emitters or γ-emitters. Promethium-147, the only β-emitter which could be used for the landed operation, suffers from some difficulties which negate its usefulness on missions of 1 yr or greater. As can be seen in Table 11, this nuclide produces a larger generator because of weight and volume requirement for the fuel. In addition, γ-radiation would be quite severe. Primarily, the low power density and high γ-radiation are due to the high impurity of the radioisotope. A consequence of this is a long storage life after the production process to allow the decay of the shorter half-life impurities. This implies a larger quantity of fuel must be processed, due to the short half-life of this fuel. Because of the preceding evaluation, Pm-147 will be eliminated as a potential source of thermal energy for this study.

Of the four remaining radioisotopes, Po-210 and Cm-242 would appear from Table 11 to provide a smaller generator than either the Pu-238 or Cm-244 long-life isotopes.

Table 10. Characteristics of radioisotope heat sources

Isotope	Co-60	Sr-90	Ce-144	Th-228	U-232	Pm-147	Po-210	Pu-238	Cm-242	Cm-244
Specific energy (pure), w/g	17.4	0.95	25.6	170	4.4	0.33	141	0.56	120	2.8
Half-life, yr	5.3	28	0.78	1.9	74	2.7	0.38	86.4	0.45	18
Estimated isotopic purity, %	10	50	18	95	85	95	95	80	90	90
Compound form	Metal	$SrTiO_3$	CeO_2	ThO_2	UO_2	Pm_2O_3	Metal	PuO_2	Cm_2O_3	Cm_2O_3
Active isotope in compound, %	10	24	15	83	75	82	95	70	82	82
Specific energy (compound), w/g	1.7	0.23	3.8	141	3.3	0.27	134	0.39	98	2.3
Density (compound), g/cc	8.9	4.6	6.4	9	10	6.6	9.3	10	11.75	11.75
Power density (compound), w/cc	15.5	1.05	24.5	1270	33	1.8	1210	3.9	1150	27
Radiation	β, γ	β	β, γ	α	α	β	α	α	α	α
Shielding required	Heavy	Heavy	Heavy	Heavy	Heavy	Minor	Minor	Minor	Minor	Minor
Curies/g (pure)	1130	142	3180	4100	114	914	4500	17	3310	84
Curies/w	65	150	124	24	26	2770	32	30	28	30
Melting point, °C	1495	1900	2680	3200	2750	2350	254	2300	1500	1500

Table 11. Summary of isotope requirements

(η_T = 4%) (t = 1.4 yr) (P_o = 165 w) (P_t = 165/0.04 = 4,130 w)

Isotope	Pm-147	Po-210	Pu-238	Cm-242	Cm-244
Initial fuel, w	5,920	49,350	4,170	34,850	4,350
Mass, g	21,900	368	10,700	356	1,890
Volume, cm³	12,200	39.6	1,070	30.3	161
Curies	1.98×10^7	1.65×10^6	1.18×10^5	1.02×10^6	1.34×10^5
γ-Dose Rate @ 100 cm, rad/hr	5×10^4	10	0.005	1.5	0.5
Neutron-Dose Rate @ 100 cm, mrep/hr	—	~15	25	2×10^3	10^3
~Cost \$ × 10^6	1.98	9.8	4.53	4.9	3.9
Availability 1970[a], c/yr × 10^6	11.6	—	46 kg	0.15	20 kg

[a] Dependent upon user requests.

However, the required initial fuel inventory to ensure efficient operation of the generator at end of life would be in excess of eight times that required at the end of 1.4 yr. The excess heat from this fuel must be removed or shunted around the conversion device to prevent the generator from reaching critical temperatures. The problems associated with rejecting heat from radioisotope generators and the complexity of the generator are discussed in Refs. 1 and 2. Figure 13 indicates the required fuel to ensure a required 4130 w at the end of 1.4 yr. The Figure assumes fuel loading at time of launch and does not consider early fuel loading for generator preflight checkout. All the energy shown in the shaded area must be removed at a rate equal to its exponential decay rate. Because of this added thermal complexity and the larger gamma dose rates, it appears more probable that either Pu-238 or Cm-244 would be used for this capsule application.

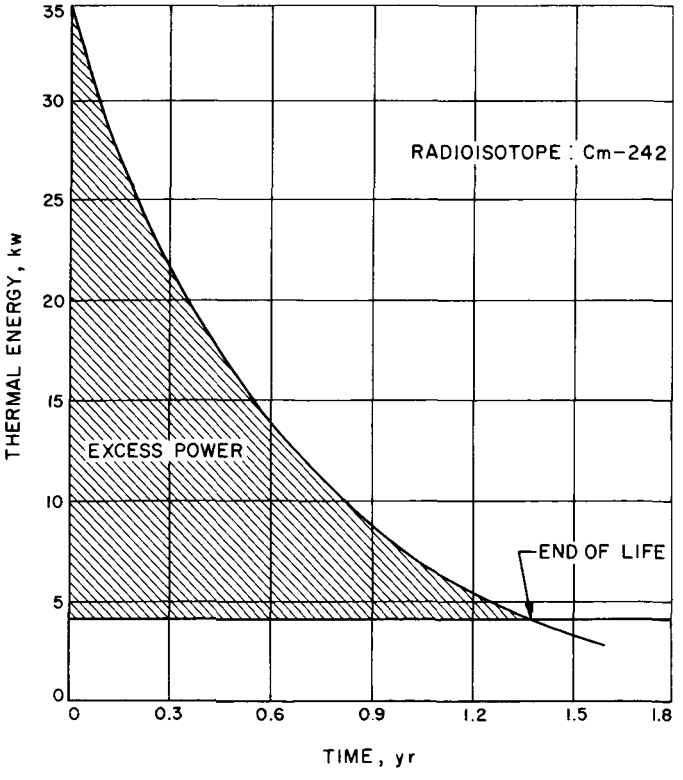

Fig. 13. Mission power showing required excess power to ensure load at end of mission

The power densities of both Pu-238 and Cm-244 are inadequate for use with thermionic conversion without the use of a thermal concentrating device such as the heat pipe. The heat pipe is a relatively new device in its early development phase which acts as an efficient heat transport mechanism. Heat generated in a compact energy source produces a phase change in a eutectic. This eutectic transports the heat from the source to the conversion device by capillary action where the heat is given up. The heat pipe shows great promise of providing thermal energy transport at temperatures in excess of those obtainable to date. Of the two remaining radioisotopes, Pu-238 is more desirable, because its important characteristics (radiation, cost, availability, temperature characteristics) are more favorable. Plutonium dioxide, a stable, easily handled radioisotope is favorably considered even though it has a lower power density than other plutonium compounds.

After selection of the radioisotope has been made, the method of conversion from thermal to electrical energy must be considered to ensure that the power density of the selected fuel is adequate. For example, thermoelectric generators require power densities of 2 to 10 w/cm³, because the hot junction temperature of the thermoelement is limited by materials technology. Thermionic conversion devices require higher power densities, on the order of 25 to 50 w/cm³, because of the higher operating temperature of the diode. Power densities for dynamic systems have a much larger range, because of the system geometry, the type of cycle involved (Rankine, Brayton, Sterling, etc.) and the power level of the system. For the

power levels considered in this Report, dynamic conversion will not be considered for reasons pointed out in Section IV.

The properties of thermoelectric and thermionic converters must, therefore, be evaluated before a design using radioisotopes can proceed.

3. Thermoelectrics

A thermoelectric energy converter is a heat engine which uses the Seebeck effect to convert heat into electrical energy. As such, its efficiency is bounded by the limits of the Carnot cycle and the properties of the thermoelectric materials. To improve the Carnot efficiency of the device, the temperature differential across the element, ΔT, must be maximized. However, this temperature difference, ΔT, is constrained at the upper limit, hot junction, by the physical limitations of thermoelectric materials and/or the fuel capsule configuration and materials and the lower limit, cold junction, by the radiator temperature. Because of the fuel capsule and radiator constraints, maximizing the efficiency does not, necessarily, minimize the system weight. The conversion efficiency of the thermoelectric material is limited by three factors:

1. Seebeck coefficient, which is a measure of the potential difference, voltage, that can be established per degree of temperature difference across the element
2. Thermal conductivity
3. Electrical resistivity

The ideal material would have a high Seebeck coefficient, low thermal conductivity and low resistivity. Unfortunately, the properties are somewhat conflicting. It is particularly difficult to realize both low thermal conductivity and resistivity. Semiconductor materials have given the best compromise between these various requirements.

The thermoelectric materials receiving the most use today are lead telluride (PbTe) and germanium silicon (GeSi). Although capable of good performance, lead telluride has poor physical strength and environmental sensitivity. It is somewhat fragile and its high thermal expansion coefficient requires great care in preventing thermal stresses from causing failures when fitted directly to structural materials. Environmental considerations further restrict the use of lead telluride. It cannot be operated in air or any atmosphere containing oxygen because the presence of oxygen is poisonous to the PbTe, resulting in material degradation and loss in performance. In addition, low vapor pressure produces sublimation of the material preventing lead telluride operation in a vacuum. The practice in generator design has been to hermetically seal the PbTe elements in a pressurized vessel with an inert atmosphere of argon.

The physical and mechanical properties of germanium silicon are considerably better than those of PbTe. These are compared in Table 12. The germanium silicon can be operated in a vacuum without sublimating. Therefore, it does not have to be hermetically sealed in a pressurized container. These features make it particularly attractive for a landing mission, where high environmental stress may be experienced.

Table 12. Comparison of physical properties of PbTe and GeSi

Properties	PbTe	GeSi
Density, g/cm^3	8.25	3.3
Coefficient of thermal expansion, $\times 10^{-6}$/°C	18	5
Tensile strength, psi	1,000	~ 5,000
Compressive strength, psi	> 10,000	150,000
Young's modulus, psi	2	–
Melting point, °C	922	> 1300
Maximum service temperature, °C	650	> 1000

To date practically all the thermoelectric generators have used lead telluride elements. This is because they have been available longer and have, therefore, been further developed. Lead telluride is more efficient over the temperature range that is compatible with the radioisotope fuels and safety philosophy. This is shown in Fig. 14. From this Figure, it is evident that germanium

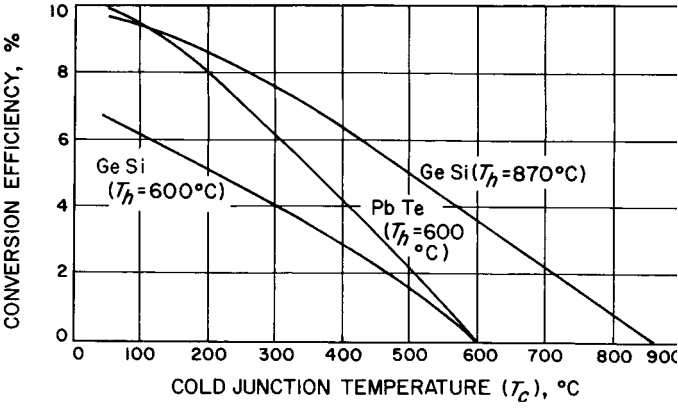

Fig. 14. Energy conversion efficiencies of PbTe and GeSi for constant hot junction temperatures and varying cold junction temperatures

silicon becomes more attractive at hot junction temperatures in excess of 600°C, which is the limit of PbTe elements. Because of fuel containment considerations, the higher hot junction temperatures have not been possible. Operation at the higher temperature has an added advantage in the final generator design. It allows the designer to raise the cold junction temperature, and thereby, reduce the size and weight of the radiator surface and still maintain a good system efficiency. The radiator is one of the largest contributors to the overall generator weight. By sacrificing some efficiency, it is possible to minimize the weight of the generator.

A thermoelectric element is essentially a low voltage device (~0.015 v @ 100° ΔT/element). However, since several hundred elements would be required in a generator for the capsule, it is possible to realize terminal voltages in excess of 20 v. (As a matter of fact, the higher terminal voltage aids the design of practical thermoelectric elements in allowing elements which are large and easily manufactured.) The multitude of elements in an RTG generator also makes it possible to arrange the elements in a series-parallel array, which will improve the generator reliability. This becomes particularly true of generators rated in excess of 40 w.

4. Thermionic Converters

Like thermoelectrics, thermionic conversion devices are heat engines, which convert heat directly into electrical energy. Input heat impressed on the emitter produces a *boiloff* of electrons from the emitter which are collected at a much lower temperature collector. Heat is then rejected to space from the collector. The efficiency of the thermionic diode is dependent upon the difference in work function between the emitter and collector and the minimizing of the space charge between the electrodes. Because the spacing between emitter and collector is as small as possible, the introduction of cesium into this space is used to reduce the space charge.

Figures 15 and 16 give the performance characteristics of a thermionic diode as a function of temperature. The area of the emitter is 2 cm². From the Figures it is evident that a thermionic system would be high current and low voltage. It is also a high power device (~30 to 50 w/diode). This implies that at low power levels (~100 w) it would be necessary to use a dc-to-dc converter near the thermionic generator to transform the voltage to a high level where it can be better utilized. There are transformation losses in this method, which reduce the overall generator efficiency. If silicon transistors must be used in the converter, this efficiency loss could be quite large. In addition

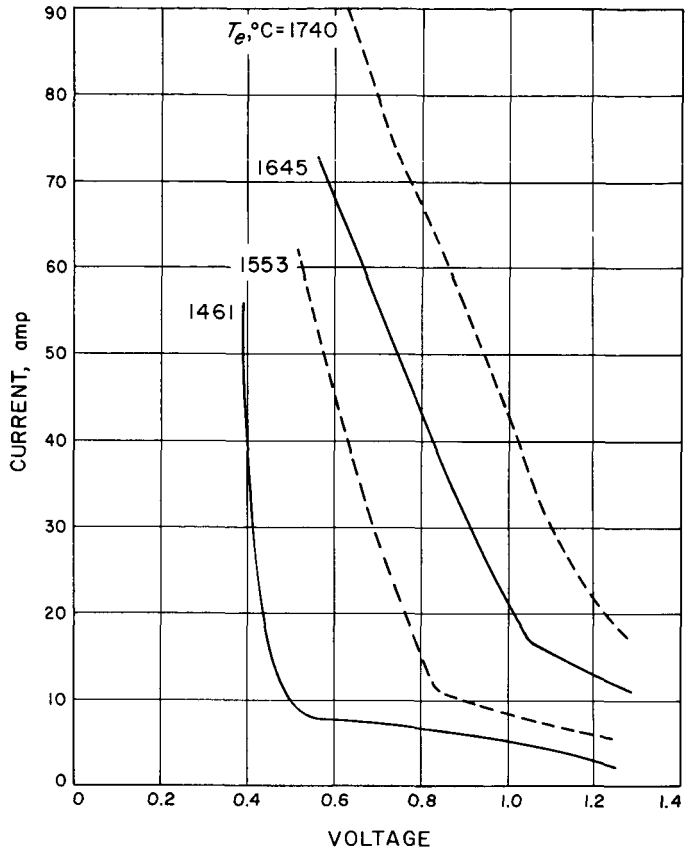

Fig. 15. Voltage/current characteristics of a 2-cm² cesium vapor thermionic diode

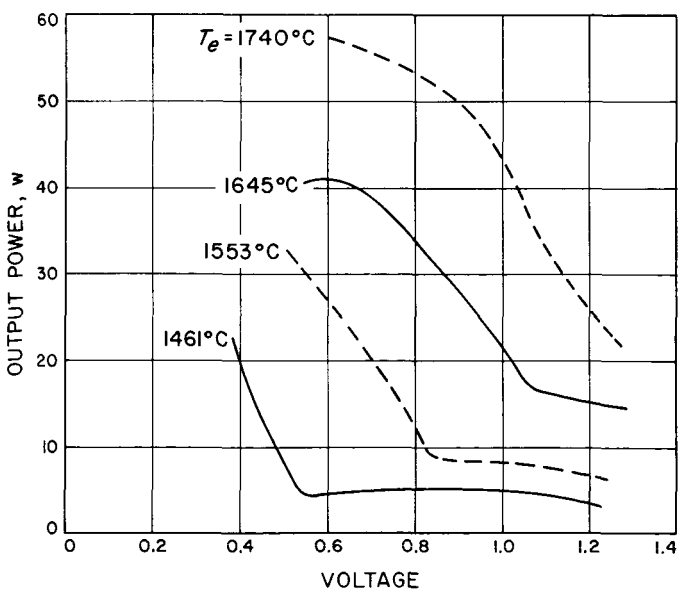

Fig. 16. Power/voltage characteristics of a 2-cm² cesium vapor thermionic diode

to the potential efficiency problems, the reliability of the diodes would have to be very high, since only two diodes are needed to produce up to 100 w.

With the thermionic diode, the absolute temperature of the device is very important. This makes the thermal design of a generator using thermionics critical. To illustrate: from Fig. 16, it can be seen that a system designed to operate at 0.8 v will have a power output drop from 53 to 34 w for a 95°C drop in emitter temperature from 1740 to 1645°C, a 35% loss of power for a 5% reduction in temperature. An additional 6% loss in temperature reduces the output power another 50% to 8.5 w output power. Optimum power output of the diode requires temperature control of the cesium reservoir adding additional complexity.

The high radiator temperature (600 to 700°C) of the thermionics generator helps to make the system lightweight and nonsensitive to the temperature changes associated with the sterilization cycle or the planetary environment. The thermionic diode is dependent upon the maintenance of close mechanical tolerances for optimum performance. Impact hardening will prove a problem in the design of a radioisotope thermionic generator for this reason, because the close spacing required between emitter and collector could easily be upset by impact.

The fact that a thermionic diode must operate at an emitter temperature in the range of 1600 to 1700°C for optimum power output, poses compatibility problems with the fuel capsule. In addition, these high temperatures require high power density fuels, which is at cross purposes with the capsule requirement of long life.

Plutonium, the selected fuel for this study cannot be concentrated enough to provide the power density required for thermionic diodes. Because the operating temperature is higher for thermionics, as shown above, α-emitters such as plutonium must be encapsulated with a void volume of approximately five times the fuel volume for helium pressure buildup. This requires operation at high power levels, kw, for efficient operation, due to large container surface area, or use of isotopes with high power densities. For short mission times, short half-life isotopes, such as Cm-242 and Th-228, could be used because they can provide the power density required. Development efforts are under way to provide materials and techniques for high temperature use of thermionics with radioisotopes. They will not be available to meet the needs of capsule systems in the early 1970's, however. Thermoelectric conversion is, therefore, considered as the method of conversion of thermal energy from the radioisotope to the electrical power required.

After selection of the fuel to be used and the conversion technique to obtain electrical energy, the generator design can proceed. The design itself is then dictated by the fuel, the conversion technique, mission constraints and the safety philosophy for radioisotope and radiation containment. This last item is of special interest and is discussed in the following paragraphs on safety. However, it is significant to point out here that a change in the design philosophy of the radioactive fuel capsule will have to be made from the present design approach to make either germanium silicon thermoelectric or thermionic conversion attractive. At present, fuel capsules for interplanetary missions must be designed for intact reentry and the containment of the helium generated in the radioactive decay of the α-emitting fuels. The fuel must not be allowed to exceed its melting point, as it becomes very corrosive and could not be contained for the length of time desired. It is the practice to allow void volumes, as mentioned earlier. This has the effect of diluting the specific output of the capsule and makes it difficult to achieve the higher temperatures required.

Programs are underway to resolve these difficulties. The first of these is the development of fuel forms of higher melting points, at the sacrifice of specific energy. The progress with Pu-238 has been good and fuel forms with melting points in excess of 2000°C are assured. Two approaches to solving the helium pressure buildup are being studied. The first is to decrease the containment lifetimes for the ceramic fuel forms as they are virtually insoluble and the other is to vent or bleed off the capsule helium.

With the programs underway the likelihood of going to higher temperature generators is quite good. This will make the germanium silicon thermoelectric generator most attractive and offers the potential of generator specific powers in excess of 2 w/lb. It will also be a boon to the development of radioisotope thermionic generators.

5. RTG Design for Capsule Operation

The method used to determine the size of a radioisotope thermoelectric generator can take several forms, (1) a design to provide all the power required, thus, precluding the use of a storage system, (2) design the RTG for an optimum power system, which must include energy storage for some of the load, and (3) design the RTG for the average load and provide energy storage to supply the load in excess to the average.

The first method, although easily mechanized, does not produce a favorable system. A method must be provided to shunt the excess power when the generator is not operating at its maximum design output. This can be achieved by design of the system to incorporate several generators in parallel. When a load is removed, such as during the landed operation passive period, those generators not required to support the lower requirement could have their outputs shorted. This would produce an increase in the generator Peltier heat reducing the temperature at the thermoelectric hot junction, thus, cooling the generator. This, of course, produces a less efficient system, requires an excessive radioisotope inventory, which is only produced in limited quantity, and increases the internal radiation level of the capsule.

The second method places heavy reliance on the energy storage system to provide peak loads. This design leads to the smallest generator and the resultant radiation level is the minimum. Although the generator may be the smallest, the system weight and volume may exceed that of the above example because of such heavy dependence on energy storage and the requirement for recharging the storage source. When the design utilizes the average load to set the generator size, the design essentially incorporates all the disadvantages of the previous two mentioned. They are less extreme, however, and may, dependent on the requirements, be acceptable in meeting the mission requirements. Because the mission experiments will be sensitive to radiation background during biological experiments, the design shall be based on minimizing the radiation hazard from onboard equipment. This leads to designing an optimum generator system, although the maximum will be presented to determine radiation levels and size.

Although the short mission time for landed operation does not require a constant power source, which has as a major advantage long life, it may be determined such a system is more favorable; and if so, has the advantage of extending the life of operation. For all the generator designs presented here, the parameters shown in Table 13 will be used in the design analysis.

Table 13. Capsule I design analysis parameters

Thermoelectric material	Ge Si
Hot junction temperature, (T_h), °C	900
Cold junction temperature, (T_c), °C	350
Temperature, (T), °C	550
Seebeck coefficient, (α_{n+p}), μv/°C	525
Resistivity, (ρ), Ω/cm	4.96×10^{-3}
Fuel	Pu-238

From Table 1 the maximum power occurs during the active communications period on the planet's surface. For this design the load voltage per couple of the generator, assuming the internal resistance as equal to the load, is

$$V_L = \tfrac{1}{2}\alpha_{n+p}\,\Delta T = 0.143 \text{ v} \tag{32}$$

the number of series couples to provide the output voltage

$$N = \frac{12}{0.143} = 84$$

to ensure no mission degradation, an allowance of 10% will make the total 92 couples. The power output of each couple is

$$P_c = \frac{(\alpha\Delta T)^2}{4\rho l/A} = 0.435 \text{ w/couple} \tag{33}$$

rearranging to determine the l/A ratio

$$\frac{l}{A} = \frac{(\alpha\Delta T)^2}{4\rho P_c} = 9.75 \text{ cm}^{-1}$$

Geometrically, 9.75 cm^{-1} corresponds to an element

17/64-in. long × 3/16-in. diam

The system current $I = P_o/E_o = 3.34$ amp

The resistance per couple $R/N = V_o/NI = 0.039\ \Omega$/couple

The heat absorbed by the heat source Q_a

$$Q_a = Q_{\text{Peltier}} + Q_{\text{conduction}} - Q_{\text{joule}} \text{ w} \tag{34}$$

$$= \alpha I T_h + 2kA/l\Delta T - \tfrac{1}{2}I^2R = 6.6 \text{ w/couple}$$

The thermoelectric efficiency is

$$\eta_t = \frac{P_c}{Q_a} = 6.6\% \tag{35}$$

The above figure represents the efficiency of a germanium silicon module under ideal conditions; i.e., no heat losses. If we assume 25% heat losses, a more realistic overall efficiency would be 4.95% for the generator. The fuel

quantity required at launch to sustain 40-hr survival on the planet would be

$$P_o = Pe^{0.664\lambda}$$
$$= \frac{40}{0.0495} e^{0.005} \quad \approx 810 \text{ w thermal}$$
$$\approx 2.08 \text{ kg} \qquad (36)$$
$$\approx 2430 \text{ C}$$

Table 14 presents a summary of four designs as outlined above. For Capsule I, since the life is relatively short, no provision is made for battery recharge, and thus, the average power and peak power are the only selections. The hot side of the GeSi thermoelectric elements consist of an array of, *floating*, hot shoes that accept heat from the radioisotope by thermal radiation. To provide the heat fluxes necessary for large, temperatures, T, the hot shoes are sized larger than the elements themselves.

Neither the 200 w generator nor the 40 w generator need to be limited to one design only; the units can be split up into several units or submodules with the following possibilities as examples; for the 200 w unit:

1. 200 w/1 module, series elements
2. 4 submodules (1) in series, 50 w each, 7 v, 7.15 amp; (2) in parallel, 50 w each, 28 v, 1.79 amp
3. 200 w/1 module, series-parallel.

The effect of paralleling modules on couple geometry indicates the l/A ratio of the thermoelectric couple increases. This can be seen also from Eq. (37). For a constant voltage and a decrease in the power per couple, the l/A ratio increases. This is highly undesirable from an impact standpoint. Although no analysis has been made of element failure due to impact, Eulers column formula (37) illustrates the dependence of buckling

$$L_{cr} = \frac{\pi^2 Y I_2}{l^2} \qquad (37)$$

failure on the l/r or l/A ratio, where L_{cr} is the critical load. The absence of experimental data makes it difficult to provide implicit impact load numbers to specific l/A ratios. However, the brittleness of bulk thermoelectric materials would make an l/A ratio greater than 10 rather suspect for impacts greater than 100g.

To stay within the l/A ratio, reference to Table 14 indicates the reduction in the generator output voltages for Capsule I. Also of significance, is the fact that designing a generator for average loads for a power profile, similar to Capsule I's, provides a power system of equal weight. Although the mechanization necessary to shunt excess load when designing for peak power may be difficult,it may offset the requirement for a secondary energy storage device.

The radioisotope thermoelectric generator could take the form shown in Fig. 17. Instead of excessive insulation, the overall case could be reduced by use of reflective material completely surrounding the fuel block and the case itself made of graphite. A similar concept has been proposed by RCA. This type design with the flat plate radiator lends itself to capsule size, as will be shown in the section on thermal control.

Table 14. Capsule power system parameters using radioisotope thermoelectric generator

Factor	Capsule			
	I peak	I average	II peak	II optimum
Power output, w	40	19	200	88.5
Voltage output V_o, v	12	6	28	28
Number of TE couples, N	92	46	216	216
Element length, in.	17/64	9/32	9/16	9/32
Element diam, in.	3/16	3/16	1/4	3/16
Thermoelectric effectivity, %	6.6	6.6	6.6	6.75
Generator effectivity, %	4.95	4.95	4.95	5.0
Thermal power, w	810	385	4350	1790
Fuel mass, kg	2.1	0.988	11.15	4.6
Curies	2.31×10^4	1.1×10^4	1.2×10^5	5.1×10^4
Battery capacity, whr	none	280	none	7210
Battery weight, lb	—	14	—	384
Generator weight, lb[a]	27	13	154	60

[a] No shielding included.

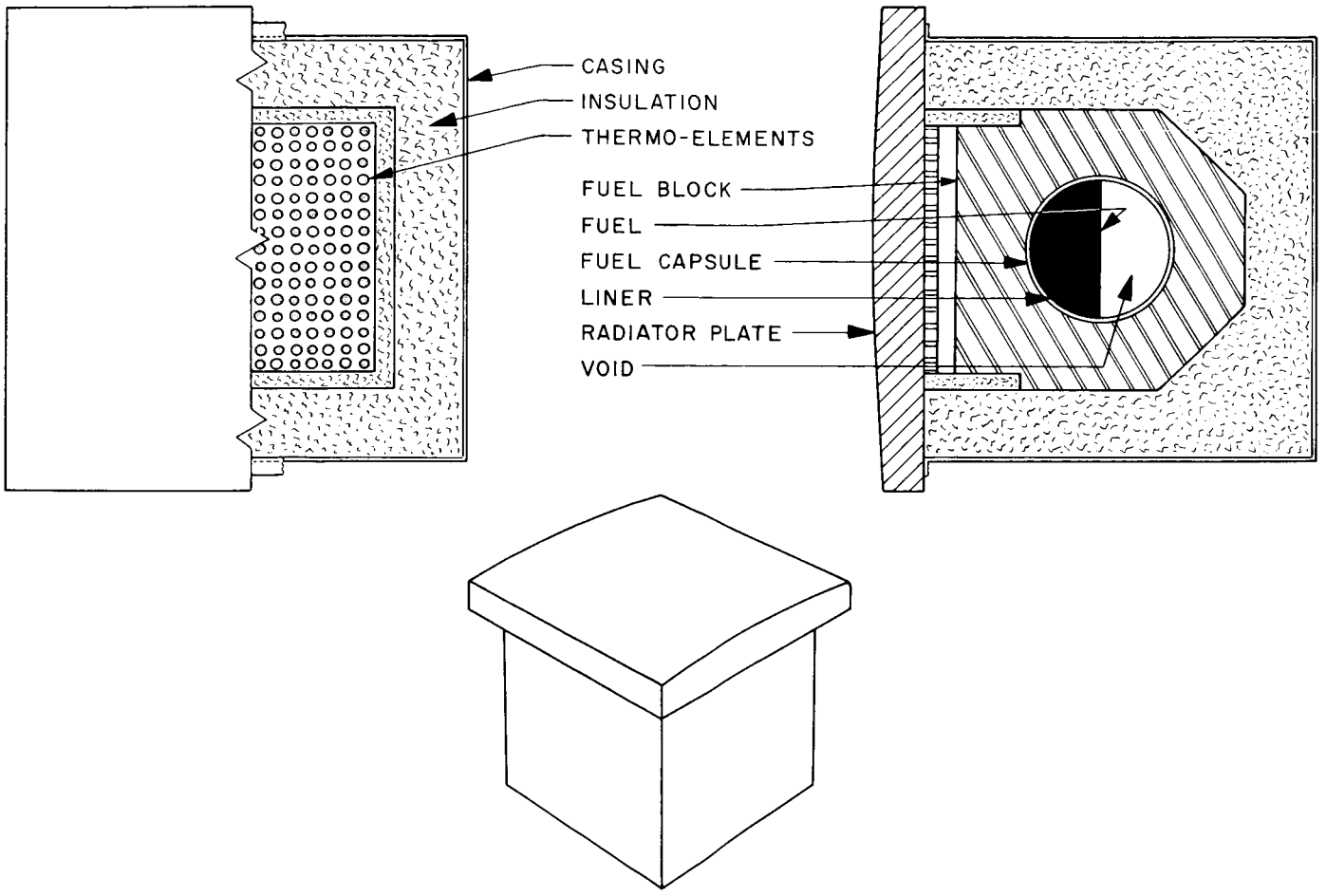

Fig. 17. Generator designed for intact reentry

6. Safety

The radioisotope, which provides the thermal energy for the power system, is a highly radioactive material that if released would cause serious problems. For this reason the generator must be designed to prevent this release should accidental reentry into the Earth's atmosphere result from a launch failure. Consideration should be given to the containment philosophy of the radioisotope on the surface of Mars, in the event of an aborted landing, so that no radioactive material contaminates the planet's environment. Studies by the AEC indicate complete containment is extremely difficult.

The method presently being studied to prevent release of the fuel, is design of the fuel capsule to remain intact during any type of reentry by use of increased structural strength in the container, use of protective coatings to absorb the heat of reentry and additional material surrounding the fuel capsule, which absorbs the heat of reentry by undergoing a change in phase. Because Mars entry abort would not cause complete burnup of the surrounding material, it would absorb a portion of the impact force. A significant penalty in efficiency and specific power results from this safety requirement. The specific capsule design with its associated material block can only be completed when an analysis of the launch trajectory and staging times are known. From this analysis the amount of thermodynamic heating, which might occur during reentry, the point of impact for propulsion or guidance failures, and the quantity of fuel and helium present can be determined. This last item is significant in determining what internal pressure is present at the maximum life requirement of the fuel containment and may require a capsule vessel design in excess of the impact and temperature during reentry requirements. In any event, the design must consider encapsulation in a container which utilizes materials of high strength, high

temperature and corrosion resistance to ensure the safe containment in the event of any conceivable adverse environment.

7. Radiation

The use of a radioisotope power source in a spacecraft or capsule design, introduces an environment which is unique to nuclear sources-radiation. The selection of this power source may well be governed by the mission and capsule design criteria for background radiation levels. As pointed out earlier, alpha- and beta-particles emitted by the particular radioisotope are absorbed within the fuel and surrounding media and do not represent a direct radiation hazard. However, secondary radiations associated with the decay process contribute, in the case of an α-emitter, penetrating photon and neutron radiation that poses severe problems at high dose rates. Beta radiation may contribute to radiation problems through production of *Bremsstrahlung*.

The concern evidenced for the radiation problem can be seen when ground handling techniques must be developed for ground protection of personnel, fuel loading of the generator and prelaunch checkout procedures, for both capsule and spacecraft. In addition, the integration of such a device into a complex space system which must be exposed to radiation for long durations must be considered. Electronic components and materials are susceptible to severe degradation without proper design and/or shielding. Scientific measurement equipment, which may be onboard a capsule system to perform radiological or biological experiments, may be hampered by a radiation flux background from a radioisotope source. Indeed, the requirements placed on background radiation by experimenters will be shown to be the limiting restriction on the use of nuclear sources. It is, therefore, necessary to minimize the radiation problem by fuel selection, separation of power source from sensitive equipment and use of shielding material where necessary to reduce the undesirable flux to an acceptable level.

As pointed out earlier in the selection of radioisotope fuels, Pu-238 represents the most acceptable fuel choice having the lowest radiation emission for isotopes, which can meet the other criteria. To determine the magnitude of the radiation problem, two RTG power units will be evaluated, corresponding to levels for Capsules I and II. The two power levels to be considered are shown in Table 15 using PuO_2 as the fuel source.

Using the decay information, the spontaneous fission and (α, n) output listed in Ref. 3, the radiation produced by the selected power sources can be determined. They are listed in Table 16.

Table 15. Capsule I and II power levels, using PO_2 as the fuel source

Factor	Capsule I	Capsule II
Electrical output, w	40	150
Thermal power, w	640	2400
Fuel mass, kg	1.8	6.87
Active isotope, C	19,700	73,800

Table 16. Unit I and II radiation produced by the selected power sources

Radiation sources	Unit I	Unit II
Prompt γ-rays from fission	6.9×10^6/sec	2.6×10^7/sec
γ-rays from fission products	7.5×10^6	2.8×10^7
γ-rays from α decay,Mev:		
0.0435	2.76×10^{11}	1.04×10^{12}
0.099	5.82×10^{10}	2.18×10^{11}
0.150	7.27×10^9	2.73×10^{10}
0.203	2.91×10^7	1.09×10^8
0.76	3.64×10^8	1.36×10^9
0.875	1.45×10^8	5.45×10^8
Neutrons from (α, n) reaction	9.1×10^7	3.47×10^8
Neutrons from spontaneous fission	6.14×10^6	2.34×10^7

To determine the significance of this magnitude of radiation, it must be compared with the absolute maximum requirements for radiation flux requested by science experimenters. Table 17 reproduces Table 1, p. 254 of Ref. 4, which represents these maximum values. The radiation levels, if they could be reached, would assure that a full set of experiments could be carried out without significant interference from nuclear sources. The values given in the table represent 1% of anticipated minimum natural radiation and would be extremely difficult to obtain. For example, at the Earth's surface, the cosmic radiation background is approximately 1% of the total cosmic background in space or 10.4 photons/cm^2-sec (Ref. 5).

This represents four orders of magnitude greater than the value specified for photon energies of $3 > E > 0.3$ Mev in Table 17. Based on this, the requested maximum values should only be used as a guide until the table can be redefined and factors of 10 or 20 difference will be considered.

However, in comparing the two tables, the radiation emitted from the generators is unacceptably large for use

Table 17. Maximum desirable flux of various radiations

Radiation	Flux at detectors, particles/cm²-sec
Protons	
E > 10 Mev	3×10^{-3}
10 > E > 0.02 Mev[a]	10^{-2}
20 kev > E > 1 ev	10^{6}/decade of energy
Alphas and heavier nuclei	
E > 10 Mev/nucleon	3×10^{-4}
10 > E > 0.02 Mev/nucleon[a]	10^{-3}
20 kev > E > 1 ev	10^{6}/decade of energy
Electrons	
E > 0.5 Bev	10^{-4}
0.5 Bev > E > 1 Mev	10^{-3}
1 > E > 0.02 Mev[a]	10^{-3}
20 kev > E > 1 ev	10^{6}/decade of energy
Neutrons	
E > 1 Mev	10^{-2}
1 > E > 0.001 Mev	10^{-2}
1 kev > E	10^{-2}
Photons[b]	
E > 50 Mev	10^{-6}
50 > E > 3 Mev	5×10^{-3}
3 > E > 0.3 Mev[c]	10^{-3}
300 > E > 100 kev	10^{-1}
100 > E > 10 kev	10^{-1}
10 kev > E > 100 ev	10^{+2}

[a] These values are estimates based on available data.
[b] This includes the electron Bremsstrahlung produced in all parts of the spacecraft and in any detector.
[c] With no resolvable peak containing more than 5% of this value.

in the vicinity of scientific instruments and must be shielded to reduce the radiation level. The problem, therefore, is to determine the shield thicknesses (and weights), which will reduce the radiation flux to acceptable levels at distances corresponding to usable instrument locations.

All the γ-rays listed in the table are of relatively low energy, and thus, their intensity can be substantially reduced by relatively thin shields of heavy material such as lead or uranium. The decay of Pu-238 consists of only 1% of photons with an energy spectrum between 0.0435 and 0.875 Mev. Although low in abundance, these photons define the amount of shielding necessary to suppress the flux level to a desirable value.

The disintegration scheme for Pu-238 shows that in the decay process 10^{-4}% photon emission is at an energy level of 0.810 Mev, the most abundant of the high energy photons. The equivalent quantity or curie equivalent of 0.810 Mev photons for Capsule II is:

$$\text{Ce} = 7.38 \times 10^{4} \text{ curies} \cdot 10^{-6} = 7.38 \times 10^{-2} \text{ curies}$$

the dose rate (D_r) at a distance of 25 cm from the 0.810 Mev source is

$$D_r = 5.2 \times 10^{6} \frac{CeE_\gamma}{d^2} \, mr/\text{hr} \tag{38}$$

$$= 5.2 \times 10^{6} \frac{7.38 \times 10^{-2} (0.81)}{625} = 500 \, mr/\text{hr}$$

and since 1 mr/hr $= 5.6 \times 10^{2} \, E_\gamma^{-1}$ photons/cm²-sec the flux at a point 25 cm from the source is

$$3.44 \times 10^{5} \text{ photons/cm}^2\text{-sec}$$

To meet the background radiation requirement of maximum photon flux of 10^{-3} (I) photon/cm²-sec (as shown in Table 17), the flux from this generator must be reduced, by a factor of 2.9×10^{-9} at the separation distance of 25 cm. This can be done with either uranium or lead shields. The γ-ray initial intensity I_o will be reduced to the intensity I after passage through a thickness t of absorber equal to

$$I = I_o \, e^{-\mu_o t} \tag{39}$$

where μ_o, the linear attenuation coefficient is a measure of the interactions of photons in the absorber. The absorber thickness required to reduce the initial intensity is, therefore,

$$t = -\frac{1}{\mu_o} \ln I/I_o \tag{40}$$

$$= -1/0.9 \ln 10^{-3}/3.44 \times 10^{5} = 21.8 \text{ cm}$$

However, the dose rate given in Eq. (38) must be altered by a buildup factor to consider both scattered plus unscattered photons from a point source. Therefore:

$$D_B = B \, D_r \tag{41}$$

and from Fig. 18 the buildup factor for an 0.81 Mev flux is 5.0 and

$$D_B = 2500 \, mr/\text{hr}.$$

The total thickness of lead becomes 23.6 cm. For any distance from the radiation source to any detector with the lead shield between, the thickness of the shield can be reduced slightly for increases in the separation distance. This is not a significant amount, however, for distances less than several hundred cm.

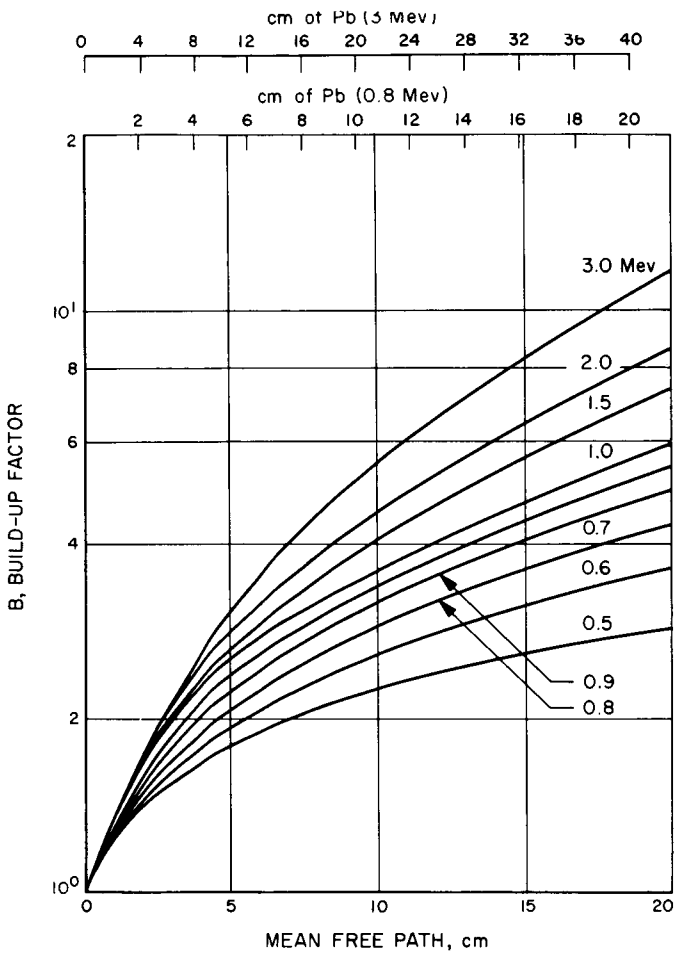

Fig. 18. Buildup factor as a function of photon energy and lead mean-free-path thickness scaled in cm units for 3 Mev and 0.8 Mev photons indicated

Shielding the radioisotope source does not present as great a problem for neutron emissions. Usually the lighter element materials such as lithium hydride (LiH) or polyethylene can adequately reduce the neutron flux at very little sacrifice in weight, but at an increase in the required volume. The total neutron emission due to (α, n) reactions from the fuel under consideration is 5.05×10^4 neutrons/g-sec. Emissions from spontaneous fission add an additional 3.41×10^3 neutrons/g-sec. For the Capsule II generator this produces a total of 3.7×10^8 neutrons/sec neutron emissions. The neutron flux at a distance of 50 cm from a point source radiating radially as found by Eq. (42) is 1.18×10^4 neutrons/cm²-sec.

$$\phi_n = \frac{\text{neutron emissions}}{4\pi d^2} \qquad (42)$$

Again from Table 17, the maximum allowable neutron dose acceptable to science is 10^{-2} neutrons/cm²-sec at the detector. Figure 19 is a graph of LiH requirements as a function of neutron flux and separation distance between source and shield. The Figure shows that for a full decade decrease in neutron flux at constant separation, the shield thickness increases by 18 cm. Conversely, at constant shield thickness, an increase in separation distance by a factor of ten decreases the neutron flux by a factor of one hundred. Therefore, reduction of the flux from the source to 10^{-2} neutrons/cm²-sec, represents an attenuation factor of 0.848×10^{-6} or 5.848 decades. The LiH shield required is 18×5.848 or 105 cm.

There is some additional attenuation of neutrons to be expected from the lead shield and of γ-rays from the LiH shield. For γ-ray attenuation in LiH, if the lead shield precedes the LiH shield, it has been determined that the lead thickness can be reduced by one decade for each 33 cm of LiH shield. This means that the lead shield could be reduced in thickness by an equivalent of 3.2 decades of attenuation. At the equivalent rate of 2.6 cm of lead per decade, the lead shield could be reduced to a thickness of 15.3 cm, when combined with 105 cm of lithium hydride. The lead shield preceding the LiH reduces the neutron flux only slightly.

An analysis for the Capsule I isotopic mass, as shown in Table 15, follows the above calculation. The results are tabulated in Table 18. As can be seen from the comparison, there is no significant reduction in shield requirements for the two different power requirements. This is true because of the logarithmic absorption effect of the shield material. A dose rate reduction of 90% of the incident radiation occurs in the first decade (2.6 cm of Pb and 18 cm of LiH) of the shielding material. The remaining 10% requires an extremely large material thickness for reduction.

Table 18. RTG radiation shield requirements

Factor	Capsule	
	I	II
Thickness of Pb to yield 10^{-3} photons/cm²-sec, cm	21.5	23.6
Thickness of LiH to yield 10^{-2} neutrons/cm²-sec, cm	98	105
Equivalent thickness of Pb due to photon absorption in LiH, cm	7.7	8.3
Required thickness of Pb shield used with LiH, cm	13.8	15.3

In determining any damage which could be sustained by the components and subsystems on the capsule or spacecraft, the radiation dose rate integrated over the life of the mission must be determined. For Capsule II, the

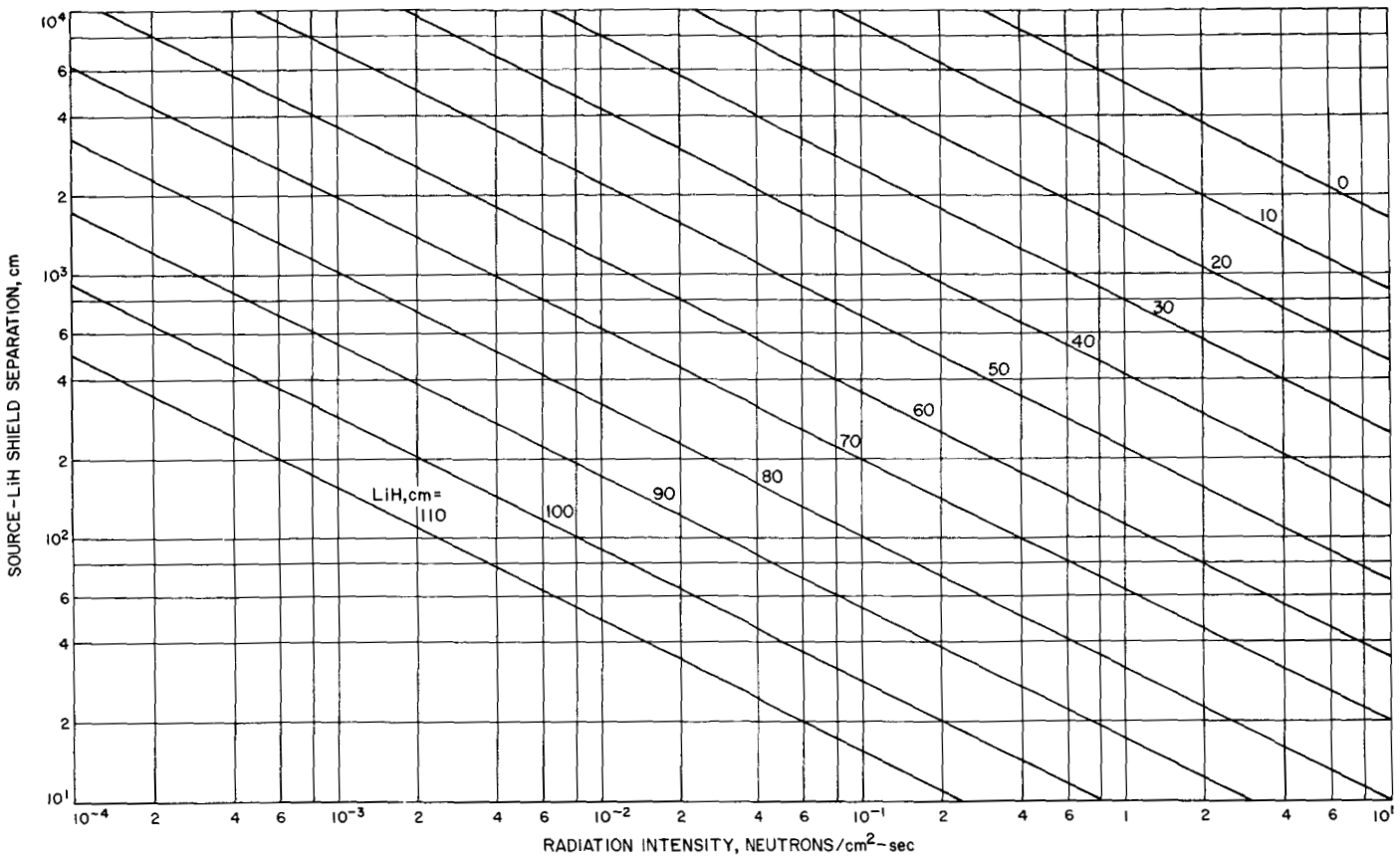

Fig. 19. Neutron radiation intensity as a function of separation between a 6.87 kg source of $Pu^{238}O_2$ and a detector (shielding thickness of LiH indicated)

photon dose rate at a distance of 50 cm from the centerline of the isotopic source integrated over the mission time of 1.4 yr with no shielding would be

$$D_r = 5.2 \times 10^6 \frac{\mathrm{CeE}_\gamma}{\mathrm{d}^2} \cdot T_m \, mr \qquad (43)$$

$$= 1.5 \times 10^3 \, r = 1.28 \times 10^3 \text{ rads}$$

The neutron dose rate at 50 cm from the centerline for neutron energy of 5 Mev is

$$D_N = \phi_n \, b\,(E_o) \qquad (44)$$

where $b\,(E_o)$ is the biological effect of unit flux of neutrons of energy E_o

$$D_N = 1.965 \times 10^3 \text{ rad}$$

The effects of photon and neutron radiation on damage to various materials have been performed to determine the level that damage occurs and the mechanism of that damage. The material having the lowest threshold of damage to an integrated photon flux is teflon with a value of 1.7×10^4 rad. The materials with the lowest threshold to neutron flux damage are capacitors at 10^{11} neutrons/cm^2 and unijunction and germanium transistors at 5×10^{11} neutrons/cm^2. The integrated neutron flux, in this example, is 5.2×10^{11} for the 1.4-yr period. Review of the above values indicates no damage would occur from the γ-radiation over the life of the mission but the neutron dose rate must be attenuated to assure no damage to electronics from neutron radiation. Because a generator design acts as a shield itself, due to internal thermal control material and the fuel block, the amount of shielding would be minimal. Safety during ground handling of a fueled source is dictated by the maximum exposure allowed for personnel (3 rad/13 wk of beta or gamma; 0.3 rad/13 wk of neutrons for total body radiation). For a 150-w RTG, safety during ground handling would be protection of personnel from γ-radiation, which can be accomplished by portable shields, automatic handling equipment and adequate procedure during test and personnel programming.

From the preceding, the requirements for radiation are not dictated by biological or material damage, which can easily be safeguarded, but by requirements to prevent interference with instruments used for scientific exploration. To date, little definitive criteria are developed for radiation constraints on background radiation. Reliance has been placed on the data presented in Table 17, which cannot at this time be fully justified. Until specific equipment is specified for a mission with its actual background radiation requirements defined, the degree of shielding with its weight and size cannot be defined. However, it is obvious there will be a shield requirement which ultimately reduces the attractiveness of the use of an RTG for space power.

It must be noted, however, that shielding is the easiest approach to the radiation problem and of course, the penalty is the added weight and volume requirements. Other methods, such as increasing the separation distance between the radiation source and the equipment, can reduce the dose rate. Another method to reduce radiation background is by anticoincidence of the background, to null it out of the measuring device. It is likely, a combination of these methods could produce the required reduction. In addition, damage to materials and electronic components and the resultant degrading of the assembly can be reduced by design methods.

The previous discussion has involved only direct radiation from source to detector. Five other sources of difficulty come to mind:

1. Capture of neutrons by spacecraft materials outside the shield *shadow*, with release of capture γ-rays and/or subsequent decay radiation
2. Scattering of neutrons and/or gammas toward the instruments by spacecraft material outside the shadow
3. Capture γ-rays created in the shield itself by absorption of neutrons in the heavy-metal component
4. Sky shine in the atmosphere of Mars
5. Penetration around the shadow shield through the Martian surface

First, the small cross section for capture, combined with the small solid angle for return of the radiation to the detector, make this an unlikely problem except for thermal neutrons on particular materials. Since the initial neutron spectrum is fast, only a large concentration of moderating material in one place could serve to create the necessary thermals. This unlikely situation can be remedied with addition of small amounts of a strong absorber.

Second, the cross section for scattering of both neutrons and γ-rays is large enough to be worthy of consideration. A value can be determined from a simple model of the capsule and detector configuration. However, it requires consideration of the varying cross section with gamma energy, the angular distribution of scattered radiation and the shape of the shield.

Third, the γ-rays from material capture of neutrons is difficult to calculate, but can be a significant problem. It can be reduced by the use of lead as opposed to uranium; however, the penalty is added shield weight. The actual shield designer must consider this problem, since it can be reduced by attenuating at least low energy neutrons before they enter the heavy material shield. Another method may be by segmenting the shield material.

Fourth, this is a familiar problem on Earth, but will be reduced by something like the ratio of atmospheric densities squared. It could only be significant in the case of an unusual sensitivity on the part of a particular lander detector.

Fifth, this also requires some definition of the lander instruments, before one even decides if it is a problem. It would require some effort for the calculation, but appropriate methods are available. Because one can always add a little shield material under the RTG, it should not be a source of real difficulty.

From the preceding discussion, the use of a nuclear source of power on the capsule can be seen to represent a problem, only in so far as the science experimentation is concerned. For power levels considered here, neutrons and photons can be attenuated to acceptable levels with shield weights in hundreds of pounds or less and separation distances in tens of centimeters. Were it not for the stringent requirements of space science experiments, no shielding would be required. To define the shielding problem more explicitly, the following problems should be resolved:

1. Reassessment of the data in Table 17, to define a more realistic maximum tolerance to radiation with better spectral resolution in the most sensitive groups
2. Definition of lander instruments, the radiation measurements to be made by them, and the sensitivity of their detectors
3. Determine radiation characteristics of all instruments

4. Measure the radiation output from an actual source with various shield configurations

Cooperation between the experimenter, designers and power systems groups could possibly reduce the inadequacy of requirements, as now known. As an example, checkout of actual experimenter equipment can be performed in cooperation with the AEC, to determine tolerance levels of the equipment and to aid in the design of final equipment. The result may indicate the use of an RTG on a capsule can be tolerated, but only as an alternative or at a sacrifice of some experiments.

8. Thermal Control Considerations

The design of the radiator, to remove the excess heat from the RTG or the radioisotope thermionic generator (RTI), is critical in setting the operating temperatures of the conversion device. In the thermoelectric system, where radiator temperatures are generally below 260°C, the radiator is one of the largest contributors to generator weight. The desire, therefore, is to go to higher temperatures without giving up too much efficiency. However, care must be exercised so that the hot junction temperature limits of the generator are not exceeded. Brief studies (presented in Appendix C) were performed to investigate the effect of capsule configuration for various mission phases, from sterilization through landed operation, determining which phase established the size of the radiator. Figure C-1 shows the capsule configuration considered. The RTG's are of the flat plate configuration, as shown in Fig. 17, and radiate heat to space through the entry capsule aft shell and sterilization canister. The studies show that for a 175-w generator, the radiator area required to hold the radiator temperature to 260°C during the sterilization cycle is 14.3 ft^2. During cruise, the radiator area required to maintain the same temperature is only 10.2 ft^2. If the radiator were designed for the cruise condition, the radiator temperature during sterilization would be about 21°C above normal. By shorting the generator output during the cycle, cooling of the generator can be obtained through the Peltier effect of the thermoelectric elements. The amount of heat removed by the Peltier effect is proportional to the current flowing through the element junction. This additional cooling would minimize the increase in hot junction temperature.

Because the radiator temperature of the thermionic system is on the order of 700°C, it is little affected by the sterilization cycle. The thermionic system radiator must maintain its thermal properties in order to realize optimum power out of the generator. As compared to the 10.2 ft^2 for the 175-w RTG, the thermionic generator would require only 0.36 ft^2. Because of this low radiator weight, the thermionic system shows promise of higher specific power than thermoelectrics, providing the problems associated with the fuel capsule can be resolved satisfactorily.

9. Conclusions

The problems involved with improved generator performance, in both thermoelectric and thermionic systems, are primarily those of fuels and materials performance at high temperatures. Because the thermoelectric systems operate at lower temperatures, the problems are not as acute, and hence, will be solved sooner than those for thermionics. At present the AEC has programs underway on thermoelectric systems, which will raise the operating temperature limits on the fuel. In addition, a well defined quality assurance program is underway on the thermoelectrics. By making more use of beryllium in the generator structure and radiator, higher specific powers (1.5 w/lb) will be realized. Higher temperature germanium silicon thermoelectric generators offer great promise for the capsule mission.

The thermionic system is less well developed and more complex, in that it is more temperature sensitive and requires temperature regulation of the cesium reservoir. There are no long-life fuels with sufficient power density to achieve the operating temperatures required. The short-life fuels, Po210 and Cm242, pose severe thermal design problems, for both the generator and capsule integration. The *heat pipe* offers a potential to the solution of generator problems for either the long-life or short-life isotopes.

Little can be said about the reliability of thermionic systems, since little data exists. Progress in diode development and lifetime have been good. Even with successful development of the heat pipe for a thermionic system, it is felt that it will remain a less reliable system than thermoelectrics, because of its greater complexity, higher operating temperatures and large power per converter, i.e., converter redundancy is difficult at lower power levels.

The thermal considerations have been discussed briefly here and more completely in the Appendix. Sterilization requirements pose no serious problem to either the thermoelectric or thermionic system as both operate at temperatures in excess of that required for sterilization. Since a radioisotope source radiates heat at a constant rate and represents a large heat load, it must be very closely integrated into the thermal design of the capsule. It may offer

a controlled means of providing heat to the spacecraft and capsule if required.

The largest unknown in the design of a radioisotope power source for the capsule involves the impact hardening of the generator. It is felt that the desired degree of impact hardening can be achieved, but the weight penalties involved are yet to be determined.

Little has been said of the effects of the radioactive source on potential spacecraft experiments. The incompatibility of the source with experiments on the spacecraft and capsule is an area of major concern. The shielding weight penalties associated with reducing the radiation levels to *acceptable* levels can be severe as shown earlier. The resolution of this problem would be required early in the capsule program.

IV. CONVERSION DEVICES

A. General

As pointed out in previous sections, the energy produced by a source, except in the case of photovoltaic devices, is not generally in the acceptable form of electrical power and must be converted from its resultant form to electrical power. In general, the usual form of energy provided by the source is heat. This thermal energy can be converted to electrical energy by various static or dynamic methods. Usually, static converters should provide a more efficient method of conversion because no intermediate step is needed, as there is with dynamic systems. However, static conversion has not achieved the level of its theoretical capability.

Of the various methods of static conversion now in existence or being developed, only two, thermoelectric and thermionic, are developed to a degree where they can be considered for a capsule system. Since they have been discussed to some length in the previous section, no further discussion will be made.

B. Dynamic Conversion

Dynamic conversion is one in which a turbine or a reciprocating engine drives an electric generator. The driving force to the turbine can be a chemical injected into the turbine chamber at high temperature and pressure or it may be a fluid which has been heated and allowed to expand and thus drive the turbine. For space power applications, three dynamic cycles have had considerable development: the Rankine Cycle, Brayton Cycle and the Sterling Cycle.

The Sterling cycle is obtained from a reciprocating engine instead of a turbine and most closely matches the Carnot cycle. Using a closed loop inert gas as a working fluid, the cycle consists of two moving pistons whose movements govern the temperature and pressure of the working fluid. This operational cycle is particularly adaptable to use with solar energy having as its principal advantage an efficiency of 20 to 30%. Other advantages are low operating temperature and low rotational speeds. Unfortunately, the Sterling cycle produces efficiencies much less than those stated above at power levels of less than several kw. This, coupled with lubrication and seal problems, rejection of heat at low temperatures, and large radiators, reduces the probability of its usefulness for the capsule mission.

The turbine system based on the Brayton cycle uses an inert working fluid which is always in the gaseous state. This gas can either be exhausted after performing mechanical work (open loop cycle) or it can be recovered, cooled in a radiator and returned to a compressor (closed loop). After compression, the gas is reheated at constant pressure, allowed to expand isentropically in the turbine chamber and recooled. The three principal elements of this dynamic system are the heat exchanger, radiator and combined rotating unit consisting of the turbine, alternator-compressor on a single shaft. This system can be made adaptable to either nuclear or solar sources of thermal energy and has predicted efficiencies of 20%. Although this cycle appears to perform at twice the efficiency of a Rankine cycle. It is less complex, and therefore more reliable; it does have a more complex radiator design because of a decreasing temperature across the radiator

Design and laboratory tests on prototype Brayton cycle systems have been successful in showing the potential of this system but no production units have been made and used on a specific application. There appear to be some problems in high temperature materials yet to be solved before this system becomes completely operational.

The Rankine cycle, also adaptable to nuclear or solar sources of thermal flux, uses a two-phase working fluid—liquid and gas. The fluid is transported to the heat source in liquid form, where it is heated to a vapor and then expanded in the turbine chamber. The heat energy at the turbine exhaust is dissipated by radiation to space until the gas is again condensed to a liquid. While this system has efficiencies of only 10% as compared to 20% for the Brayton cycle, it has been further developed.

Open-cycle systems, which require heat to be added to a working fluid, appear to be far too inefficient to be used on a lander. The system must carry the heat source and sufficient fuel to operate for the mission life requirement. Even for short durations of a few days the design of storage equipment would be complex but could be achieved. For longer missions, this fuel and its container become too gross to be practical. Problems such as protection of the fuel and the exhaust mechanism during impact would be difficult to solve not to mention the problem of exhausting a gas or liquid on the Martian surface. Possible use of nitrogen as a gas and obtaining this from the Martian atmosphere has been discounted, because of the separation problem and the uncertainty of the atmospheric content.

The major problem derived from the use of a dynamic conversion device is due directly to the mechanical step in the conversion of thermal flux to electrical energy. Problems with shaft bearings, materials for turbines, boilers and condensers, seals and liquid flow problems must be adequately solved before the dynamic system can be considered as a planetary power source. A choice between Brayton or Rankine cycles would be difficult to make at this time but since more constructive work has been achieved on the Rankine cycle, it is assumed it would be more readily available. However, neither has ever been extrapolated to power levels below 500 w. To do so would produce a corresponding loss in efficiency and specific energy which is limited by mechanical design. To provide such a system, a development time far in excess of the available time would be needed.

The use of turboalternators cannot be discounted for levels in excess of 500 w, but their selection would have to be made on a comparison of the physical characteristics and availability as compared to static conversion devices. They are not recommended for applications described in this study.

V. SUMMARY

A. General

The one outstanding conclusion which can be made from this study is that there is no power system available today for a Mars landing capsule. No one power source can be selected to meet all the requirements of a capsule from spacecraft separation until end of the mission life on the planet's surface.

Solar cells, primary and secondary batteries, radioisotope thermoelectric generators and monopropellant fueled turboalternators are the most promising systems for utilization on a capsule system. The selection of any one or a combination of these systems will be dependent upon the final mission and spacecraft criteria. Each of these systems can be made available but none can completely satisfy the entire list of requirements.

There are several important points to be considered in the selection of a capsule power system. Neither the solar cells nor the chemical dynamic system can supply the total load requirements for the complete capsule missions considered. They must be supplemented by either primary or secondary batteries to provide power during peak loads, non-oriented and landed periods for the solar cell system and for startup and thermal control on the dynamic system. Batteries can be used as the total energy source

for the capsule at a tremendous cost in weight, volume and reliability. Radioisotope generators offer the only potential for reliable long life operation without regard to the external environment. Although RTG's can be designed to provide power without the requirement for energy storage, use of batteries will produce a more optimum design. The data in Fig. 20 and Table 19 present summary comparisons of the four acceptable systems. Both indicate an RTG alone would produce a lighter system than an RTG-battery combination. However, radioisotope fuel and the attendant radiation are greater in this case, requiring more shielding to meet the science requirements. In addition, it may be necessary that the larger unit be a combination of series-parallel units, to provide for variations in the load. These factors tend to escalate the size and weight of the RTG only system to a less desirable system. The requirement for added fuel, when compared with that available, must also be considered, as well as criticality of the large mass. However, if the present program to provide a sterilized battery does not produce a device as now anticipated, only the RTG power system could be designed to absorb this deficiency without too great a penalty.

Although it has been shown that chemically fueled turboalternators are feasible, development time, fuel mass and expulsion of combustion products into the planet's atmosphere outweigh the usefulness of this unit. It offers no advantages when compared to solar cells for cruise to the planet, and it does not provide as much potential as an RTG for landed operation on the planet's surface. Whereas, the RTG can provide uninterrupted power for a long period of operation, yr, the turboalternator must be alternated with a secondary power source to extend its operations to days.

With the present state of knowledge of the surface of Mars, systems using the Sun as a source of energy appear

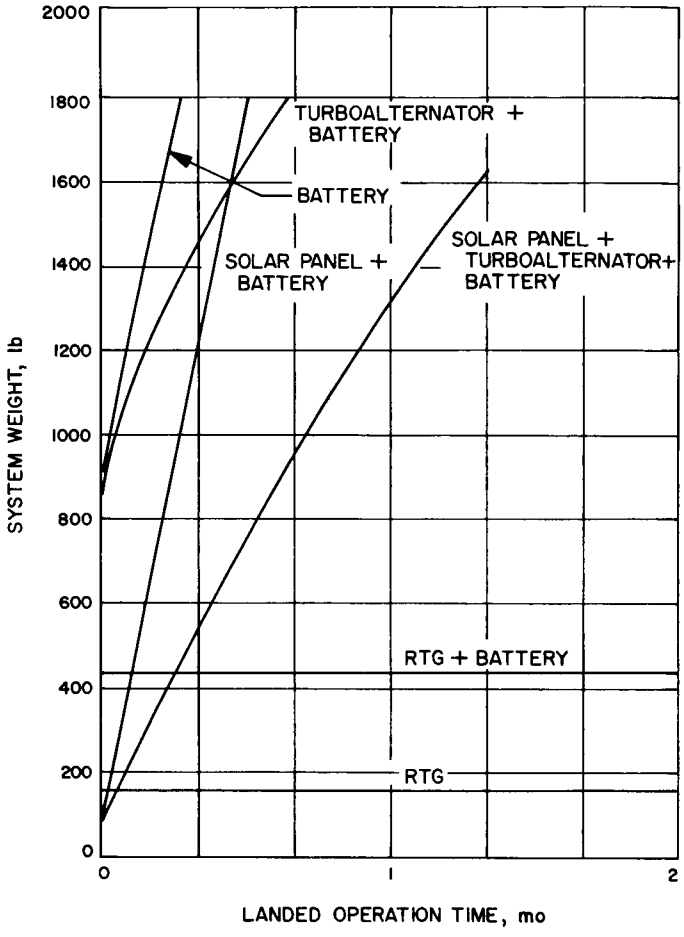

Fig. 20. Capsule II power system weight as a function of operational time and selected system

to be restricted to use outside the planet's environment Solar systems can be further restricted to solar cells used in conjunction with energy storage. The decrease in solar insolation at the Sun–Mars distance would require solar

Table 19. Power subsystem weight comparison of acceptable capsule systems for capsule I and II

Power subsystem	Operational phase							
	D_1	D_2	S	L_1	L_2	$D_1 + S$	$D_2 + L_1$	$D_2 + L_2$
	Weight, lb							
Battery only	126	927	42	22,200	583	183	23,000	1,500
Oriented solar cell & battery	8	54	—	310	310	50	364	364
Nonoriented solar cell & battery	11	—	—	—	—	53	—	—
Body mounted solar cell & battery	—	48	—	—	—	—	22,200	631
Turboalternator & battery	—	—	18	2,300	293	144	3,250	1,225
RTG	27	154	27	127	127	27	154	154
RTG & battery	20	353	23	151	151	25	443	443

systems other than photovoltaic cells to have large collector areas and/or too great a degree of accuracy to obtain the thermal energy required for efficient operation of the conversion device.

Table 20 is a summary of systems studied in this Report. They are categorized into acceptable and nonacceptable systems. Of the systems studied, growth potential is most significant for the radioisotope thermal source at low power levels (1 kw). Growth potential for solar photovoltaic systems is limited by structural and geometrical considerations because of the constant power per unit area relationship for cells. The limiting value has not been reached yet, however, and will continue to be employed almost exclusively for long duration missions with batteries for off Sun operation. Solar-thermal systems appear useful in the medium power range and on exploration of the inner planets while reactor systems appear the most favorable at high power levels.

Table 20. Power sources considered for capsule study

Acceptability	Power sources
Acceptable	Solar photovoltaic cells (silicon)
	Batteries
	Chemically fueled turboalternator
	Radioisotope thermoelectric generator
Nonacceptable	Nuclear
	Thermoelectric
	Thermionic
	Dynamic
	Batteries
	Fuel cells
	Solar
	Thermoelectric
	Thermionic
	Dynamic
	Solar cells (other than silicon)
	Thermal batteries

Although this Report does not presume to be all inclusive in reporting on all power systems adaptable to landed operation on a foreign planet, it does consider those which appear most favorable from the standpoint of state-of-art and development. Indeed, devices of systems such as magnetohydrodynamics, nuclear batteries, electrostatic generators, and biological fuel cells are only a few of the concepts not covered. This was not an oversight, however; they were omitted on the grounds of incomplete development or inadequacy for this particular capsule definition. The projection of their performance is particularly difficult because of the lack of practical technology in solving a great many practical problems. Estimates of reliability and the effects of both the space and planet environments are in many cases little more than conjecture, due to lack of concrete data. Factoring in this new data, once such is obtained, would require a new study of reliability and of space and planet environment effects.

The major basis of comparison throughout this study has been by system weight. This has been done only because the various systems are amenable to this type of analysis as the results show. As the Voyager program progresses, less emphasis will be placed on weight and directed more appropriately to the other criteria listed in Section II. These other factors have been considered in this study but cannot in most cases be tabulated for comparison. An example, is the comparative analysis of an RTG system as opposed to a solar photovoltaic system for landed operation (Appendix B). A great many criteria are factored into the analysis but again the best method of comparison is by weight. In this particular case the study concludes that the RTG can weigh 40 to 50% less than the equivalent solar cell system.

B. Recommendations

To provide a system or systems for capsule cruise and landed operation, intensive development of three of the four acceptable systems is recommended. As pointed out in Section III-3, a program is now underway which will lead to a sterilized, impactable battery. Similar activity should be initiated in the development of radioisotope thermoelectric generators and solar cells. Specifically, to provide growth of capability and flexibility for future missions, assuming a minimum life mission for a first capsule, solar cells will have to be improved in mechanical design to survive the Martian environment as well as the landing impact. This can be implemented by tests under simulated conditions in the laboratory and by planning to carry at least one square foot of solar cells on the first capsule as an experiment. Cell erosion, reduction in output from dust and atmospheric attenuation of the solar insolation, can be determined under actual conditions, which could result in conclusive information on the usefulness of solar systems on the planet's surface.

In addition to problems of designing an RTG of 150 w or greater, methods of sterilization to ensure thermal control and design for high impact must be started. Radiation effects produced by the radioisotope must be studied to indicate the requirements and restrictions placed on

integration of an RTG into a spacecraft-capsule system. Effects of radiation on scientific experiments must be more clearly defined for each particular experiment proposed. This will aid in determining any tradeoff in power system-science design in designing shielding and/or ancillary equipment to null out the background radiation from the generator.

Without effort being applied to both the solar cell and RTG systems for landed operation, there is no growth capability in extensions to present technology. In the same way, there is no possibility of extending the operational life or experiment sophistication of present capsule designs without a power system having more capability than now proposed for batteries.

NOMENCLATURE, TEXT

a_g specific weight of solar cells, lb/w

A area, cm^2

b electrical resistivity per cell for fuel cell, ohm/cm^2

$b(E_o)$ biological effect of unit flux of neutrons having an energy E_o, mrad/hr

B buildup factor for gamma ray transport through shield

C_1 battery capacity discharged from battery during time T_1

C and C_e curie and curie equivalent of a radioisotope source

d diameter, cm

d distance, cm

D gamma dose rate and mr/hr

D_n neutron dose rate, mr/hr

D_1 capsule system requiring low power during delivery to planet

D_2 capsule system requiring high power during delivery to planet

E voltage, v

E energy of gamma ray, Mev

E_r battery capacity, whr

h battery recharge efficiency

I current amp, gamma intensity

I_L least moment of inertia

I_s solar insulation, mw/cm^2

$I_{(\gamma)}, I_{o(\gamma)}$ light intensity as a function of wavelength, mw/cm^2

J current density, ma/cm^2

K fraction of the peak load period occurring within the solar eclipse period, see Appendix B

l length, cm

L_{cr} critical collapsing load

L_1 and L_2 capsule II survival systems for 6-mo and 5-day planet operations, respectively

N number of individual fuel cells

P power, w

P pressure, psi

Q thermal energy, w

R attenuation coefficient

R charge rate, hr

R resistance, ohm

S capsule I survival system for 40 hr of planet operation

t material thickness, cm

T time

T temperature

$T_{1/2}$ isotope half life

v ratio of cell voltage to open circuit voltage of a fuel cell

V voltage, v

W fuel cell consumption rates, lb/hr

W weight, lb

X constant-cell weight/10^3 cm^2 of fuel cell

Y Young's modulus, dynes/cm^2

α constant-cell weight/10^3 cm^2 of fuel cell electrode area

α ratio of eclipse time to total cycle length, T_e/T_o

α_{n+p} Seebeck coefficient, v/°C

$\alpha_{(\lambda)}$ absorption coefficient at a discrete wavelength

β constant, a conversion factor (2.2×10^{-3} lb/g)

δP ratio of peak power to average power, P_p/P_1

$\Delta S/S$ spectral response ratio

S_e specific energy, w/ft²

η efficiency, %

θ angular difference between solar radiation vector and surface normal

λ radioisotope decay constant, $\ln 2/T_{1/2}$

μ_o linear attenuation coefficient, cm^{-1}

μ_r recharge overcapacity, w/w

ρ resistivity, ohm-cm

σ electrochemical equivalent of hydrogen, amp-hr/lb

ϕ ratio of peak load time to total cycle length, T_p/T_o

ϕ_n neutron flux density, neutrons/cm²

APPENDIX A

Photovoltaic Power System Analysis for a Mars Lander

This Appendix presents an analysis for an asynchronously loaded photovoltaic (PV), power system. The peak load power is asynchronous with respect to solar eclipse of the system. The system considered consists of a non-oriented photovoltaic power source and electrochemical, AgCd, energy storage. The analysis includes the effect on system size of solar energy attenuation through the atmosphere, battery charge rate limitations and battery temperature variations.

I. MISSION DESCRIPTION

The load profile is shown in Fig. A-1. Power level P_1 corresponds to the mission's passive observation period and power level P_p corresponds to the mission's active communications period. The peak load may occur at any time within a given planetary rotation depending on the Earth-Mars communication look-angle. The duration, αT_o, is that portion of the Mars rotation period (T_o) during which no solar insolation is incident on the lander's solar array (this is referred to as the eclipse period, T_e). The time ϕT_o is the duration of the active communication period. The parameter K represents that fraction of the peak load period (ϕ) occurring within the solar eclipse period (α).

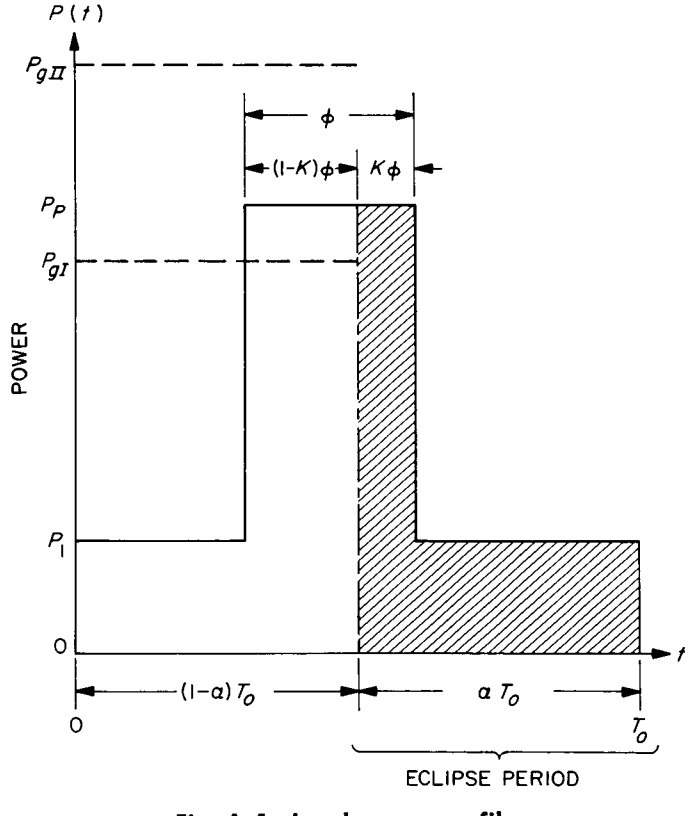

Fig. A-1. Load power profile

II. ENERGY BALANCE

Two energy balance equations must be written because of the discontinuity at $P_g = P_p$:

$$\text{I} \quad P_g < P_p; \qquad h(P_g - P_1)\beta = (P_g - P_p)(K-1)\phi + (P_p - P_1)K\phi + \alpha P_1 \tag{A-1}$$

$$\text{II} \quad P_g > P_p; \qquad h(P_g - P_1)\beta + h(P_g - P_p)(1-K)\phi = (P_p - P_1)K\phi + \alpha P_1 \tag{A-2}$$

where $\beta = 1 - \alpha - (1-k)\phi$. Recharge overcapacity can be derived for each case and is as follows:

$$\text{I} \quad P_g < P_p; \qquad \mu_{RI} = \frac{\alpha + \phi\,\delta P}{h(1-\alpha) + \phi(1-h)(1-K)} \tag{A-3}$$

$$\text{II} \quad P_g > P_p; \qquad \mu_{RII} = \frac{\alpha}{h(1-\alpha)} + \frac{\phi\,\delta P\,[h + K(1-h)]}{h(1-\alpha)} \tag{A-4}$$

where

$$\delta P = \frac{P_p}{P_1} - 1 = \bar{P}_p - 1,$$

and

$$\mu_R = \frac{P_g}{P_1} - 1 = \bar{P}_g - 1$$

A limiting case for each μ_R occurs when $P_g = P_p$, and at this value of P_g the calculation of μ_R transfers from μ_{RI} to μ_{RII};

$$\phi_T = \phi_{\text{transfer}} = \frac{h(1-\alpha) - \alpha/\delta P}{h + K(1-h)} \tag{A-5}$$

Figure A-2 shows μ_R as a function of ϕ for various values of the parameter K, and also shows the locus of ϕ_T for various δP.

III. POWER SOURCE SIZING

A worst case, from the viewpoint of system weight, occurs for $\alpha = 0.5$ which corresponds approximately to the solar eclipse encountered by an equatorial lander. For illustrative purposes the recharge efficiency, h, is assumed to be 50% and $\bar{P}_p$ is assumed to be 400% ($\delta P = \bar{P}_p - 1 = 3$).

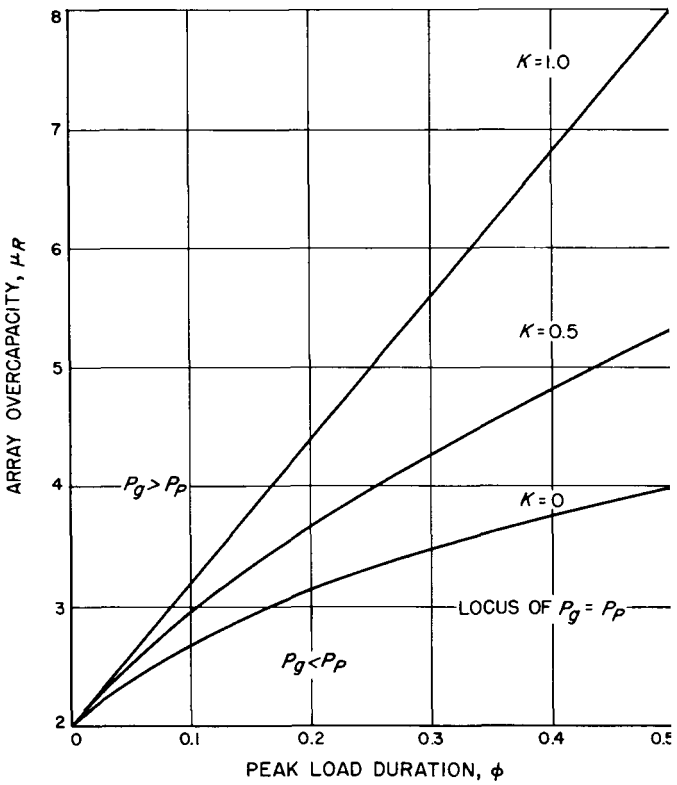

Fig. A-2. Recharge overcapacity

For sizing the solar array, the equations of interest Eq. (A-3), (A-4), and (A-5) reduce to the simple function of K, ϕ given below;

$$\mu_{RI} = \frac{2 + 12\phi}{1 + 2\phi(1-K)} \tag{A-6}$$

$$\mu_{RII} = 2 + 6\phi(1+K) \tag{A-7}$$

and

$$\phi_T = [6(1+K)]^{-1} \tag{A-8}$$

Equations (A-6), (A-7), and (A-8) are the actual function plotted in Figs. A-2 and A-3.

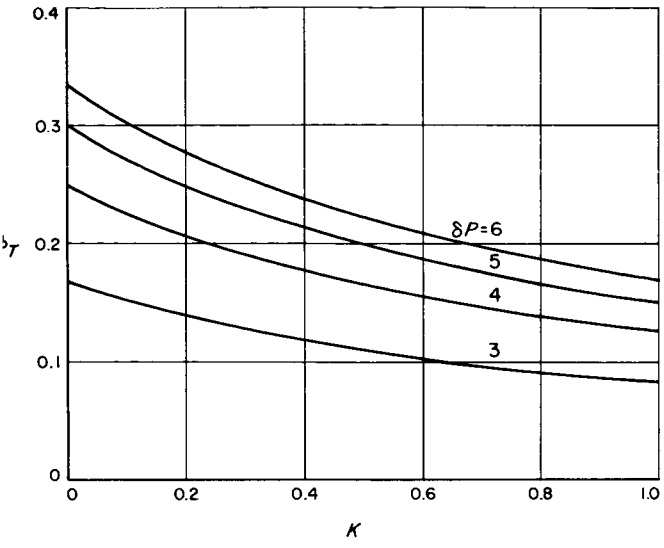

Fig. A-3. Values of peak load fraction for $\bar{P}_g = \bar{P}_p (\phi = \phi_T)$

Evidently, from Fig. A-2, a minimum value of μ_R occurs when $\phi = 0$, or more realistically when $(\phi \neq 0)$ $K = 0$. A minimum μ_R when $K = 0$ is reasonable because the power source is not penalized by the recharge losses during the period $K\phi$.

Although the recharge overcapacity due to any realistically proportioned load power profile is already quite high, the solar array weight is penalized even more. Assuming that solar array weight at *Mariner Mars* encounter is 0.22 lb/w (1.55 AU), we can derive the average specific weight on the Martian surface.

Power output decreases approximately as a function of the cosine of the angle of solar incidence (θ), thus, specific weight (a_g) at a given θ becomes:

$$a_g = 0.22 \frac{1}{\cos \theta}$$

A further decrease in output is caused by solar energy absorption through the atmosphere. This attenuation factor is calculated in footnote A-1. On the basis of that referenced calculation, the specific weight at any θ becomes:

$$a_g = \frac{0.22}{\cos \theta} (0.75)^{-\sec \theta} \qquad \text{(A-9)}$$

A-1 J. A. Zoutendyk, "The Effect of Solar Cosmic Radiation on Solar Cell Power Sources in Interplanetary Space," Jet Propulsion Laboratory, June 7, 1965.

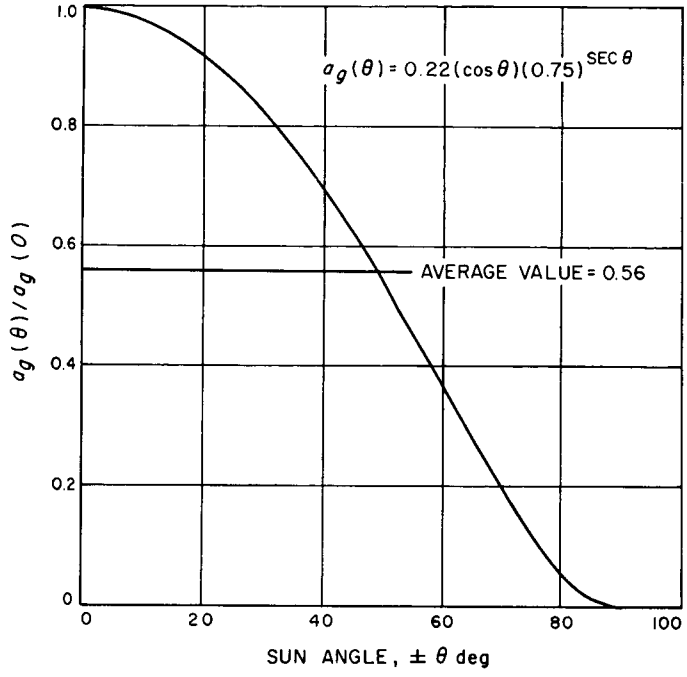

Fig. A-4. Normalized power degradation

The overall, normalized, power degradation factor $a_g/a_g(o)$ is plotted in Fig. A-4.

The average power output, taking into account both power degradation factors, is 56%. Thus, the effective specific weight should be: $a_g = 0.22/0.56 = 0.40$ lb/w. However, an additional penalty is sustained because for approximately 5% of the sunlight period, the value of $P_g(\theta) < P_1$. Therefore, the actual specific weight is probably no lower than 0.44 lb/w—double the Mars free-space value at 1.55 AU.

IV. DUTY CYCLING BY PLANETARY PERIOD

Reduction in the value of μ_R is achievable by means of duty-cycling by orbit. This is an operational mode, whereby, the active communication period is inhibited for one or more consecutive rotations of the planet. For instance, the energy balance relationship, Eq. (A-3), is modified by the parameter n, where n is the number of rotational periods for which the peak load is inhibited. The modified relationship results in a recharge overcapacity as given below:

$$\mu_R(n) = \frac{\alpha(n+1) + \phi\,\delta P}{h(1-\alpha)(n+1) + \phi(1-K)(1-h)} \qquad \text{(A-10)}$$

Equation (10) may be rewritten to give the value of $\mu_R(n)$ in terms of the recharge overcapacity with no duty-cycling by orbit, $\mu_R(o)$, and a modifying factor. This is given below in Eq. (A-11):

$$\frac{\mu_R(n)}{\mu_R(o)} = \frac{1 + \dfrac{n}{1+6\phi}}{1 + \dfrac{n}{1+2\phi(1-K)}} \qquad \text{(A-11)}$$

Also the value of ϕ at which $P_g = P_p$ (and at which μ_{RI} should be replaced by μ_{RII}) increases as given below:

$$\frac{\phi_T(n)}{\phi_T(o)} = n + 1 \qquad \text{(A-12)}$$

The reduction in μ_R with n is given in Figs. A-5 and A-6 for various values of ϕ and K. A least value of $\mu_R(n)/\mu_R(o)$ is calculable and corresponds to the case when n is very large:

$$\lim_{n\to\infty}\left|\frac{\mu_R(n)}{\mu_R(o)} = \frac{1+2\phi(1-K)}{1+6\phi}\right. \qquad \text{(A-13)}$$

The locus of the right-hand expression of Eq. (A-13) is shown in Figs. A-5 and A-6 along the line marked $n = \infty$.

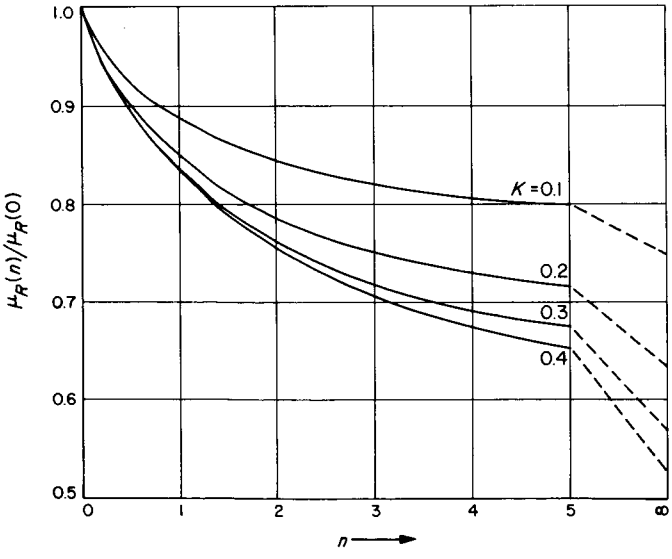

Fig. A-5. Reduction in solar panel overcapacity requirements as a function of the number of inhibited peak load periods (no peak load occurs during solar eclipse period, K = 0)

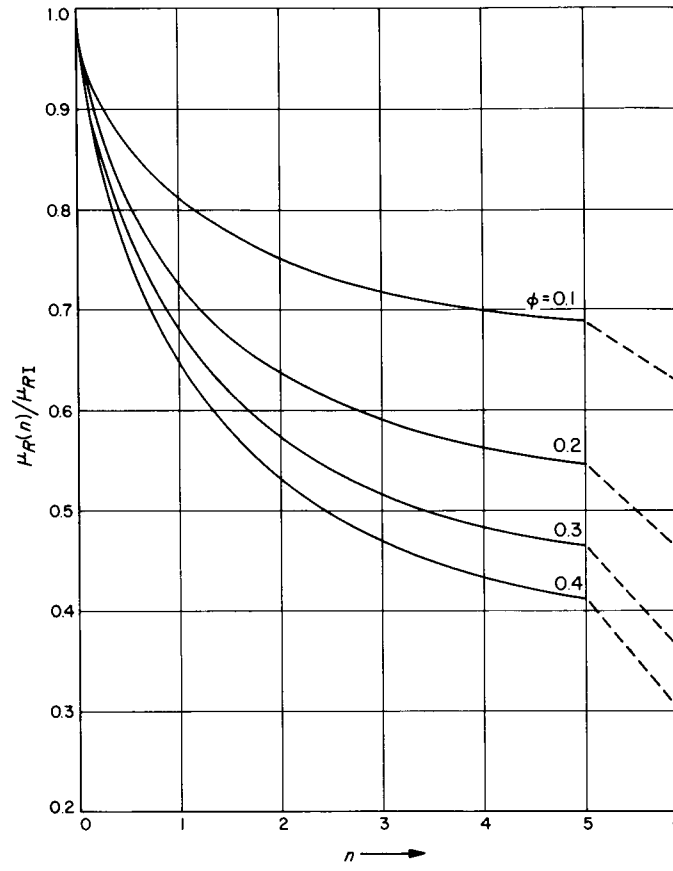

Fig. A-6. Reduction in solar panel overcapacity requirements as a function of the number of inhibited peak load periods (one peak load occurs during solar eclipse period, K = 1)

V. BATTERY SIZING

Basically, the battery rating is given simply by the energy discharged and the depth of discharge allowable. This is calculated below:

Energy out of battery (whr/w):

$$\bar{E}_{BI} = \left\{\alpha + \phi\,\delta P\left[1 - (1-K)\frac{\mu_{RI}}{\delta P}\right]\right\} T_o \qquad \text{(A-14)}$$

$$\bar{E}_{BII} = T_o(\alpha + K\phi\,\delta P) \qquad \text{(A-15)}$$

Energy rating of battery:

$$\bar{E}_R = \frac{\bar{E}_B}{d} \qquad \text{(A-16)}$$

where d = depth of discharge. To calculate the amp-hr rating of the battery we divide by the discharge voltage, V_D:

$$\bar{C}_R = \frac{\bar{E}_B}{V_D d} \tag{A-17}$$

Battery sizing is complicated further by the fact that charge-rate-limitation is reached. Because of the relatively long dark time ($\alpha = 0.5$), the Martian planetary period of rotation allows a maximum of only 12.5 hr to recharge the battery. This time is decreased if the active communication period (ϕ) uses an appreciable portion of the sunlight time.

The recharge time is also decreased (charge rate increased) because of the shape of the $P_g(\theta)$ curve. For P_g to provide charge current we must have $P_g > P_1$. However with $P_g(\theta)$ as shown in Fig. A-4, we have a period of approximately $0.05(1 - \alpha)T_o$ in which $P_g \leqq P_1$. This is an effective increase in α from $\alpha = 0.5$ to $\alpha = 0.55$. This situation also causes an increase in μ_R and a subsequent decrease in charge time (R_c).

Now, the discharge energy (E_B) and the recharge overcapacity (μ_R) increase as the peak load period moves into eclipse (K approaches unity), and one would be led to believe that maximum system weight occurs when $K = 1$ (and that minimum system weight occurs when $K = 0$). However, the effect of charge-rate-limitation and temperature are such that this may not be entirely the case.

To calculate the effect on battery size of charge-rate-limitations, we first calculate the charge current, I_c:

$$\text{I} \quad P_g < P_p; \quad \bar{I}_{cI} = \frac{h\mu_{RI}}{V_c} \tag{A-18}$$

$$\text{II} \quad P_g > P_p; \quad \bar{I}_{cII} = \frac{h\mu_{RII}}{V_c} \tag{A-19}$$

$$\bar{I}_{cII} = \left(\frac{h\mu_{RII}}{V_c}\right)\left(\frac{1 - \delta P}{\mu_{RII}}\right) \tag{A-20}$$

where V_c is the battery charge voltage. There are two discrete values of I_c for the case where P_g = constant, because charging takes place both during the passive period when $h(P_g - P_1)$ is available and during the active period when only $h(P_g - P_p)$ is available.

A fairly good case can be made for using the higher value of charge current (in evaluating the effect of charge rate) as given by Eq. (A-19):

1. The battery temperature is lowest at the start of charge.
2. The battery efficiency is highest at start of charge.
3. The charge control efficiency is higher at the higher charge current level.
4. Charge voltage is lower at start of charge.
5. It is not possible to completely utilize the source overcapacity (because P_g is not constant, but a complex function of angle of incidence).

For the above reasons we use the charge current as given by Eq. (A-19) and disregard the charge current given by Eq. (A-20). The charge rate (R_c, hr) can now be calculated as follows:

$$R_C = \frac{C_R}{I_c} = \frac{\bar{C}_R}{\bar{I}_c} \tag{A-21}$$

This yields, for the two cases considered:

$$R_{cI} = \frac{T_o}{h_v d}\left[1 - \alpha - (1 - K)\phi\right] \tag{A-22}$$

and

$$R_{cII} = \frac{T_o}{h_v d}\left[\frac{1 - \alpha}{1 + \dfrac{h(1 - K)}{K + \dfrac{\alpha}{\phi\,\delta P}}}\right] \tag{A-23}$$

where

$$h_v = \frac{V_C}{V_D}$$

Obviously, the maximum charge rate (minimum charge time) occurs when $K = 0$, i.e., when the active communication period is in sunlight. Under these conditions Eqs. (A-22) and (A-23) reduce to the following:

$$R_{cI} = \frac{T_o}{h_v d}(1 - \alpha - \phi) \tag{A-24}$$

$$R_{cII} = \frac{T_o}{h_v d}\left[\frac{1 - \alpha}{1 + \dfrac{h\phi\,\delta P}{\alpha}}\right] \tag{A-25}$$

These calculations of charge rate are based on an *average* value of $P_g(\theta)$. However, a glance at Fig. A-7 will show that, at least intuitively, the effect of charge rate limitation should be worse than that calculated by using average P_g. This is because of the large peak charge currents necessary to maximally utilize the array output. As an approximation to this, we decrease the equivalent charge time by the rms-to-average ratio of $P_g(\theta)$. A typical calculation of R_c proceeds as follows:

$$R_{cII} = \frac{25}{0.75(0.7)} \cdot \frac{1 - 0.5}{1 + (0.5)\,0.2\,(3/0.5)} = 14.8\text{ hr}$$

Effect of using rms instead of average charge current yields:

$$R_{cII} = \frac{0.56}{0.66} \times 14.8 = 12.6\text{ hr}$$

Effect of increasing α to 0.55 gives $R_{cII} = 11.7$ hr. These values of R_{cII} are typical of the situation for $\phi = 0.2$ and $\delta P = 3$. A rapid decrease of R_{cII} occurs for increasing peak power ratio, $\phi\delta P$.

Charge rate, R_{cII}, and rate-limited battery overcapacity are shown in Fig. A-8 as a function of the peak load energy; the product $\phi\delta P$. The two capsule modes (I & II) indicated are those given in Section II of this Report. From Fig. A-8 can be seen the drastic effect on battery size caused by temperature (T_B) and peak load energy (ϕP).

It should be noted that (although the battery is initially sized by its discharge energy, depth of discharge allowable, and cycle-life considerations) the charge-rate-limitation imposes a first-order increase in the basic battery rating.

One other point: It seems likely that battery temperature is higher at the start of charge when the peak load discharge occurs immediately prior to the eclipse period (as shown in Fig. A-7), than if the peak load occurs immediately after the eclipse period. Due to the asynchronism extant between the Earth and Mars periods of revolution, both conditions relating to the locus of the peak load exist. Thus, in Fig. A-8 we have shown the rate-limited overcapacity for mean battery temperatures of +50°F and +60°F. The difference in the theoretical rate-limited overcapacity is remarkable.

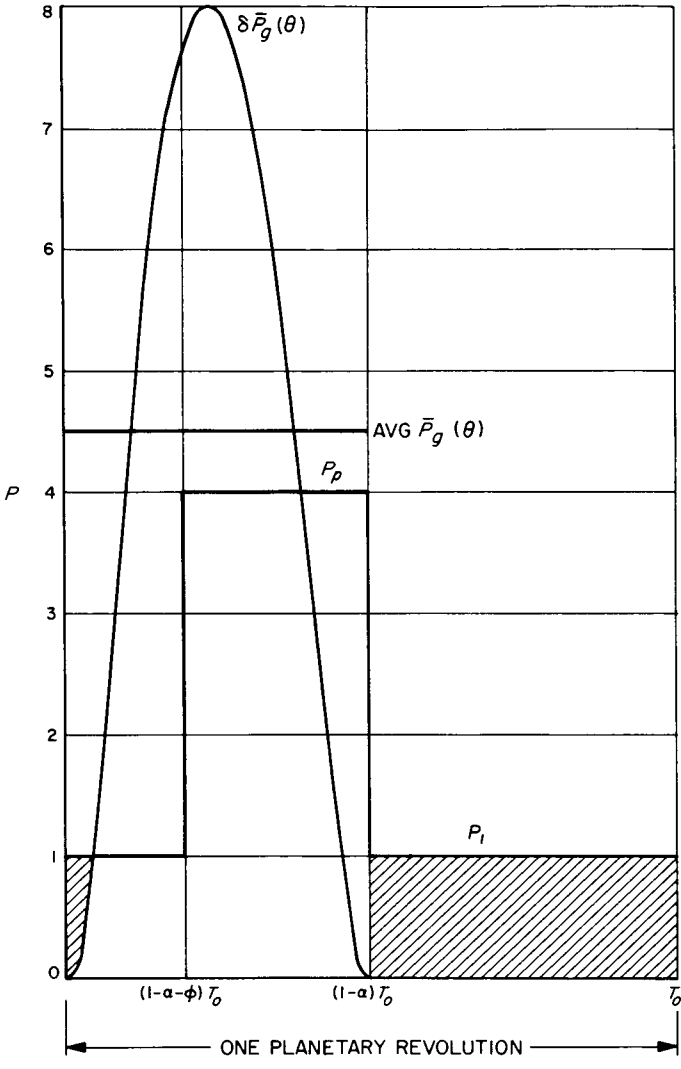

Fig. A-7. Load and source profile

For Capsule I, with the battery temperature at 50°F the effective specific energy of a AgCd battery would be approximately 14.4 whr/lb at 100% depth of discharge

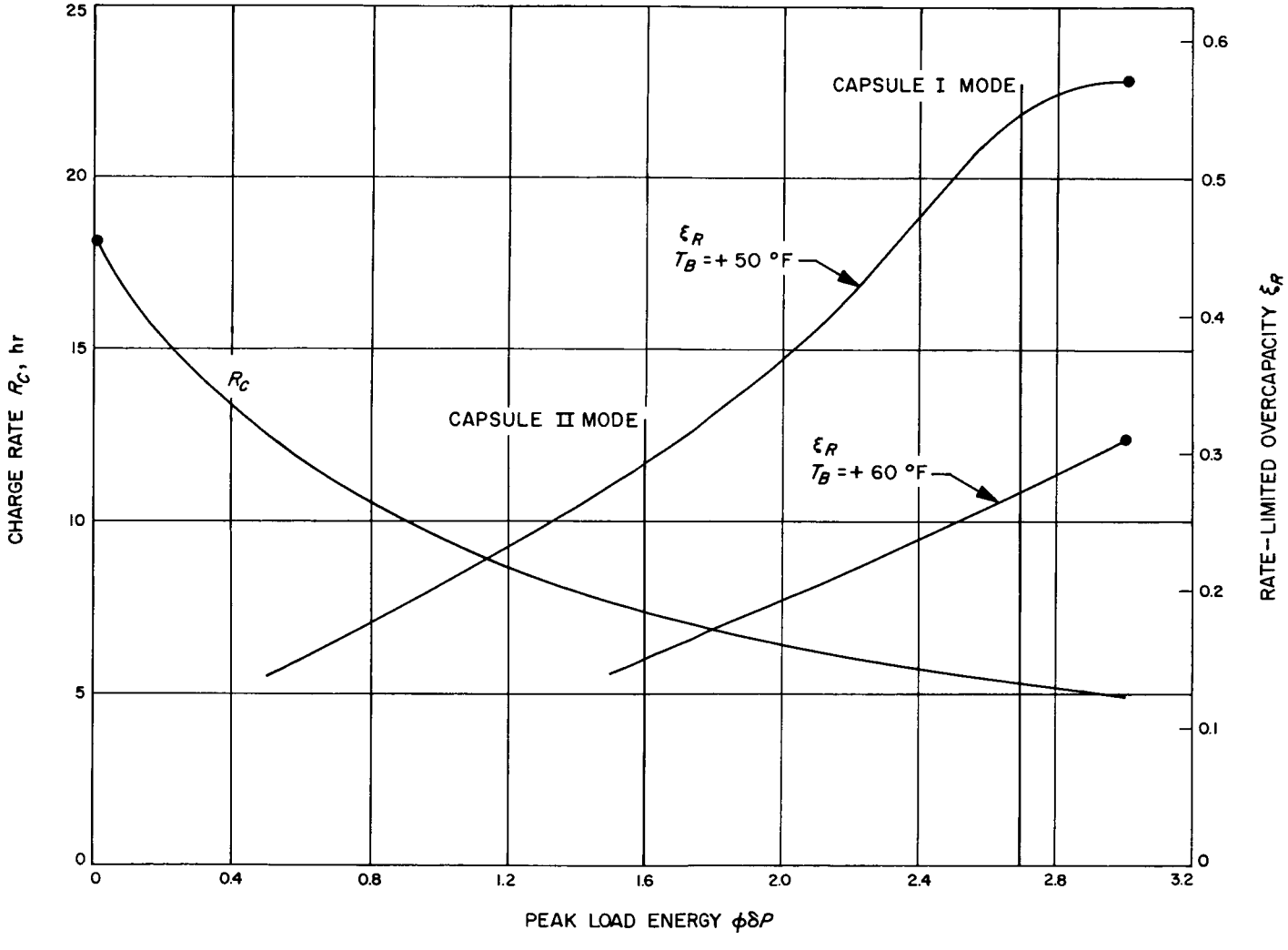

Fig. A-8. Battery charge rate and battery overcapacity due to limited charging time as a function of peak load energy

APPENDIX B

A Mars Lander Tradeoff Study of Solar Cells and Radioisotope Thermoelectric Generators

This study has been performed to determine the margin and weight tradeoff between photovoltaic, PV, and thermoelectric, TE, power sources. The study considered a Mars landing vehicle using these power sources.

The major conclusion of this study is that for Martian surface operation, thermoelectric systems weigh 40 to 50% less than an equivalent solar cell system.

I. MISSION DESCRIPTION

A landing vehicle is assumed at or near the Martian equator. It is supposed that the scientific and communications loads are constant and that the vehicle is in darkness half of each planetary rotation. The power profile considered is shown in Fig. B-1.

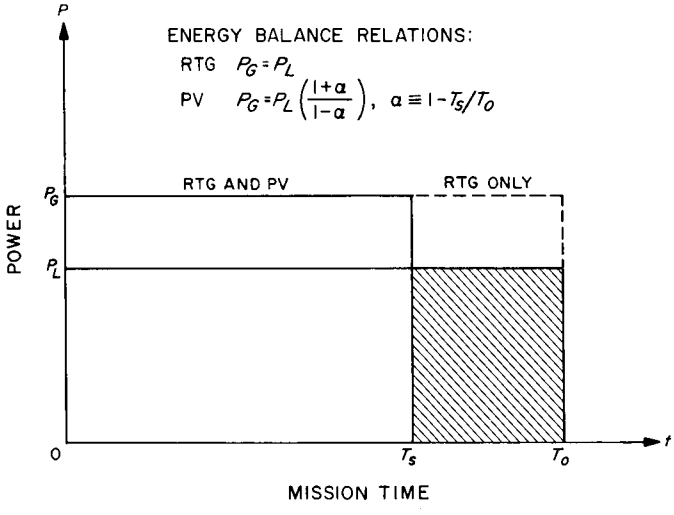

Fig. B-1. Mission power profile

Some simplifying assumptions (which should yield valid results to a first approximation) are:

a. The effect of atmospheric dust is no larger on solar panels than on RTG radiators, this is conservative in favor of a PV system.

b. The effect of ambient air temperature variations on solar panels or RTG radiators is not considered. This is conservative in favor of a PV system.

c. The shock effect of a hard landing does not affect the solar panels, battery, and associated attitude control equipment any more than it affects an RTG system.

Referring back to Fig. B-1, an energy balance can be performed for both the TE and PV systems. From the energy balance we derive the bare minimum size of the generator (P_G, w) and the battery capacity (C_B, amp-hr).

For the *TE* system we obtain,

$$P_G = P_L \tag{B-1}$$

and for the *PV* system we obtain,

$$P_G = P_L \frac{1+\alpha}{1-\alpha} \tag{B-2}$$

where $\alpha = 1 - T_s/T_o$, (eclipse fraction).

The overcapacity (μ_R) for recharging the battery after each solar eclipse is a strong function of the eclipse fraction (α) and is shown in Fig. B-2. The curve of Fig. B-2

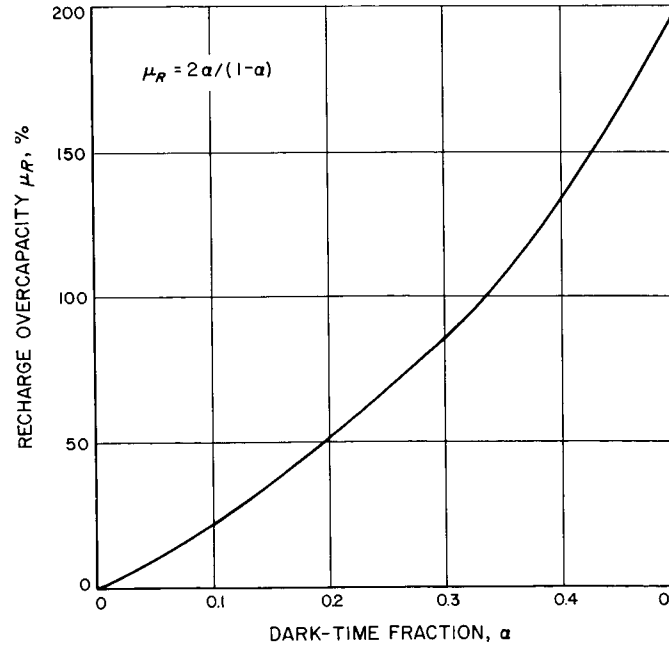

Fig. B-2. Effect of eclipse on photovoltaic source size

was derived on the basis of a recharge efficiency (h) of 50%.

The recharge efficiency accounts for battery and charge control losses in the charge mode. Symbolically we have:

$$h = h_c h_i h_v \tag{B-3}$$

where

h_c = converter efficiency (assumed 80%),

h_i = battery amp-hr efficiency (assumed 95%), and

h_v = battery discharge-voltage to charge-voltage ratio (assumed 65%).

The voltage ratio, h_v, used herein is calculated from the minimum battery discharge voltage (1.02 v/cell) and the maximum battery charge voltage (1.55 v/cell). This is a very conservative estimate because considerable energy is available from the battery at voltages greater than the minimum discharge voltage, and may be replaced in the battery at voltages less than the maximum charge voltage. However, the value $h = 0.5$ is used because it simplifies many, otherwise inelegant, expressions.

The installed capacity of the battery with no margin is derived from the energy balance consideration and is:

$$C_B = P_L T_o \alpha / V_c d \tag{B-4}$$

II. SYSTEM DESCRIPTION

The system which implements the requirements imposed by the energy balance is shown in Fig. B-3. Such a system using an RTG source can dispense with the battery and charge control equipment because power is available over the complete planetary rotation.

However, with a PV source, the battery and charge control are indispensable: In sunlight (T_s) the photovoltaic generator, PVG, supplies all required load power plus battery recharge power. As the planet turns, the insolation of the PVG decreases, its current capability decreases and an increasing proportion of the load current is drawn from the battery (commonly referred to as *load sharing*). Finally the vehicle passes into total darkness and the battery must provide full load power. As

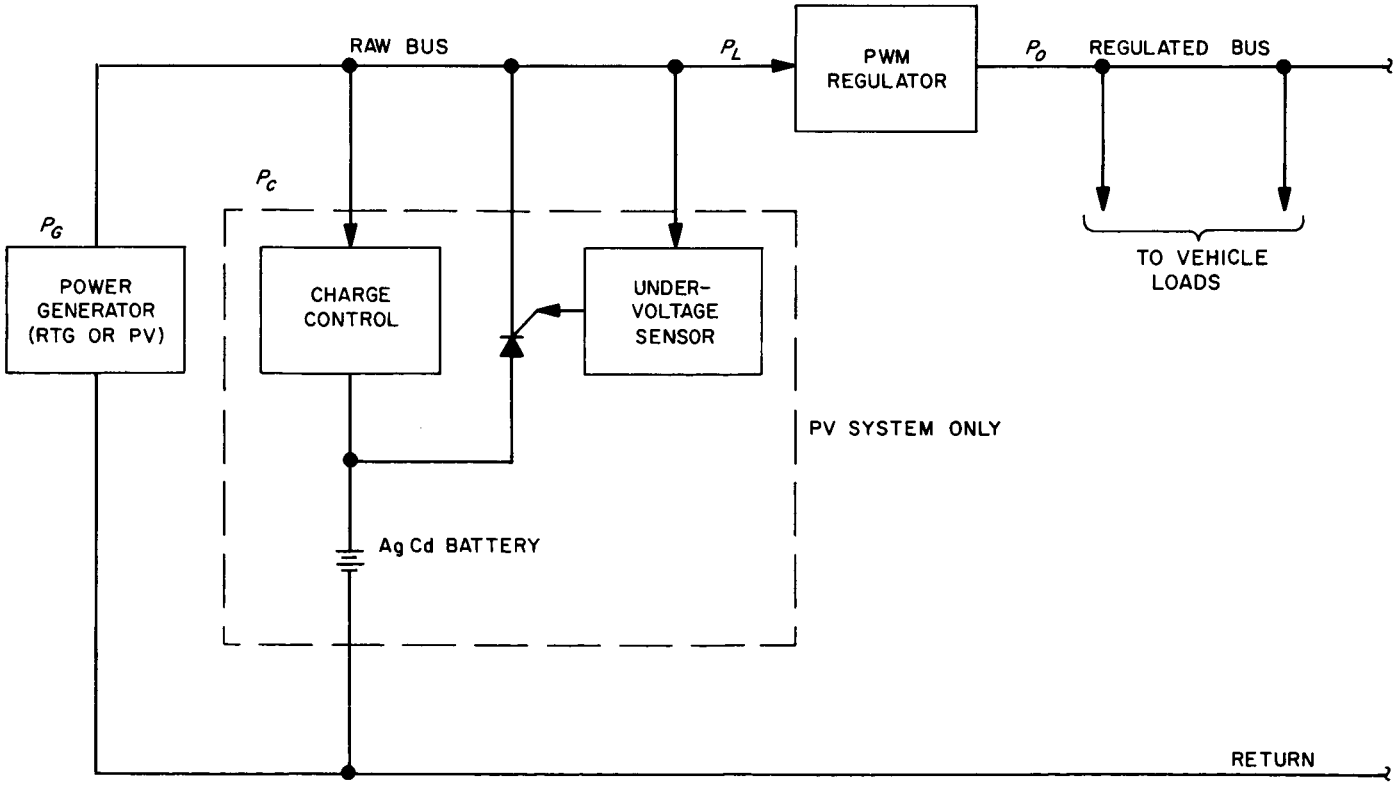

Fig. B-3. System block diagram

the vehicle subsequently emerges into sunlight two effects are manifest:

1. The PVG being extremely cold (200°K) produces a high voltage and a slowly increasing current capability, thus taking over the load carrying capability from the battery (and automatically resetting the discharge current switch—the silicon controlled rectifier, SCR, in Fig. B-3).
2. The battery is cold and is not capable of absorbing more than a fraction of its installed capacity because of the high charge rate, R_c, requirements.

   The effect of a cold battery and a high charge rate on battery size and system weight is analyzed in Sections 5 and 6 below.

III. SYSTEM INTERACTIONS

Two major assumptions are necessarily made in relation to the interaction of PV system components: (1) no load sharing in sunlight at maximum load and (2) undervoltage, U/V, actuation at the maximum power point voltage.

A. Assumption 1

No load sharing in sunlight implies that the PVG must be sufficiently large so that it can support the load without any unstable or undesirable operating modes. This consideration actually defines the margin for the source.

B. Assumption 2

Undervoltage actuation at the maximum power point voltage, implies that maximum use of the PVG occurs (although the maximum power point voltage varies, we can select its minimum value, which should correspond roughly to the minimum PVG power capability, and state that maximum PVG utilization occurs when minimum PVG capability exists).

IV. GENERATOR MARGIN

The generator overcapacity due to operating margin requirements is

$$\mu_m = \frac{P_{lm}}{P_m} - 1 \qquad \text{(B-5)}$$

The margins for both thermoelectric and photovoltaic sources operating into constant-power loads are shown in Fig. B-4. From the Figure, it is quite evident that PV systems require significantly larger margins than TE systems for a given range of bus voltage, R.

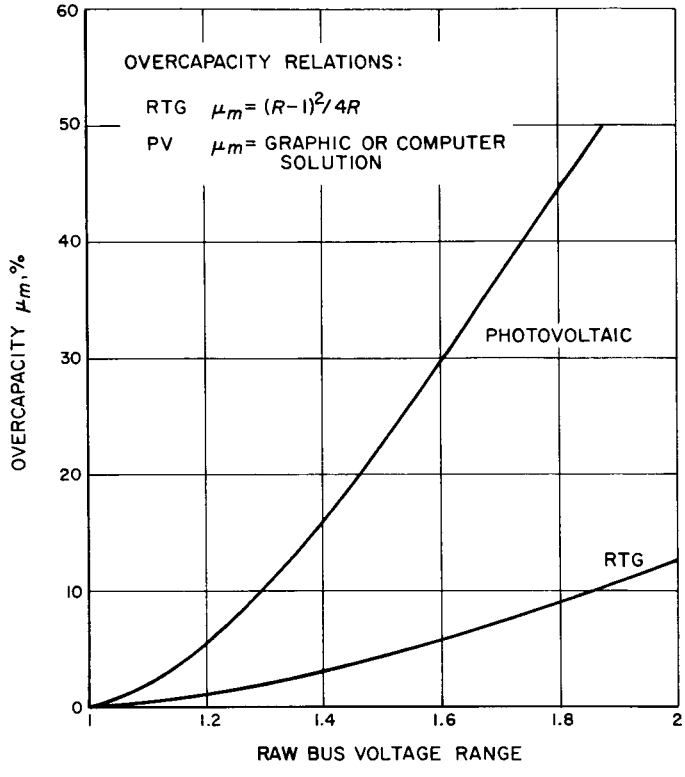

Fig. B-4. Comparison of operating margins

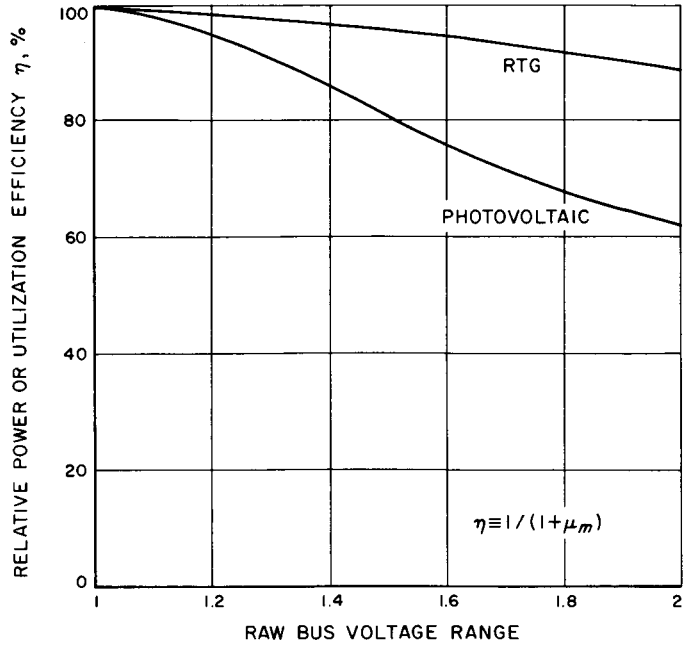

Fig. B-5. Comparison of source utilization

It should be noted that the values of margin given are for the following models:

$$\text{RTG,}\quad y = 1 - x \tag{B-6}$$

$$\text{PVG,}\quad y = 1 - \xi^{b_1(x-1)} \tag{B-7}$$

Although the margin is readily enough calculable for an RTG, it is quite involved for a PVG because of the number of variables. One way of presenting the comparison of margins is shown in Fig. B-5. The given curves answer the following question: What is the maximum bus voltage range allowable while maintaining a given fraction of the maximum power out of either an RTG or PVG? If the power fraction assumed is 90%, then for a PVG the allowable bus range $R \leqq 1.32$, and for an RTG the allowable bus range $R \leqq 1.93$.

V. BATTERY MARGIN

Battery margin, as used herein, refers to excess battery capacity necessitated by charge-rate limitation. When a battery is to be charged rapidly it is not always possible to return all of its initial capacity. Thus, the installed capacity must be increased to account for this effect. Figure B-6 shows the maximum capacity to which a AgCd cell can be recharged at various cell temperatures and rates. Figure B-7 shows this same information plotted such that the overcapacity is given directly as a fraction of the assumed installed capacity value. Note that the overcapacity due to charge rate limitation is an extremely strong function of cell temperature.

In the case under consideration, the vehicle interior was assumed to be fairly cool (approximately 10°C) because the Martian temperature environment on and near the surface is quite low.[B-1] Given the various mission parameters, a simple calculation yields a recharge rate. The assumed installed capacity is given by Eq. (B-4) and charge current is given by:

$$I_c = \mu_R h_C P_L / V_C \tag{B-8}$$

and

$$R_c = (1 - \alpha)\, T_o h_v^2 h_i / d \tag{B-9}$$

where h_i is the cell amp-hr efficiency and h_v, α, T_o, and d are as defined above

and

$$R_c = 7.1 \text{ hr.}$$

[B-1] R. L. Newburn, Jr., "The Environment in the Vicinity of the Surface of Mars," Jet Propulsion Laboratory, EPD 271, March 1, 1965.

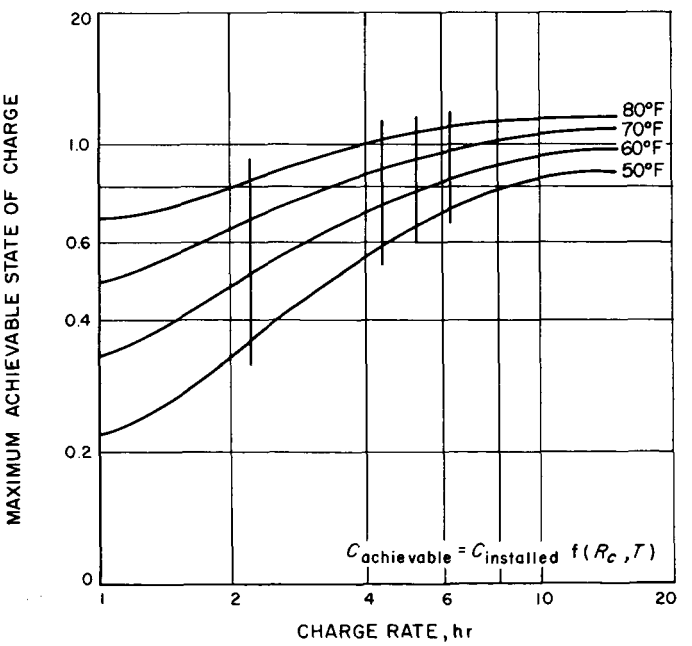

Fig. B-6. Maximum capacity to which a AgCd cell can be recharged as a function of cell temperature and charge rates

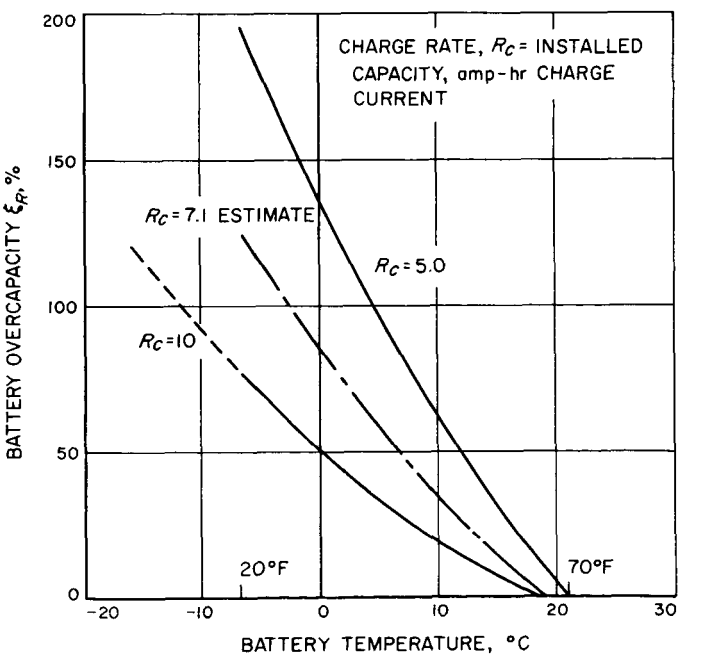

Fig. B-7. Overcapacity due to charge-rate limitation of AgCd batteries

At the 10°C temperature assumed and at the charge rate (7.1 hr) calculated, the battery overcapacity is given by the curves of Fig. B-7 as approximately 34%. The increase in overcapacity with temperature is so rapid, that at 5°C the overcapacity is 58%.

VI. WEIGHT TRADEOFF

A. Generator Weight

The weight of the RTG and PVG may be calculated from the mission parameters and from the specific weights of the various equipments:

$$W_{PVG} = (a_{PV})_E S^2 \frac{1+\alpha}{1-\alpha} P_L \qquad \text{(B-10)}$$

$$W_{RTG} = a_{TE} P_L \qquad \text{(B-11)}$$

where S is the distance from the Sun in AU, and all a's are lb/w or lb/whr as applicable.

Taking the ratio of W_{PVG} to W_{RTG} and setting this ratio equal to unity (equal generator weights), we obtain:

$$\frac{a_{TE}}{(a_{PV})_E} = S^2 \frac{1+\alpha}{1-\alpha} \qquad \text{(B-12)}$$

This relation is shown in Fig. B-8 as curves A, B, and C. Curve A shows the solar distance at which the generator

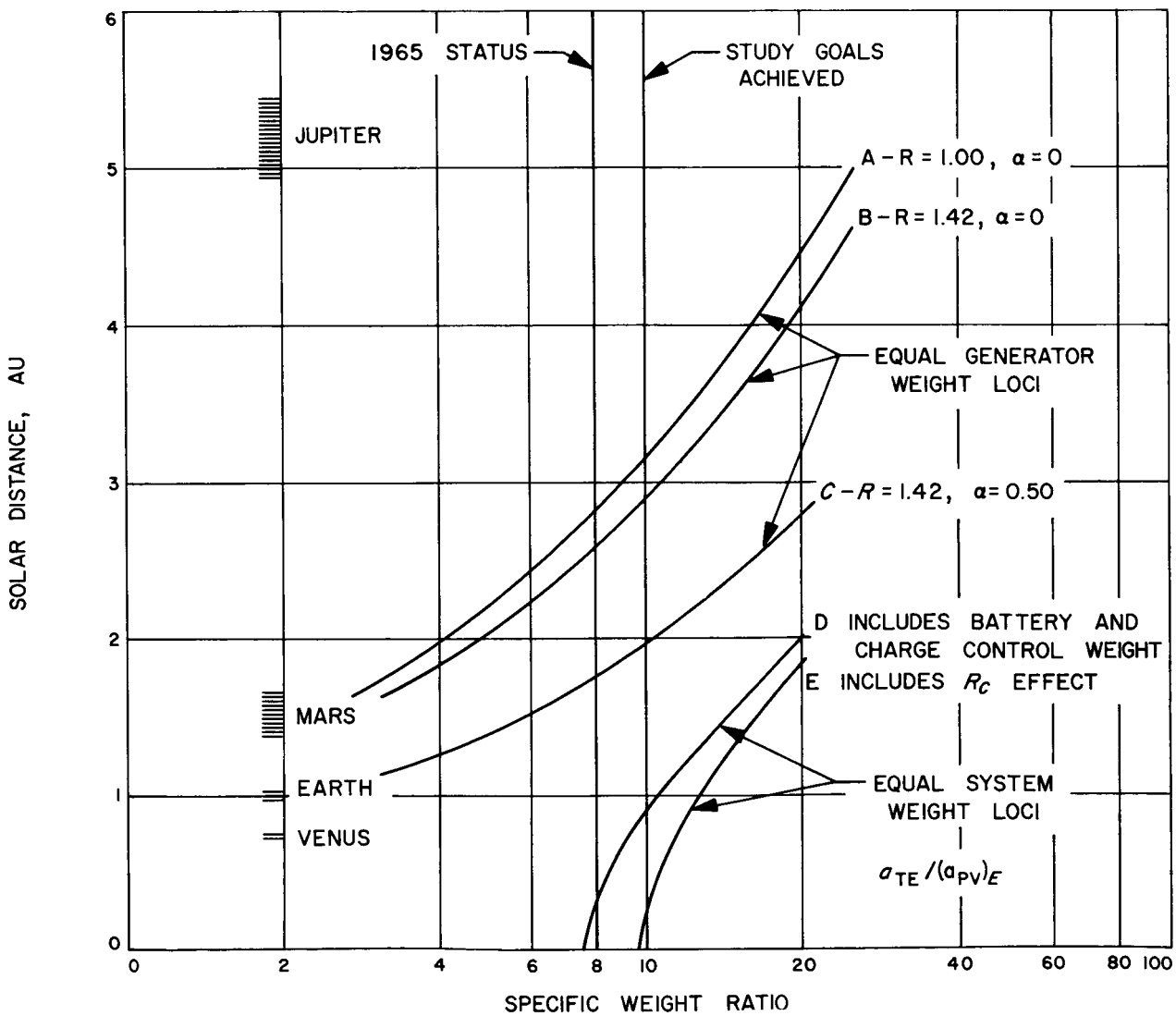

Fig. B-8. Relative system specific weight ratios as a function of operational distance from the Sun

weights are equal for a bus range of $R = 1.0$ and no eclipse ($\alpha = 0$). Curve B is a variation of curve A in that it shows the effect of a bus voltage range of $R = 1.42$, which is the expected range for a system using AgCd batteries.

Curve C includes the effect of a 50% eclipse and shows a radical decrease in the solar distance at which equal generator weight occurs.

B. System Weight

The weight of a complete system using a PVG, battery, and charge control was calculated and compared to the weight of an RTG only. The weight of a photovoltaic system is:

$$W_{PV} = (a_{PV})_E S^2 \frac{1+\alpha}{1-\alpha} P_L + a_B V_D C_B + a_C P_C \qquad \text{(B-13)}$$

where a_B is the unit weight of a AgCd battery, a_C is the unit weight of the associated charge control, and P_c is the average recharge power.

The weight of a thermoelectric system is:

$$W_{TE} = W_{RTG} = a_{TE} P_L \qquad \text{(B-14)}$$

Taking the ratio W_{TE} to W_{PV} we derive the locus of equal system weights:

$$\frac{a_{TE}}{(a_{PV})_E} = S^2 \frac{1+\alpha}{1-\alpha} + 11 + \frac{1.2}{1-\alpha} \qquad \text{(B-15)}$$

Given $h = 0.50$, the specific weight ratio becomes:

$$\frac{a_{TE}}{(a_{PV})_E} = 3S^2 + 7.6 \qquad \text{(B-16)}$$

Equation (B-16) is plotted in Fig. B-8, curve D, and the solar distance at which equal system weight occurs is $S = 1.54$ AU.

C. Charge Rate Effect

If the effect of battery charge rate limitation is taken into account, we obtain curve E of Fig. B-6. Assuming an average battery temperature during recharge of $+10°C$, we have for the equal weight locus:

$$\frac{a_{TE}}{(a_{PV})_E} = 3S^2 + 9.7 \qquad \text{(B-17)}$$

From curve E, and for the present (1965) weight ratio, it can be seen that a thermoelectric system weighs less than a photovoltaic system—even at Mars perihelion (1.38 AU).

If it is assumed that both the RTG and PVG study goals (2 w/lb and 20 w/lb, respectively) are achieved the TE system still weighs less than the PV system.

Actual system weight ratios are given in Fig. B-9. From the Figure we see that, with the present state-of-art, a photovoltaic system weighs 64 to 96% more than an equivalent thermoelectric system.

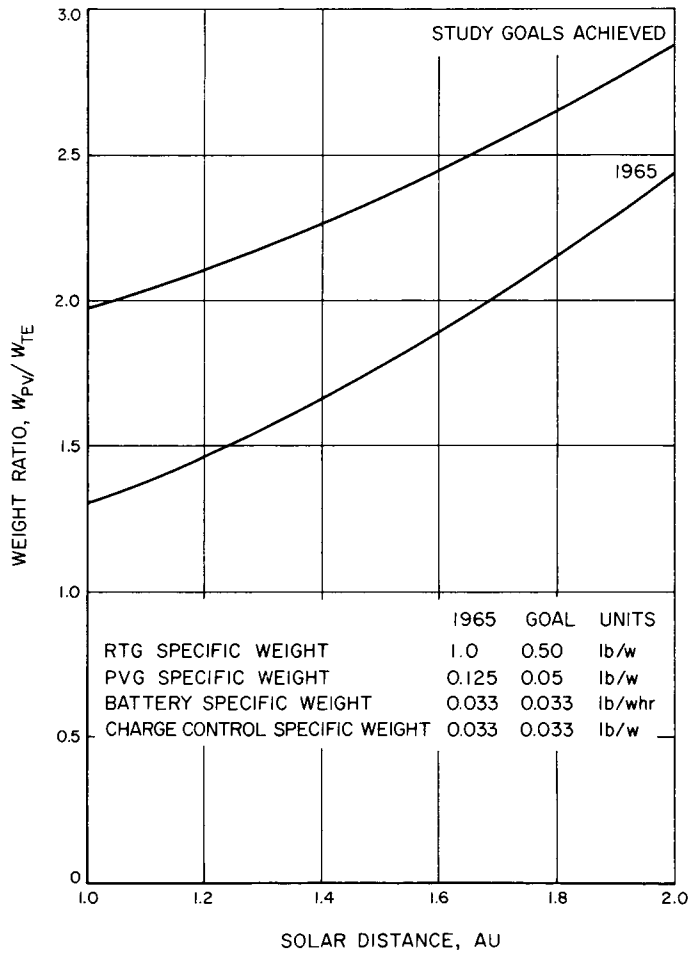

Fig. B-9. Ratio of weights of photovoltaic to thermal electric systems as a function of operational distance from the Sun

NOMENCLATURE, APPENDIXES A AND B

a_B AgCd battery unit weight, lb/whr

a_c charge control unit weight, lb/w

a_g solar array specific weight, lb/w

$\bar{C}$ normalized battery capacity, amp-hr/w

C_B, C_R rated battery capacity at start of mission, amp-hr

d depth of discharge allowable as a fraction of C_b

$\bar{E}$ energy required from battery, whr

$E_{b,R}$ rated battery energy capacity, whr

E_B normalized energy, whr/w

h recharge efficiency, product of battery whr efficiency and charge control unit efficiency, $h = h_w h_c$

h_c charge control conversion efficiency

h_i battery amp-hr efficiency

h_r battery voltage efficiency, V_c/V_D

$\bar{I}$ normalized current, $\bar{I} = I/P_1$, amp/w

I_c battery charge current, amp

n number of orbital rotational periods for which peak power loads are inhibited

$\bar{P}$ normalized power, with respect to P_1

P_e eclipse load; average power during eclipse periods, w

P_G, P_g source power; average source (array, generator) power available at end of mission life, w

P_p peak load; average of all load power levels greater than P_g, w

P_1 average of all load power levels less than P_g, v

R raw bus voltage range

R_c battery charge rate, hr

S distance of object from Sun, AU

T_B temperature, °F

T_e duration of solar eclipse, hr

T_p duration of peak load, hr

T_o orbital period or cycle length, hr

T_s duration of sunlight, hr

V_C battery charge voltage, v

V_D battery discharge voltage, v

x normalized source voltage, $x = V/V_{OC}$

y normalized source current, $y = I/I_{SC}$

α T_e/T_o

δP normalized peak power differential, $\delta P = P_P/P_1 - 1$

θ angle of solar incidence

μ_m margin overcapacity, overcapacity due t operating margin requirements, w/w

μ_R recharge overcapacity, overcapacity due t battery recharge requirements, w/w

ξ overcapacity of storage device on an energ basis (fraction of energy required in a give time period due to margin or other opera tional requirements), whr/w

ξ_{RC} charge limited overcapacity; overcapacity o battery due to limited charging time, whr/v

ϕ T_p/T_o

APPENDIX C

Thermal Considerations of a Radioisotope Power System for a Mars Lander

The purpose of the thermal portion of this study was to determine the amount of radiator area required for various types of radioisotope-fueled power systems. To accomplish this, the various mission phases from sterilization through landed operations were studied to determine the relative thermal severity of the various environments. The missions phases studied included: sterilization, cruise with sterilization canister on, near Earth midcourse maneuver with sterilization canister off, separated capsule, entry, and surface operation. The power systems studied were radioisotope-fueled systems of the following types: thermoelectric, closed loop vapor cycle (Rankine), closed loop gas cycle (Brayton), and thermionic. The purpose of this study, then, was to find the operational phase which sizes the radiator area for each of these systems.

One of the criteria for selecting a Mars lander power system will be total power system weight. Part of the total weight will be contributed by the area required to radiate the heat rejected from the power system. Because radiator weight will be directly proportional to radiator area, estimates of the amount of radiator area required are necessary to compare competing power systems.

Required radiator area is a function of items (1) total heat to be dissipated, (2) radiator temperature, (3) radiator emissivity, (4) heat sink temperature, (5) heat sink area, (6) heat sink emissivity, and (7) radiator/heat sink geometry. Item (1) is a function of the type of power system and in this study assumed constant for a given power system, since radioisotope fuel is used. Item (2) is a power system parameter, which for this study was assumed to be a given requirement only when electrical power was required. When electrical power is not required, it was assumed another, higher temperature requirement would apply. Items (3) and (6) are a material property and a reasonably high value (0.85) was

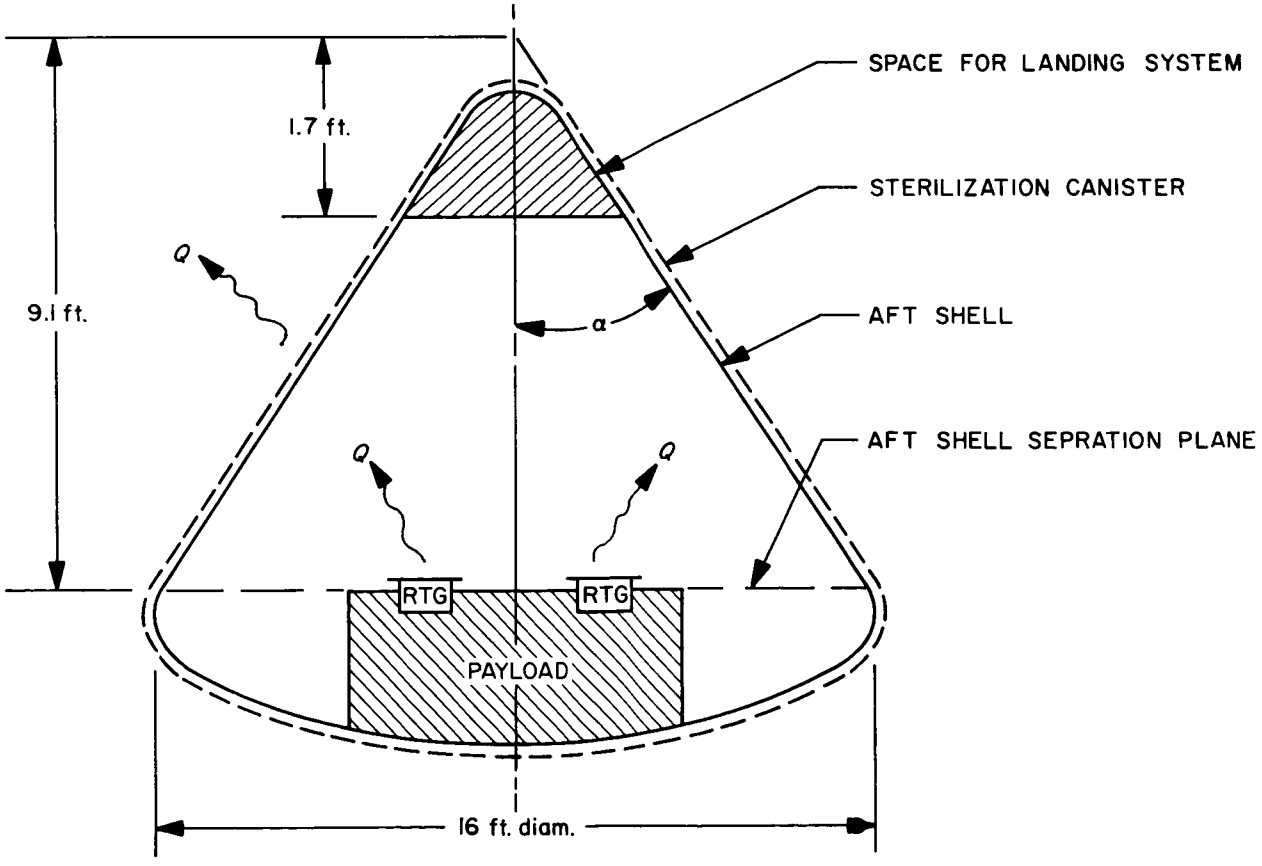

Fig. C-1. Capsule configuration

assumed, since radiator area varies inversely with this property. Items (5) and (7) are functions of the entry body/payload geometry, which are affected by many factors. Here the simplifying assumption was that the radiator had an unobstructed radiative view to the afterbody of a 16-ft diam Apollo-shaped entry body, as depicted in Fig. C-1. The effects on capsule temperature due to the presence of a biological barrier (sterilization canister) and a capsule aft-shell were determined in a separate study using RTG's with thermal powers up to 6000 w. Only the cruise phase was considered. The results of the study are shown in Figs. C-2 and C-3. Figure C-2 indicates the temperatures of the shells and radiator, for various radiator sizes, as a function of thermal power. Figure C-3 shows the effect on the radiator temperature by the presence of the canister and aft-shell. As can be seen, their presence does not greatly affect the radiator temperature. The equations used to describe this transfer of heat from the RTG to the aft-shell, from the aft-shell to the sterilization canister, and hence to space are summarized at the end of this Appendix.

The heat sink temperature listed as item (4) in the preceding paragraph, is dependent upon the amount of heat rejected and operational phase. Because this temperature significantly affects the size of the radiator, the operational phases were surveyed to determine which was most severe, and thereby sizes the radiator. The operational phases surveyed were: sterilization, near Earth cruise with biological barrier (sterilization canister) on, near Earth midcourse maneuver with sterilization canister off, separated capsule, entry, and surface operation.

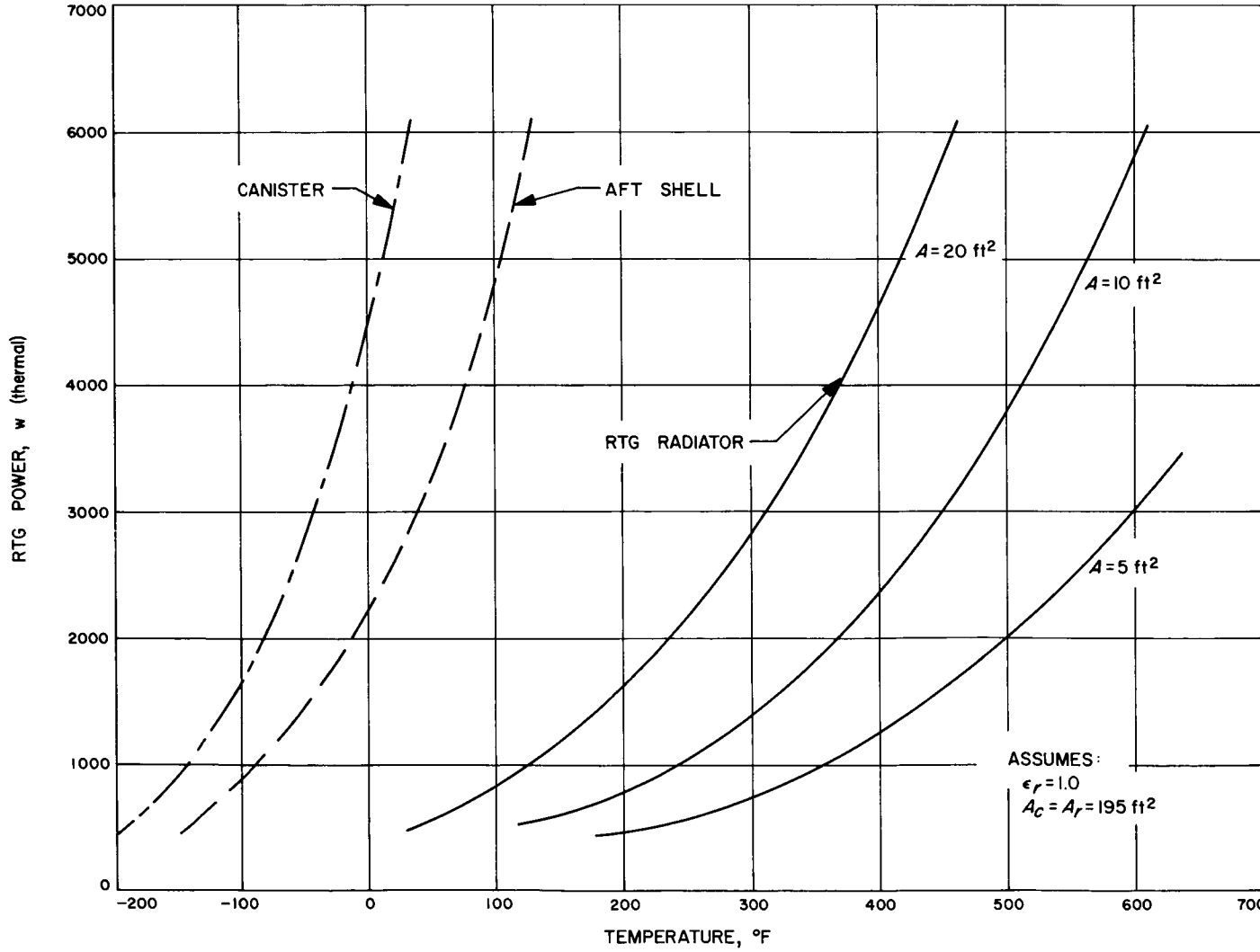

Fig. C-2. Capsule-RTG temperatures in pre-release configuration

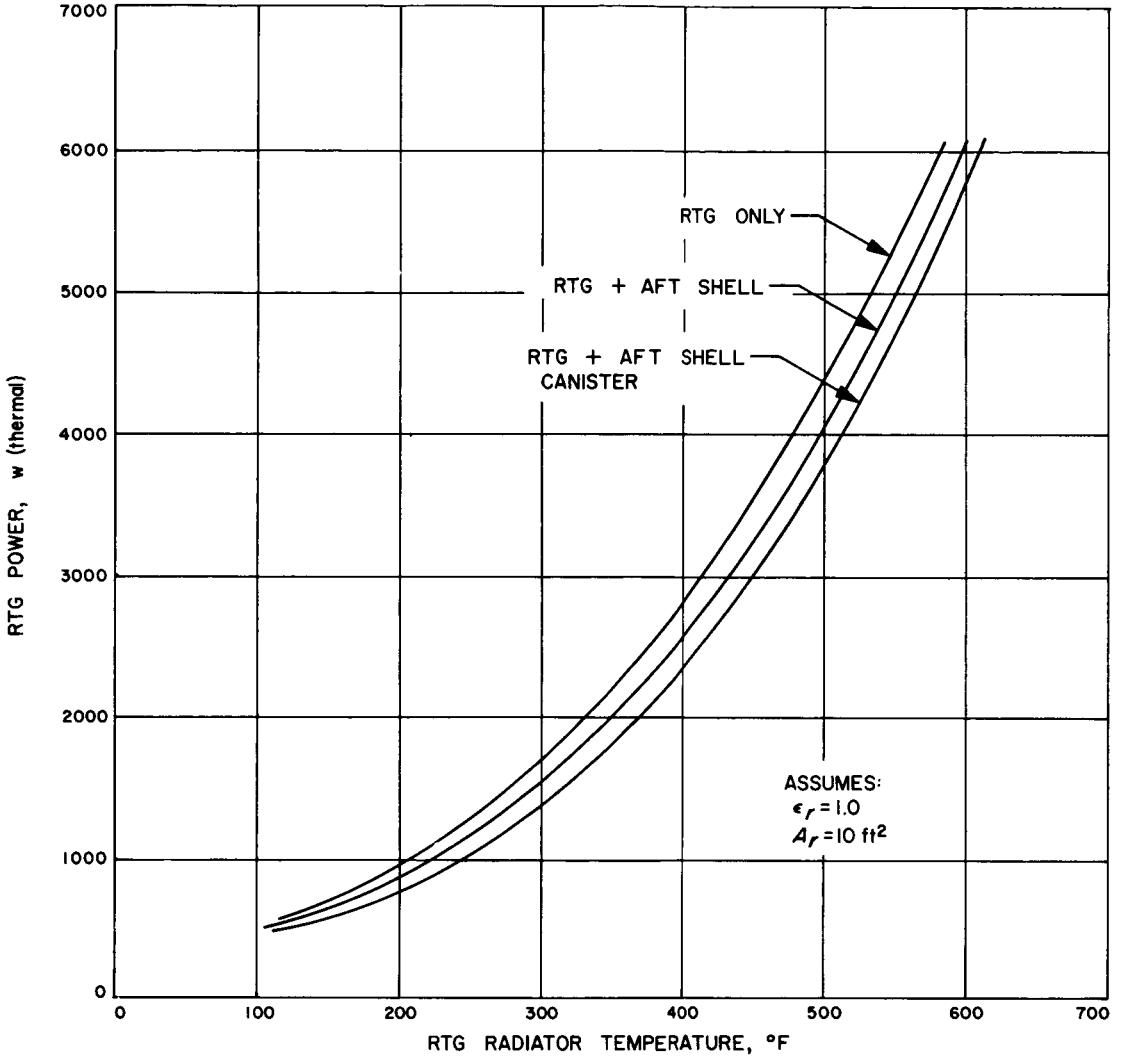

Fig. C-3. The effect of the aft shell and canister on RTG temperature

I. ASSUMPTIONS AND OPERATING CONDITIONS

A. Thermoelectric Generator

1. Power output, 175 watts (raw)
2. RTG overall efficiency, 5%
3. Maximum allowable cold junction temperature, 400°F
4. Radiator area sized to dissipate all of isotope thermal energy when electrical power is not required
5. The RTG configuration of Fig. C-4 is used, whereby the heat is rejected upward from the flat plate radiator as shown in Fig. C-1

B. Closed Loop Rankine System

1. Power output, 175 watts (raw)

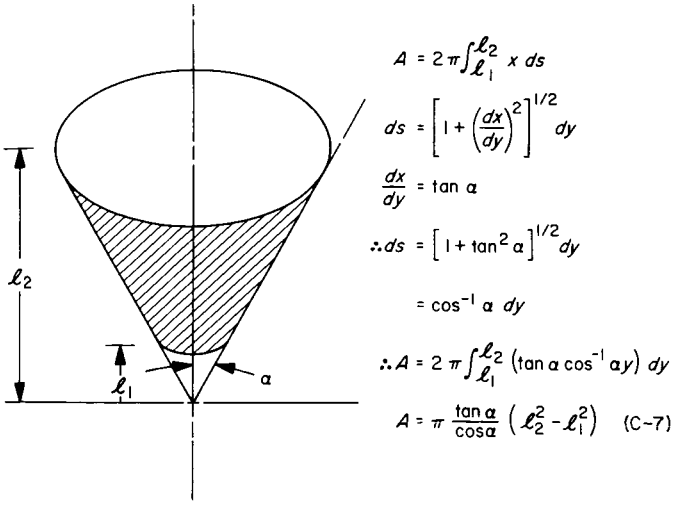

Fig. C-4. Radiator surface area of aft shell

2. Heat rejected
   a. Condenser 1540 w
   b. Subcooler 282 w
3. Condenser temperature, 305°F
4. Subcooler temperature (average), 277°F

C. Closed Loop Brayton System

1. Power output, 175 watts (raw)
2. Heat rejected 1180 w
3. Radiator temperature (average), 247°F

D. Thermionic

1. Power output, 175 watts (raw)
2. Overall efficiency, 11%
3. Heat rejection temperature, 1300°F (700°C)

E. Entry Body

1. *Apollo* shape
2. Aft body surface area, 400 ft² (approximately 16-ft-diam cone)
3. Negligible temperature gradients through aft body during steady state
4. Radiators with unobstructed view to aft body as illustrated in Fig. C-1
5. Entry body shaded during cruise

F. Sterilization

1. Temperature, 300°F
2. Inside of sterilization canister maintained at 300°F
3. Interior of entry body and sterilization canister at atmospheric pressure

G. Operational

1. Sterilization canister is attached until spacecraft attains interplanetary cruise mode
2. Auxiliary cooling is provided for encapsulated spacecraft when radioisotope fuel is aboard during transit to launch pad, on pad, and during pre-flight checkout
3. Power systems cooled passively, if possible; i.e., no coolant loops considered as part of the flight equipment unless already part of the power conversion system (Rankine or Brayton systems)

H. Surface Properties

1. Solar absorptivity = 0.25.
2. Thermal emissivity = 0.85.

As might be expected, of the phases considered, sterilization presents the most severe environment for the power system radiator, in that sterilization temperature approaches and in some cases exceeds normal radiator operating temperatures. Of the power systems included in this study, only the RTG and the thermionic systems have heat rejection temperatures that are reasonably above the sterilization temperature of 300°F. Both the Rankine and Brayton systems studied had condenser or effective radiator temperatures near or below the sterilization temperature. Because the high heat sink temperature imposed by sterilization necessitates a large radiator area for an RTG and will essentially preclude operation of the dynamic systems during sterilization, some alternate approaches are required for this phase. For the RTG, possible alternatives are: (1) allow higher cold and hot junction temperatures, (2) allow a higher cold junction temperature but reduce the hot to cold junction temperature gradient, and (3) provide auxiliary ground cooling. For the dynamic systems, possible alternatives are: (1) allow higher radiator temperatures by using the fluid system as a cooling loop for the fuel and (2) provide auxiliary ground cooling. Item (1) here may require a bypass on the turbine such that only enough work is provided to circulate the working fluid through the loop. Because implementation of any of these alternatives would require judgment from an overall mission viewpoint, the required radiator areas were determined for an RTG at three different radiator temperatures during sterilization, at two different radiator temperatures during the hot-test phase of the mission, and of one radiator temperature for the remaining phases. For the dynamic systems, radiator areas were determined for the phases of the mission during which electrical power was required. These areas are shown in Table C-1.

During the period from aft body jettison to impact, air flow will probably cool the radiator and payload. Because of the uncertainties in configuration definition and descent time, no estimate was made of the magnitude of this effect. It may suffice to say cooling will occur, and some form of movable thermal shielding (e.g., louvers) will be required on the power system radiator as well as the remainder of the payload to accommodate this abrupt cooling period as well as other variable heat loads and thermal uncertainties.

Table C-1. Radiator area as a function of system and radiator temperature

System	Radiator temp., °F	Mission phase/radiator area, ft²					
		Sterilization	Cruise	Midcourse/ Maneuver	Separated capsule	Entry	Surface ops
RTG	400	37.9	16.4[a]	16.3	16	See Below[b]	15
	500	14.3	10.2[a]				
	650	6.9					
Rankine	305				13.8[a]		12.8
Brayton	65–347				12.0[a]		11.1
Thermionic	1300	0.36			0.35		

[a] Indicates flight phase that sizes radiator.

[b] To assess the severity of aft body entry heating as experienced by the power system radiator, an estimate was made of the radiator temperature rise during this period. For most entry conditions aft body heating during this period should not significantly affect the radiator. The reasons for this are: (1) There is a significant time lag between (a) the temperature rise on the outside and inside skin and (b) the inside skin and the radiator; and (2) the aft body is jettisoned before the inside surface gets extremely hot. However, under the most severe (relative to aft body heating) entry conditions studied, the radiator temperature rise was significant. Assumed *worst* case entry conditions were entry angle = 20 deg; angle of attack = 170 deg; ballistic coefficient = 0.35; entry velocity = 25,000 ft/sec; a 16-ft-diam *Apollo*-shaped entry body and aft body jettisoned at sonic velocity. Under these conditions, a 1-lb/ft² radiator that is only radiatively coupled with the aft body would experience approximately a 20°F temperature rise. This is not an extremely large temperature increase and occurs over a 2-min period; therefore, it probably will not be important unless the power system is operating near a high temperature limit at this time.

II. CONCLUSION

From a power system radiator viewpoint, the cruise phase with the capsule in the shade of the spacecraft and with the sterilization canister on is approximately the same thermal condition as the separated capsule in sunlight near the Mars orbit (16.4 ft² vs 16 ft²). Therefore, leaving the sterilization canister aboard until sometime prior to capsule separation should not have a significant thermal effect on the radiator. However, if midcourse maneuver is performed near Earth with the canister on, it could obviously be a hotter condition than either the nominal cruise configuration or the separated capsule, depending upon spacecraft attitude and duration of the maneuver. In the worst case, the radiator area required for an RTG during this phase would be 17 ft² (at 400°F).

As can be seen from the preceding table, the closed loop dynamic systems will require about the same size radiators and compare with the RTG operating at 500°F. At 500°F and above, the RTG radiator is less sensitive to sterilization. The thermionic system requires very little radiator area because it utilizes a high rejection temperature. However, the high temperatures associated with the thermionic system pose material problems that preclude its use.

The entry heating pulse probably will not have a significant effect on the power system radiator, particularly if movable devices are employed to handle this as well as other variable heat loads.

Sterilization may or may not be a problem, depending on what flexibility is available in operating the radiators at higher temperatures during this phase.

The RTG, Rankine, and Brayton systems are competitive on a *radiator area* basis for this mission.

Changing any of the assumptions, on which this study was based, may significantly effect these area estimates. For example, changing the entry body configuration from an Apollo shape to a sphere/cone shape such as to reduce the aft body surface area will increase the temperature of the aft body and change the radiator to aft body geometry. Both of these effects will cause the radiator area requirements to increase.

Equations used to determine heat transfer from RTG to space through the capsule aerodynamic shell and sterilization canister use the following expressions:

q_i total thermal energy removed from the RTG

q_o total thermal energy into the RTG

A_c area of canister

A_s area of aft shell

A_r area of RTG radiator

ε_c emissivity of canister

ε_s emissivity of aft shell

ε_r emissivity of RTG radiator

T_c temperature of canister

T_s temperature of aft shell

T_r temperature of RTG radiator

Q thermal output of RTG

Now for simplification it is assumed that the view factors are as given below:

$$F_{r-s} = 1.0$$

$$F_{s-r} = \frac{A_r}{A_s}$$

$$F_{s-c} = 1.0$$

$$F_{c-s} = 1.0$$

Further it is assumed that secondary reflections are negligible.

Therefore, the net Q transferred from one RTG to the aft shell is given by

$$Q = Q_{\text{net}} = q_{o(\text{RTG})} - q_{i(\text{RTG})} \tag{C-1}$$

$$q_o = \sigma \varepsilon_r A_r T_r^4 \tag{C-2}$$

$$q_i = \sigma \varepsilon_r \varepsilon_s F_{s-r} A_s T_s^4 + \sigma \varepsilon_r^2 (1 - \varepsilon_s) F_{s-r} A_r T_r^4 \tag{C-3}$$

Combining Eqs. (C-2) and (C-3) into (C-1) gives

$$Q = Q_{\text{net}} = \sigma \varepsilon_r A_r \left\{ T_r^4 \left[1 - \frac{A_r}{A_s} (\varepsilon_r - \varepsilon_s \varepsilon_r) \right] - \varepsilon_s T_s^4 \right\} \tag{C-4}$$

The net heat transferred from the aft shell to the canister is given by

$$Q_{\text{net}} = \sigma A_s (T_s^4 - T_c^4) \frac{1}{(1/\varepsilon_s) + (1/\varepsilon_c) - 1} \tag{C-5}$$

The net heat transmitted to space is given by

$$Q_{\text{net}} = \sigma A_c \varepsilon_c T_c^4 \tag{C-6}$$

REFERENCES

1. Rohsenow, W. M., *Developments in Heat Transfer*, Massachusetts Institute of Technology Press, Cambridge, Mass., 1964, Chap. 15.
2. Corliss, W. R., and Harvey, D. G., *Radioisotopic Power Generation*, Prentice-Hall, Inc., Englewood Cliffs, New Jersey, 1964.
3. Arnold, E. D., *Handbook of Shielding Requirements and Radiation Characteristics of Isotopic Power Sources for Terrestrial, Marine, and Space Applications*, ORNL-3576, Oak Ridge National Laboratory, April 1964.
4. Anderson, H. R., and Craven, J. D., "Artificial Sources of Radiation on Spacecraft," *Space Programs Summary No. 37-25, Volume IV*, Jet Propulsion Laboratory, Pasadena, Calif., February 29, 1964, pp. 253–255.
5. Hughes, D. J., *Pile Neutron Research*, Addison-Wesley Publishing Company, Inc., Massachusetts, 1953.

BIBLIOGRAPHY

Broadway, N. J., and Palinchak, S., "The Effect of Nuclear Radiation on Elastomeric and Plastic Components and Materials," Report No. 20 (Addendum), Battelle Memorial Institute, Radiation Effects Information Center, Columbus, Ohio, August 31, 1964.

Cheney, E. O. Jr., Farris, P. J., and King, J. M., Jr., "Open Cycle Fuel Cell System for Space Applications," ASME Paper 64-WA/AV-15, November 29, 1964.

Cherry, W. and Zoutendyk, J. A., "The State-of-the-Art in Solar Cell Arrays for Space Electrical Power," AIAA Paper No. 64-738, September 4, 1964.

Coffman, S. W., Fono, P., and Gould, C. L., "Advanced Fuel Cell Applications for Space Missions," AIAA Paper No. 64-723, September 1, 1964.

Etherington, H., *Nuclear Engineering Handbook,* McGraw-Hill Book Company, Inc., New York, N.Y., 1958.

Evans, D. E., Pitts, D. E., and Kraus, G. L., "Venus and Mars Nominal Natural Environment for Advanced Manned Planetary Mission Programs," NASA SP-3016, 1965.

Fleischer, A., Shulz, E., Tyler, R. D., Uchiyama, A. A., and Banes, R. S., *Background Material for the Study of the National Space Power Program, Vol. I,* DDC TAB No. 452617, Electrochemical, Power Information Center, November 1964.

Francis, H. T., *Space Battery Handbook,* NASA CR-56514, April 15, 1963.

Frankel, P., AIAA Space Power System Lecture Series, LR 17558, February 1964.

Glasstone, S., *Principles of Nuclear Reactor Engineering,* D. Van Nostrand Company, Inc., New York, 1960.

Heath, A. R., Jr., and Hoffman, E. L., "NASA Solar Concentrator Development," AIAA Paper No. 64-730, September 1964.

Houck, O. K., and Heath, A. R., Jr., "Characteristics of Solar Concentrators as Applied to Space Power Systems," SAE-ASME Paper 867C, April 27, 1964.

Johnson, F. S., *Satellite Environment Handbook,* Stanford University Press, Stanford, California, 1965. 2nd ed., Chap. 4.

Mackay, D. B., *Design of Space Power Plants,* Prentice-Hall, Inc., New Jersey, 1963.

Menetrey, W. R., and Neustein, J., *Analysis of Ancillary Equipment for Solar Thermionic System, Final Report,* Jet Propulsion Laboratory, Contract 950699–Task III, EOS Report No. 4326, March 10, 1965.

Menetrey, W. R., and Fisher, L. H., *Energy Conversion Systems Reference Handbook,* WADD Technical Report 60-699, 1961.

Menetrey, W., "Estimates of Solar-Thermionic System Performance," AIAA Paper No. 64-718, September 1964.

Morse, Dr. J. G., "Radioisotope Fueled Power Supplies," Space Power Systems–Szego, UCLA Short Course, x494.

Pedersen, E. S., *Heat-Sterilizable Power Source Study for Advanced Mariner Missions,* TM-33-180, Jet Propulsion Laboratory, Pasadena, Calif., July 1, 1964.

Rockwell, T., *Reactor Shielding Design Manual,* McGraw-Hill Book Company, Inc., New York, 1958.

Rouklove, P., and Blake, F. A., "Performance Testing of a Solar Electrical Thermionic Generator System, Paper presented to the Solar Energy Society Conference, Phoenix, Arizona, March 15, 1965.

Rouklove, P., Status Report on Solar Thermionic Power Systems, AIAA Paper No. 64-734, September 1964.

Rush, R. E., *Solar Flat Plate Thermoelectric Generator Research,* APL-TDR64-87, AF Aero Propulsion Laboratory, September 14, 1964.

Seaborg, G. T., Tape, G. F., Palfrey, J. G., and Raney, J. T., *Systems for Nuclear Auxiliary Power,* TID-20103, U.S. Atomic Energy Commission, February 1964.

Stewart, D. H., Anderson, G. M., Jordy, J. Y., and Weiner, M., An *Evaluation of Systems for Nuclear Auxiliary Power,* TID-20079, Office of Program Evaluation, U.S. Atomic Energy Commission, January 1964.

Thatcher, R. K., et al., *The Effect of Nuclear Radiation on Electronic Components, Including Semiconductors,* Report No. 36, Battelle Memorial Institute, Radiation Effects Information Center, Columbus, Ohio, October 1, 1964.

ACKNOWLEDGMENTS

The author gratefully acknowledges the contributions of the following personnel for their assistance in compiling data for this study: G. C. Cleven and W. L. Long for their assistance in the definition of batteries; J. H. Kelly and E. L. Floyd for their helpful definition of a hydrazine turboalternator; R. J. Spehalski for his analysis of thermal requirements for this capsule study; Dr. C. F. Heindl for his aid in defining the radiation characteristics and requirements; K. Willner for the analysis which appear in Appendixes A and B; K. M. Dawson for his contributions in the area of system analysis. Special acknowledgment is made to C. D. Fredrickson for his contributions in the area of radioisotopic systems, thermal analysis and his many suggestions as this study evolved, and to J. D. Acord, Manager of the Voyager Guidance and Control Section, for his patient guidance during this study.